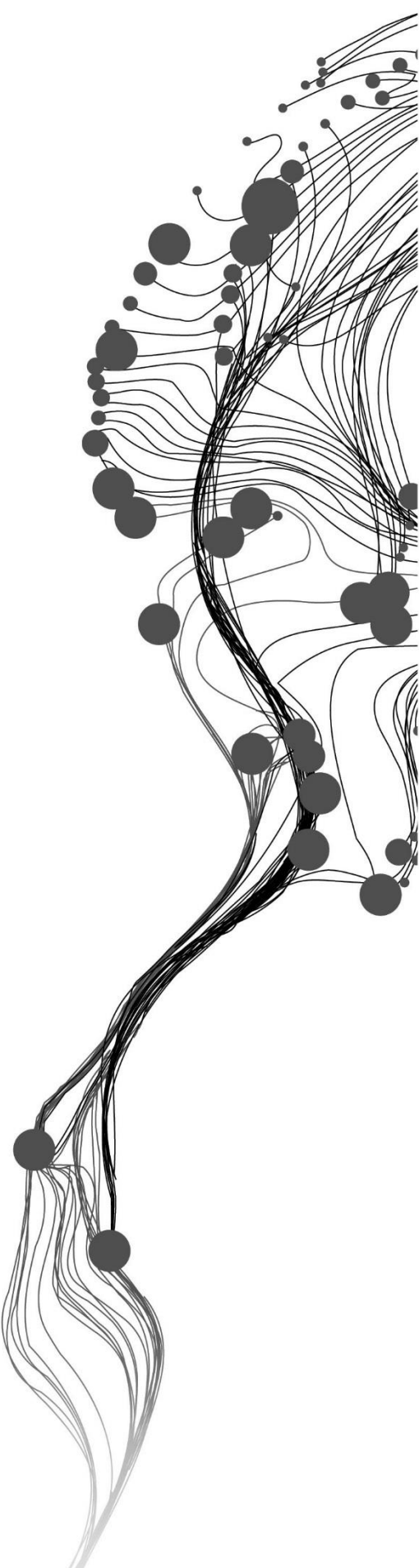


**[TERRESTRIAL LASER
SCANNING BASED MODELLING
FOR FOREST STRUCTURAL
PARAMETER RETRIEVAL]**

[AMIT KUMAR HALDAR]
[March, 2016]

SUPERVISORS:
[Mr. S. Kumar, Mr. S. Raghavendra]
[Prof. Dr. Ir. G. Vosselman]



[TERRESTRIAL LASER SCANNING BASED MODELLING FOR FOREST STRUCTURAL PARAMETER RETRIEVAL]

[AMIT KUMAR HALDAR]

Enschede, The Netherlands, [March, 2016]

Thesis submitted to the Faculty of Geo-Information Science and Earth Observation of the University of Twente in partial fulfilment of the requirements for the degree of Master of Science in Geo-information Science and Earth Observation.

Specialization: [Geoinformatics]

SUPERVISORS:

[Mr. S. Kumar, Mr. S. Raghavendra, IIRS, Dehradun]

[Prof. Dr. Ir. G. Vosselman, ITC, Netherlands]

THESIS ASSESSMENT BOARD:

[Chair: Dr. A. A Voinov]

[External Examiner: Dr. R. D. Garg, IIT, Roorkee]

[Supervisors (IIRS): Mr. S. Kumar, Mr. S. Raghavendra]

[Supervisor (ITC): Prof. Dr. Ir. G. Vosselman]

[Observers: Dr. S. K. Srivastav, Dr. Sameer Saran, dr. V. A. Tolpekin, dr. N.A.S. Hamm]

DISCLAIMER

This document describes work undertaken as part of a programme of study at the Faculty of Geo-Information Science and Earth Observation of the University of Twente. All views and opinions expressed therein remain the sole responsibility of the author, and do not necessarily represent those of the Faculty.

*"An experiment is a question which science poses to
Nature, and a measurement is the recording of
Nature's answer"*

- Max Planck (Theoretical Physicist), 1858 to 1947

Dedicated to my Parents.....

ABSTRACT

Retrieval of forest structural parameters such as Diameter at Breast Height (DBH), Tree height, volume estimation etc. is often difficult to quantify on a large scale as it is time consuming and destructive sampling is not much feasible. The tree parameters are essentially required to estimate the woody biomass accurately. Various remote sensing techniques such as SAR, Airborne LiDAR, etc are being used to estimate the same. Terrestrial Laser Scanning (TLS) which is a ground based technique which is one of the best technique to obtain the forest structural information compare to others. In this project a TLS based modelling has been carried out to retrieve the tree parameters. The data were acquired from mainly three sites, one plot of size 31.6mx31.6m at Barkot Forest Range, two plots at Thano Forest Range and one at the IIRS (only 7 trees), Campus in Dehradun, Uttarakhand State of India. The field based measurements were also taken using Nikon Forestry Pro – Laser Range Finder for height measurement and measuring tape for measuring the circumference of the trees. For each tree 10 measurements were taken in order to get the uncertainty in manual measurements. The post processing of the acquired datasets were done through RiSCAN Pro (In built application with the scanner Riegl VZ-400 model) and ClouCompare (open-source). For estimating the tree parameters an algorithm was created in Python.

The main objective of the project was to retrieve the tree parameters automatically. Then to do a comparative analysis between TLS based estimated volume with the estimated volume using field based DBH using Forest Survey of India (FSI) based volumetric equation established in 1996. For the selected sites local volume equation was used: $V = 0.0308585 - 0.77794D + 8.42051D^2 + 5.91067D^3$ (n = 710, $R^2 = 0.96135$) here n is the no. of samples. The coefficient of determination (R^2) for estimated volumes in this project using TLS and field based parameters at four plots are coming as follows Barkot: $R^2 = 0.99$, RMSE = 0.45 m, IIRS: $R^2 = 0.77$, RMSE = 0.37 m, Thano-Plot-I: $R^2 = 0.95$, RMSE = 0.37 m, and in Thano – Plot-II: $R^2 = 0.97$, RMSE = 0.32 m. Except IIRS plot the R^2 for almost plot is greater than the R^2 of the FSI which could be considered as the success of the project and the adopted algorithm. The IIRS plot was taken for getting point clouds of the trees with variable shapes such as multiple stem, tilt, bending trees, irregular branches etc. Therefore, the bending shape of the trees was addressed by doing modification in the algorithm. Now the diameter at every 50 cm slice of the tree stem has been obtain and using truncated volume formula the volume was estimated with limitation of considering only stem point cloud in the algorithm. Rest trees with variable shapes were addressed by creating the meshed models. In CloudCompare application Poisson's Surface Reconstruction tool was used to create the meshed model and to estimate their volume. However, there was some drastic difference found especially in trees with multiple stems due to which and overestimation is taking place. All these shortcomings may addressed via various open sourc applications such as SimpleTree, Computree, 3D-Forest etc.

Keywords: 3D Point Cloud, Registration Quality, Individual Tree Extraction, Connected Component, Octree Filtration, FSI, TLS based modelling Volume estimation, Surface Reconstruction

ACKNOWLEDGEMENTS

This project wouldn't be completed successfully without few to many people who were there behind me to push forward with their continuous guidance, support and encouragement. I would like to start by expressing my deepest gratitude to my IIRS supervisors Mr. Shashi Kumar, and Mr. Raghavendra S., for giving me opportunity to work in this excellent project. They have taught and directed me, how to gain in-depth knowledge and develop skills which were essentially required in this research project. They have guided me to sharpen my capability in order to bring best out of me. I would like to show my deepest gratitude to my ITC supervisor Prof. Dr. Ir. George Vosselman, he has enlighten me continuously with his great wisdom, without his regular feedback and direction, the completion of this project would not have been easy going.

I would like to express my sincere gratitude to our former director IIRS Dr. Y.V.N. Krishna Murthy and Dr. A. Senthil Kumar, Director, IIRS for providing all the opportunities and facilities which were required for successful completion of the project. My sincere thanks to former course coordinator Dr. S. K. Srivastav, Group Head, IIRS and Dr. N. Hamm, Asst. Professor, ITC, and present course coordinator Dr. Sameer Saran, HOD, GID, IIRS and Dr. V.A. Tolpekin (Valenty), Asst. Professor, ITC for their continuous concern and encouragement.

I would like to thank my best friend Manit Biswas and Pruthvi for rescuing me from the trap of Python by helping me out in coding. I would like to thank, Gautam, Sudheer and all my juniors Ajit, Sourav for assisting me in the field for acquiring the data. Special thanks to my batch mate Susheel for helping me out in data analysis. I would like to appreciate and thanks to all my friends Danish, Anchit, Ajit, Rajan, Aparna, Gautam, Sayan, Nitin, Shrija, Rohit, Vineet, Raj, Arnav, Arsh, Nikita, Ashu Sir, Feras, Mindougus, Yirka, Gabriel, Ariho, Ipsit, Sheila, Gunjan, Linus, Maral, John, Honore, Anthony and Rahul sir for the all wonderful moments we spent together who all made my IIRS and ITC days memorable. I would like to thank love of my life Raksha my best friends Hridendra, Manit, Rachit, Pramod and Vikas for being there in my life for their love and support in all ups and downs of my life.

At last but not the least I would like to thank mummy and papa for their immense love and support in all respect, for their continuous encouragement and believing in me. Once a great scientist Albert Einstein said "In the middle of difficulties, opportunity lies" with this believe I would like to thank my whole family Anoop da, Sheela bhabhi and my dearest nephew Adish for bearing such a hard time in all respect in order to support me LOVE YOU ALL.

TABLE OF CONTENTS

1.	INTRODUCTION.....	1
1.1.	Motivation and problem statement.....	2
1.2.	Title sub-section.....	3
1.3.	Research questions:.....	3
1.4.	Innovation aimed at.....	4
1.5.	Thesis structure	4
2.	LITERATURE REVIEW.....	5
2.1.	Importance of forest biophysical parameters.....	5
2.2.	Traditional approaches and field based forest inventories.....	6
2.3.	Remote Sensing based Techniques	6
2.3.1.	Satellite and aerial imagery systems	7
2.3.2.	Microwave Remote Sensing.....	8
2.3.3.	Optical Remote Sensing	8
2.3.4.	LiDAR Technology.....	9
2.3.4.1.	Space borne/Airborne LiDAR Systems	9
2.3.4.2.	Ground based LiDAR systems	10
2.3.5.	Surface Reconstruction	11
3.	STUDY AREA	13
3.1.	Significance of the study area.....	13
3.2.	Topography.....	14
4.	METHODOLOGY.....	15
4.1.	Site Planning	16
4.2.	TLS Based Data Acquisition	16
4.2.1.	Terrestrial Laser Scanner settings.....	18
4.3.	Field Based Measurements:	20
4.3.1.	Multiple Measurements:.....	21
4.4.	Post processing the data	21
4.4.1.	Co-Registration of the point clouds	22
4.4.1.1.	Registration quality	23
4.4.2.	Individual tree extraction.....	28
4.4.3.	Removal of outliers.....	29
4.4.3.1.	Connected Component:	29
4.4.3.2.	Octree 3-D grid.....	30
4.5.	Modelling of tree for parameters retrieval	31
4.5.1.	Tree Height.....	32
4.5.2.	Diameter at Breast Height (DBH)	32
4.5.3.	Volume Estimation using Forest Survey of India (FSI) based volumetric equations	33
5.	RESULT AND DISCUSSION.....	35
5.1.	Field measurements and it's uncertainty	35
5.1.1.	Regression Statistics	35
5.2.	The regression analysis of the data acquired at Barkot forest area	36
5.3.	The regression analysis of the data acquired at IIRS Campus.....	41

5.4.	The regression analysis of the data acquired at Thano forest range: Plot-I.....	45
5.5.	The regression analysis of the data acquired at Thano forest range: Plot-II.....	49
5.6.	Comparative analysis of DBH vs Height.....	55
5.7.	Discussion.....	57
5.7.1.	Limitation of the Nikon Forestry Pro Laser Rangefinder:.....	57
5.8.	Volume of the bent trees.....	58
5.9.	Trees with varying shapes.....	61
6.	CONCLUSION AND RECOMMENDATION	62
6.1.	Conclusion.....	62
6.1.1.	Answers of Research Questions.....	63
6.2.	Recommendations	64
References:	65
Appendix a:	Tables of the field measurements and its uncertainty.....	72
A.1	Uncertainty in Barkot Forest Area	72
A.2	Uncertainty in IIRS.....	72
A.3	Uncertainty in Thano Forest Range: Plot-I	73
A.4	Uncertainty in Thano Forest Range: Plot-II.....	74
Appendix B:	Predicted Volume Residual and Probability Tables	75
B.1	PV Residual and Probability Table: Barkot Forest Area.....	75
B.2	PV Residual and Probability Table – IIRS Plot.....	76
B.3	PV Residual and Probability Table – Thano Forest Range: Plot-I	76
B.4	PV Residual and Probability Table – Thano Forest Range: Plot-II.....	78
Appendix C:	Relative errors in DBH, height and volume in all plots	81
C.1	Relative errors in Barkot Forest Area	81
C.2	Relative errors in IIRS Campus	81
C.3	Relative errors in Thano Forest Area: Plot-I	82
C.4	Relative errors in Thano Forest Area: Plot-II.....	83
Appendix D:	3D View of the point Clouds.....	84
Appendix E:	Field Visits – Phtographs	86
Appendix F:	Registration quality	88
F.1	First and last iterations during Multi-Station Adjustments at Barkot Forest Area	88
F.2	First and last iterations during Multi-Station Adjustments at IIRS Campus	89
F.3	First and last iterations during Multi-Station Adjustments at Thano Forest Area: Plot-I.....	90
F.3	First and last iterations during Multi-Station Adjustments at Thano Forest Area: Plot-II	91

LIST OF FIGURES

Figure 1: Study area location map.....	13
Figure 2: Methodology flowchart.....	15
Figure 3: Plot measurements and data acquisition plan – Barkot forest area, Dehradun.....	17
Figure 4: Plot measurements and data acquisition plan – Guest house garden, IIRS Campus, Dehradun.	17
Figure 5: Plot measurements and data acquisition plan – Thano Forest Range, Dehradun	17
Figure 6: Views of all five scans on the plot in Barkot forest area	18
Figure 7: Views of all five scans along the plot at Guest House, IIRS Campus	19
Figure 8: Views of all five scans on the plot in Thano forest area-1.....	19
Figure 9: Views of all five scans on the plot in Thano forest area-2.....	20
Figure 10: Vertical Separation mode as explained in (Forestry-Suppliers, 2016) and field measurements using Forestry Pro and measuring tape.....	20
Figure 11: Survey Performa	21
Figure 12: A 3D view of the plot at Barkot forest areas after registration.....	22
Figure 13: Adjustment after first Iteration: Barkot Forest.....	25
Figure 14: Adjustment after second Iteration: Barkot Forest	26
Figure 15: Adjustment after third Iteration: Barkot Forest	26
Figure 16: Adjustment after first Iteration: Thano Forest (Dataset-1)	27
Figure 17: Adjustment after second Iteration: Thano Forest (Dataset-1).....	27
Figure 18: Adjustment after third Iteration: Thano Forest (Dataset-1).....	28
Figure 19: Individual Tree extraction	29
Figure 20: Three components example.....	29
Figure 21: Octree illustration	30
Figure 22: The removal of outliers using connected component analysis	30
Figure 23: Tilted tree height calculation.....	32
Figure 24: (a, b) Diameter estimation.....	33
Figure 25: The estimation of the volume w.r.t. modelled DBH at Barkot Forest.....	37
Figure 26: RMSE assessment in both field measured and TLS based Height.....	37
Figure 27: RMSE assessment in both field measured and TLS based Height.....	38
Figure 28: RMSE assessment in both field measured and TLS based Height.....	38
Figure 29: The volume residual plot w.r.t. TLS based DBH.....	40
Figure 30: The non-linear regression after transformation.....	40
Figure 31: The estimation of the volume w.r.t. modelled DBH at IIRS Campus	41
Figure 32: RMSE assessment in both field measured and TLS based Height.....	42
Figure 33: RMSE assessment in both field measured and TLS based Height.....	42
Figure 34: RMSE assessment in both field measured and TLS based Height.....	43
Figure 35: The volume residual plot w.r.t. TLS based DBH.....	44
Figure 36: The estimation of the volume w.r.t. modelled DBH at Thano Range: Plot-I.....	46
Figure 37: RMSE assessment in both field measured and TLS based Height.....	47
Figure 38: RMSE assessment in both field measured and TLS based Height.....	47
Figure 39: RMSE assessment in both field measured and TLS based Height.....	47
Figure 40: Volume residual plot w.r.t. TLS based DBH	49
Figure 41: The estimation of the volume w.r.t. modelled DBH at Thano Range: Plot-II	51
Figure 42: RMSE assessment in both field measured and TLS based Height.....	52

Figure 43: RMSE assessment in both field measured and TLS based DBH.....	52
Figure 44: RMSE assessment in both field measured and TLS based volume	52
Figure 45: Scatter Plot of Measured Volume and Measured DBH at Thano Forest: Plot-2	53
Figure 46: Scatter Plot of Modelled Volume and Modelled DBH at Thano Forest: Plot-2	53
Figure 47: Volume residual plot w.r.t TLS based DBH.....	55
Figure 48: DBH vs Height, Barkot.....	56
Figure 49: DBH vs Height, Thano-Plot-I	56
Figure 50: DBH vs Height Thano-Plot-II.....	56
Figure 51: Methods to estimate the tree diameter.....	57
Figure 52: The measured height through the distance measurement tool in CloudCompare	58
Figure 53: The method adopted for the bending trees	59
Figure 54: Correlation between modelled and measured volumes of tilted trees.....	60
Figure 55: Bent Trees as listed in Table 27	60
Figure 56: Meshed models of few variable trees	61

LIST OF TABLES

Table 1: Field based measured parameters and TLS based modelled parameters	36
Table 2:Regression Statistics by using modelled Volume and DBH.....	39
Table 3: ANOVA	39
Table 4: Measured and modelled parameters:.....	41
Table 5: Regression Statistics by using modelled Volume and DBH.....	44
Table 6: ANOVA	44
Table 7: Measured and modelled parameters.....	45
Table 8: Regression Statistics by using modelled Volume and DBH.....	48
Table 9: ANOVA	49
Table 10: Measured and modelled parameters.....	50
Table 11: Regression Statistics by using modelled Volume and DBH	54
Table 12: ANOVA	54
Table 13: Uncertainties in height measurements using Laser Rangefinder.....	58
Table 14: Estimated volume using algorithm for different sections at different heights and DBH.....	59
Table 15: Summarization of the results.....	62

ACRONYMS

LiDAR	– Light Detection and Ranging
LASER	– Light Amplification by Stimulated Emission of Radiation
RADAR	– Radio Detection and Ranging
SAR	– Synthetic Aperture Radar
IRS	– Indian Remote Sensing Satellites
LISS	– Linear Imaging Self Scanning
TLS	– Terrestrial Laser Scanner
MLS	– Mobile Laser Scanner
ALS	– Airborne Laser Scanner
SOCS	– Scanner’s Own Coordinate System
PRCS	– Project Coordinate System
GLCS	– Global Coordinate System
TPL	– Tie Point List
GCP	– Ground Control Point
DBH	– Diameter at Breast Height
LAI	– Leaf Area Index
PCD	– Point Cloud Data
PCL	– Point Cloud Library
DTM	– Digital Terrain Model
FSI	– Forest Survey of India
ASCII	– American Standard Code for Information Interchange
ANOVA	– Analysis of Variance

1. INTRODUCTION

Searching for renewable and non-conventional sources of energy is becoming the prime concern in most of the countries. The forest biomass is renewable and has potential to substitute fossil fuel effectively to minimize carbon emission and climate change. As per the Google trends tracks of searching for biomass, India and South Africa are under five most countries which have been searched for biomass energy (Charles, 2011). Across the world approximately 2 billion tones dry wood are being used by human for various purposes. In Asia and Africa half of it is being used for only domestic purpose (West, 2009). For a better decision making, planning and development process the use of remote sensing techniques have become essential base for sustainable forest management.

The forest inventories such as the estimation of the biomass, or information about the vegetation characteristics, its classification, quantification and measuring the ecological status of the environment such as controlling nutrients, water and solar resources are essential for ecological balance. The usefulness can be seen in many applications like for assessing the rangeland condition to get the productivity of the agricultural lands, the dominance of the species affecting biodiversity, hydrologic properties of the land, detecting and measuring the woody plants constitute potential fuels etc. are some of the fields of study wherein the estimation of the tree parameters plays great role (Launchbaugh, 2009). Now days due to the rapid growth of population is leading urbanization haphazardly, high level of deforestation, fossil fuel combustion, degradation of the forest ecology which is causing for production of the greenhouse gases in most of the tropical countries (Gibbs et al., 2007). Therefore, for quantifying all associated factors the estimation of the forest parameters gives an overall and crucial understanding of the carbon cycle and its impact on the global warming (Sierra et al., 2007). In recent years airborne laser scan, SAR tomography have been used for forest inventories but for the accurate estimation of stem volume, breast height, density etc. ground based remote sensing technique which is Terrestrial Laser Scanning (TLS) has essentially become more efficient and appropriate.

For estimating the size and volume of the tree the diameter at breast height which is 1.3 m from the trunk base is an important parameter. There are various techniques such as via aerial photographs, satellite images, SAR tomography, LiDAR etc, which are being used to estimate the biomass, carbon emission etc. The direct measurements of the DBH from airborne techniques are real challenge, since the requirement of the large scale oblique measurements or photographs; also in dense forest area the accurate tree height measurement is again very difficult. To estimate the diameters the regression equations are being used with the crown diameters obtained from aerial photographs. The wood volume is the most important tree parameter for the accurate estimation of the biomass, but to obtain such information directly is a hard to do, therefore, it is perhaps preferable to estimate the volume of the forest stand using regression equations comprising of

set of dependent and independent variables. The said technique has many disadvantages such as the getting accuracy, scale dependent, costly, lack of positional information, lack of clarity, time consuming etc. (Rosillo-Calle et al., 2012). LiDAR technology is becoming more popular in order to get a detailed 3D modelling of the real world with accurate measurements of the object parameters. Same as RADAR, LIDAR (Light Detection and Ranging) sensors work on the same principle as it fires the pulses with a shorter wavelength to measure even smaller objects accurately and ranges calculated as per the delay in returns to the source from the objects. From the airborne platform the LiDAR technology is capable of collecting and generating highly dense and accurate elevation data. Till late 80's, determining the location of the airborne LiDAR sensor was a challenge, which was resolved due to the introduction of the Global Positioning System (GPS). The direct and accurate densely topographic data acquisition the LiDAR technology becomes one of the significant techniques to acquires such information (Mursa, 2013). The recent developments in LiDAR technology is in full waveform scanners which gives higher point density along with the reflecting characteristics of the tree structures and the vegetation classifications (W. Yao et al., 2012). In LiDAR technology all dimensions of the data are individually geo-referenced, which gives high accuracy in horizontal and vertical data information (Suárez et al., 2005). In forestry precisely if we say there is some under or overestimation is always there in case of airborne LiDAR technology especially in case of dense forest area due the presence of the trees with vertical denser canopy distribution. However the ground based LiDAR equipment are more efficient and provides accurate information comparatively. The Terrestrial Laser Scanner (TLS) is proficient enough to get detailed and direct measurement of the tree parameters like diameters, height and locational information in forest areas (Maan et al., 2014).

1.1. Motivation and problem statement

In context of Indian scenario, the measurement of the tree parameters to estimate biomass still is a big challenge. A study has been carried out by Giri & Rawat, 2013, wherein, they used volumetric equations developed by Forest Survey of India in 1996 for estimation of the biomass in the Barkot forest area. The said volumetric equation used only one parameter which was diameter, but forestry is becoming very precise science now days, it involves more parameters such as basal area, tree height, leaf index etc. (Dassot et al., 2011a). 3D Laser scanning imaging system is replacing the traditional manual measurement methods and the accuracy of the technique could meet the requirement of the precision forestry inventories. So the automation of estimating forest parameters for replacing the conventional method of computing tree parameters needs to be addressed in the forestry projects. There are many challenges to proceed with as one them is the detection of the trees and its location could be the real challenge. The appropriate and efficient locations of the scanner plays great role to minimize the effort and time consumption effectively. The study area selected at Barkot forest area in Doon valley is relatively disperse and has lot of varieties in terms of tree species along with the shape and size of the trees. Normally the diameters of the trees vary from 10 cm to 100 cm in the study area. Therefore, the presumption is to scan from 5 locations, 4 corners and centre of the plot of size 31.6 m * 31.6 m would be sufficient enough to detect all the trees. The next challenge could

be the registration of the obtained point cloud, since the location information in a dense forest area would be interesting task. Bae & Lichti, 2004, have used Iterative Closest Point (ICT) method for two partially overlapping point clouds by thresholding the minimum distances from points of first cloud to the corresponding points of second cloud. The distance from a point and the corresponding surface was used as error metric in order to achieve more accuracy.

The project will focus on retrieving the tree parameters such as stem volume, basal area, diameter at breast height and tree height by using combination of appropriate methodologies and algorithms as it is very difficult to obtain by using conventional methods. Since the diameters of trees on the study area are varying from 10 cm to 100 cm which would lead to acquire adequate point density on the tree stems, therefore by using triangulation the diameters at different heights on the stem could be acquired for the better result. Then by using triangulation to reconstruct the stem and truncated cone volume formula the estimation of the stem volume and other parameters could be done. This project will mainly emphasize on automated retrieval of tree parameters through TLS based modelling. Accuracy of the estimated parameters could be validated with the field based measurements of the same tree. The accuracy in the modelled parameters could be achieved via combination of the algorithms, subsequently the appropriate method to register the obtained point cloud from the identified scanning locations. After obtaining the modelled parameters it was validated with the field measured parameters and then volume was calculated using FSI based volumetric equations.

1.2. Title sub-section

- The main objective of the project is to estimate tree parameters such as stem volume, diameter at breast height (DBH) and tree height of the tree automatically using TLS based modelling.
- Sub-objective is to do a comparative analysis of the TLS based modelled stem volume of different tree species with the stem volume obtained from FSI based empirical equation also with the field based manually measured tree parameters.

1.3. Research questions:

- How the modelling of stem diameter can be ensured in case of data gaps due to occlusion and extreme tree shape variation?
- Identification of the appropriate linear or polynomial function of the interpolation of the irregularities of stem circumference?
- The projection of the underestimated or overestimated measurement could be mitigated via using correction factor in appropriate function but how can the obtained values will be validated?

1.4. Innovation aimed at

- Automation of conventional method for estimating tree parameters especially in case of India is been interest for various organization. Hence, the algorithm for retrieving the tree parameters automatically and an overall assessment in the uncertainties in the modelled and measured volume, could be considered as partial innovation.
- Formulating function by using correction factor from the reference and measured data to project the accurate estimation of the tree parameters (Volume, Height and DBH).

1.5. Thesis structure

This thesis work will comprise six chapters, starting with introductory part explaining the importance of the LiDAR technologies over other remote sensing techniques especially for the forestry inventories in the first chapter along with the research motivation and problem statements, objectives, research questions and innovation. Chapter-2 will be on the literature review, wherein a summary of various research work done by many researchers using techniques and approaches are explained precisely. The study area and the data acquisition part will be covered in chapter-3. Chapter-4 will be about the methodology adopted in this thesis work and the post processing techniques and algorithms will be explained. Chapter-5 will be on the result analysis and discussion and in the last chapter conclusion and future recommendations will be suggested.

2. LITERATURE REVIEW

Forest inventories means to acquire the information about the forest structure such as the timber resources. The first step is the mapping of the forest stands, species composition, density, structural parameters such as height, diameters, volume etc. Such information are essentially basis for the sustainable forest management (Mohren et al., 2012). The retrieval of forest parameters and the estimation could be done using various techniques such as with satellite and aerial imagery systems, SAR technology, airborne and ground based LiDAR technologies. This chapter comprises various segments, starting with the importance of forest structure, why we need to estimate the structural parameters, significance of the biomass, various remote sensing and mathematical approach to acquire the information about the classes, species etc. along with the estimation of the retrieved forest structural parameters.

2.1. Importance of forest biophysical parameters

Forest ecology comprises the all interrelated patterns, various processes and phenomenon of the flora and fauna and ecosystems in the forest. Forest is the woodland for all biotic components such as plants, animals and micro-organisms. With growing trees the diversity and complexity of the forest ecology increases. IT helps in developing various micro-environments within the existing systems which makes it highly heterogeneous. The physical changes in the existing vegetation lead various dependent variables such as temperature, relative humidity, air quality, and water quality and minerals presence in it. The current and future responses of climate change depend on the amount of carbon emission in the environment. The modelling of estimating the carbon stocks in the forest ecosystem is challenging, but for various climate change mitigation strategies requires the accurate estimation of different parameters (Shaw et al., 2015). The carbon cycles globally link climate, atmospheric CO₂ and the terrestrial and oceanic biosphere carbon balance and management. For getting the temporal changes of environmental condition and the forest condition the tree growth is one of the most important parameters (Ferretti, 2013). The large no. of standing biomass which has great potential in order change in the climatic condition (Otto, 1998). Therefore, it is very important to take the estimation of these parameters into account for getting accurate estimates of biomass. As earlier mentioned the biomass can be the alternative solution for today's energy demands. It is renewable, low carbon fuel which is available in abundance and brings social benefits as it generates lower level of pollutants such as Sulphur dioxides, improves biodiversity, ecosystems ("Why use BIOMASS?" 2015).

2.2. Traditional approaches and field based forest inventories

Prior to the recent technology such as remote sensing comes into the existence, the forest inventories were taken place manually which was a tough task to do though it is considered as the most accurate method for quantification of the forest parameters. It is classified as (i) Destructive method and (ii) non-destructive method. In destructive method also known as Harvest method, we have to cut down the tree to measure its parameters height, diameter at the breast height (DBH), its weight of the different tree components etc. and then by using relevant allometric equations the calculation of the volume and biomass takes place. This method is expensive, limited to the scale, very time consuming, therefore not applicable for the degraded forest comprising rare species (T. Vashum, 2012). Whereas the non-destructive method is based on developing a relational allometric equations between the tree height and the diameters of the tree. Adhikari, 2005, has used the remotely sensed data and image classification techniques combining with the ground based non-destructive volume assessment method to estimate the volume and biomass of the individual tree. Then concluded that the Montes method is not reliable in terms of estimating volume as it was not sufficient while considering the tilt in the direction. The field measurement of the tree parameters such as the tree height, diameter at the breast height, canopy, density, identification of the tree species etc. are very cost intensive and time consuming tasks (Pal, 2008). For example a research was carried out on similar aspect wherein the tree root was extracted mechanically and after cleaning the root system was suspended and scanned through TLS from various angles and the root surface obtained through co-registered 3D point clouds model to determine the root volume and its complete structure (Smith et al., 2014). That could have been possible with the use of ground based LiDAR techniques, now we can imagine if the sample size is large specifically in case of dense and heterogeneous forest, it is almost impossible to estimate the required parameters for calculating biomass or any prediction related with climate change.

2.3. Remote Sensing based Techniques

Forest is one of the most diverse and wide distributed habitations on Earth comprising various ecosystems. Remote sensing is the valuable monitoring system, which allows the collection of digital information about the forest structures in timely manner. The remotely sensed images helps us for mapping the forest areas in large scale with digital information of the forest parameters which helps us in the assessment and decision making (Wulder, 1998). Remote sensors are categorized in two segments active and passive. In active sensors are optical – IR(OIR) comprising LiDAR technology and microwaves comprising Scatterometer, SAR which do not requires sun light to sense the object's characteristics, it radiates its own electromagnetic energy to do so. On the other hand the passive sensors like in optical-IR(OIR) comprising photographic camera, opto mechanical scanner (MSS), Push-broom scanner (IRS-LISS), and in Microwaves comprising scanning microwaves radiometer (MSMR) requires a different source of energy to acquire the information remotely (Joseph, 2005). For quantifying the forest biomass and categorization of the forest properties mainly three types of remote sensing techniques are being used. For vegetation structures (Leaf area index – LAI), crown

size, shadow, texture and tree density optical remote sensing are adequate, whereas, radar data measures the dielectric and geometric properties of the forest and LiDAR technology helps in detecting the vertical heights and other parameters such as diameter, locational information etc. (Zhang & Ni-meister, 2014). In forest management systems both active and passive sensors are being used. The techniques and methods of retrieving forest structural parameters by using various remote sensing techniques are explained below in details:

2.3.1. Satellite and aerial imagery systems

In ecosystem management the mapping of landscape assessment is very important. The detail level of object information using higher resolution imagery could be provided using aerial photography. This technique is one adequate technique to assess the longest available temporal spatial records of the terrain objects (Morgan et al., 2010). Vohland et al., 2007, have used Landsat-5 TM covering the Hunsruck area, which has the multispectral reflective segment of the visible, near infrared and the shortwave infrared which are actually appropriate for the study of the vegetation. They have carried out the project with the supervised parametric classification of the test site in Germany with the radiometric corrected Landsat-5 TM scene. A critical assessment of the land and resources could be done through terrestrial ecosystem mapping by incorporating the information of the climate, vegetation structures, physiographic, surface materials and soil.

A study has been done by Johansen et al., 2007, to determine the capability of the satellite imagery data to discriminate the forest structure stages in riparian and adjacent forested ecosystems as defined in British Columbia Terrestrial Ecosystem Mapping (TEM) scheme by using a high spatial resolution Quick-Bird image. Another research was on the atomization of extracting the spectral and spatial information of the forest structure. Wherein, Beguet et al., 2014, have used very high resolution satellite imagery and adopted the approach based on linear regressions between the forest structure variables (which is to be estimated) and various spectral and Haralick's texture features. A study at the Euro region Tyrol-South-Tretino in Italy was carried out by Pasolli et al., 2015, where they used MODIS imagery acquired by AQUA and TERRA satellites to determine the Leaf Area Index (LAI) of the trees at the study area. The research of Wimmer et al., 2000, clearly state the potential of the satellite remote sensing by demonstrating the high resolution satellite data such as Thematic Mapper and SPOTIV data. The classification on the basis of spectral responses of various vegetation species can be done easily with the help of aerial imagery but has limited potential in terms of the accurate estimation of the tree parameters such as tree height, diameter, volume etc. One advantage of using satellite imagery is that we get the temporal resolution but in case of aerial photographs the flight plan is limited. Though the aerial photographs have very high spatial and radiometric resolution and spectral sensitivity over the visible range to the near infrared range of the electromagnetic spectrum (400 nm to 1100 nm) (Koch, n.d.).

2.3.2. Microwave Remote Sensing

The classification of the space borne sensors is as visible, infrared and microwave sensors. The optical sensors are usually influenced by the atmospheric elements such as cloud; humidity etc. but the microwave sensors has the ability to deal with such conditions. It has good penetration capacity also very sensitive to the water in variant forms such as water contents in vegetation, soil and snow (Shi et al., 2012). The range of wavelength of the microwave is from 1 mm to 1 m. The electromagnetic radiation of the microwave is used radar remote sensing is useful in various Earth observations as in atmospheric study, oceanography, ecology etc. The ranging radar is capable of efficient measurement of the mean and dominant tree heights than the field measurements. A study has been carried out by Hyyppä & Hallikainen, 1996, wherein they acquired the data using helicopter-borne ranging scatterometer, the radar variables were analysed from the standing forest profiles to obtain the accurate measurement of the mean and dominant height of the vegetation, height of the crown base line and stem volume per hectare.

Peregon & Yamagata, 2013, have demonstrated the similar approach by using ALOS/PALSAR for estimating the above ground biomass in a mixed and deciduous forest at the southern edge of the boreal region in western Siberia. Tanase et al., 2014, have used airborne Polarimetric L-band imaging synthetic aperture radar (PLIS) for retrieving the biomass, wherein polarimetry showed similar sensitivity to biomass levels as backscatter intensity. In Malaysia and Indonesia the oil plantation resulted large scale environmental degradation, therefore a study has been carried out for the assessment of the carbon stock, carbon emission etc. by using the ALOS PALSAR (Advanced Land Observing Satellite Phased Array L-Band Synthetic Aperture RADAR) imageries for discriminating the palm plantation in the forest (Morel et al., 2011). The microwave sensed data assessment could be reliable at large scale specially in case of forest inventories for instance estimation of the tree heights but may comprise redundancies due to the multiple scattering phenomenon. Sexton et al., 2009, have done a comparative study using both LiDAR and radar datasets of Pine and Hardwood forest of the Piedmont region of North Carolina, USA. It was observed that the LiDAR data provided the intuitive representation of the vertical structure with greater accuracy and fewer systematic errors.

2.3.3. Optical Remote Sensing

The remote sensing broadly classified into three types with respect to the wavelength region of the spectrum (i) Ultraviolet and visible region (Atmosphere) (ii) Visible and reflective infrared RS (lands and sea) (iii) Thermal infrared and (iv) Microwave remote sensing. The sensors which covers the wavelength region from 0.4 μm to 20 μm falls under the optical –IR (OIR) sensors. The OIR sensors are further classified into two major categories one is photographic wherein the images are formed directly on the film whereas in second category i.e. electro-optical sensors the optical images converts into the electrical signal and then further processed to record or transmit the information. The basic elements of the OIR image systems are collecting image systems, colour separation systems, detectors, in-flight calibration systems and associated electronics (Joseph, 2005). For the assessment of the vegetation properties such as the volume of the tree stem, biomass

estimation several methods have been developed using optical remote sensing techniques. A research has been carried out using optical reflectance model and radar backscattering coefficients and height of scattering centre of the L-band generated by forest growth model. The result showed the improved estimation of the forest parameters, later the obtained parameters were validated with the LiDAR based derived data of the same area (Sun et al., 2013).

2.3.4. LiDAR Technology

The new and advanced technology which is LiDAR (Light detection and Ranging) is certainly attracting the forestry community due to its fast and efficient tools for retrieving the information used in forest inventories. It is similar to the radar which uses the electromagnetism in order to detect and ranging the object properties. It uses the similar functionality as the optical remote sensing as it uses the optics for the refraction of the electromagnetic waves (van Leeuwen & Nieuwenhuis, 2010).

2.3.4.1. Space borne/Airborne LiDAR Systems

For a detailed level of study of the forest stand biomass terrestrial measurements are more accurate but is very cost effective and time consuming. A study has been done by Latifi et al., 2015, at the highly heterogeneous forest of Bavarian Forest National Park, Germany. They have estimated the individual tree parameters, tree density, and height variation area wise and done a comparative analysis with the ground based inventories. The methods adopted were single tree segment based and area based method, as compared in terms of cost effectiveness and time consumption the ground based technique showed significant results for all structures. The tropical forest with complex and heterogeneous topography is challenging for space borne or airborne remote sensing because of difficulties in penetrating the canopy and multi scattering effects.

For estimating above ground biomass Leitold et al., 2015, have used airborne LiDAR data sets. The digital terrain model (DTM) was derived from the airborne data from a mountainous region of Atlantic forest in Brazil which was compared with the 35 ground control points measured in a survey with GNSS receivers. The derived DTM was highly accurate, then the canopy height was measured. The similar study was carried out at the mountainous forest of the northern Italy by Montagnoli et al., 2015. Wherein they have investigate the low density LiDAR data (less than 2 points/m²) to estimate the above ground biomass (AGB). The estimation of the AGB from the study has shown the acceptable accuracies. The height result showed a $R^2 = 0.87$ with a mean RMSE of 1.02 m (8.3% of the mean). The retrieval of the tree parameters using TLS based modelling is comparably easy as compare to the other techniques as it gives the 3D information about the objects under observation. The optimization of the space borne full waveform LiDAR system for vegetation analysis. The strength of the signals from the ground and the vegetation varies as per the sensor specifications. The results obtained showed a great accuracy in vegetation height after the optimization even in the extreme forest conditions. The reduced footprints allowed improved confidence in the distribution of the forest parameters (Rosette et al., 2013). A study carried out by Romanczyk et al., 2014, simulates the

impact of the structural component on the full waveform signals received during pulse outgoing and the scanning angles. The result showed that the back scattered waveform has great impact by the leaf of the trees rather than the stem, branches, twigs etc. Therefore, it is somehow states that the accurate assessment of the tree parameters other than tree height the ground based techniques could be more appropriate in order to estimate those parameters. The Terrestrial Laser Scanner (TLS) based forest inventories essentially showed more accurate estimation in forest inventories.

2.3.4.2. Ground based LiDAR systems

For the study of ecosystem studies the use of terrestrial laser scanning (TLS) technique with small footprint laser for resolving 3D structures of the objects is more precise and faster than the other remote sensing techniques. In forest inventory the precise and accurate assessment of the standing structures was a challenge, but now by merging several ground based methods with TLS based data we can get the improved characteristics of the forest structures. Statistics to derive foliage profile, leaf area index (LAI), height of the tree, diameter at breast height etc. can be easily obtained by the said technology (Zhao et al., 2015). A study has been done by Wu et al., 2008, wherein they used TLS based point cloud to estimate the volume. Using cylindrical and truncated cones to model the tree stem and then traditional method of subsection integration they estimate the volume of the tree. For the better understanding of the forest structures, 3D point clouds collecting with the Terrestrial Laser Scanning (TLS) from multiple point angles plays a great role in order to assess the 3D architecture and information of the forest structures.

It is observed that to get accurate information of the vertical structures in a forest is difficult due to heterogeneity. In another study by Moskal & Zheng, 2011, which was based on voxel data structure derived from TLS PCD showed an underestimate result in DBH and tree height when compared with field based measurements. On the other hand through Tree wrapping method (Kato et al., 2009) and Crown geometry volume method (Jung et al., 2011) the same results for all tree parameters were overestimated. Similar research has been carried out by Park et al., 2010, wherein they have used K-Dimensional algorithm to the voxelisation of the point cloud data of tree with the size 10 cm, 50 cm and 100 cm and later they compared the TLS based result with the ALS based result to validate the accuracy. Another study by Olofsson et al., 2014, where they used Hough transformation and RANSAC algorithms to detect and estimate tree parameters. Dassot et al., 2011, have established the state-of-the-art of TLS based tree modelling, wherein they have elaborated the methods like point cloud voxelisation (Tree topology), bark texture analysis (Species/defects), geometric fitting (Diameter/Height/Volume) and plot cartography (DTM/Stem detection and location) for tree measurement. The Echidna Validation Instrument (EVI) built by CSIRO Australia was used by Yao et al., 2011, which is capable of retrieving forest stand structural parameters including DBH, density, basal area with good accuracy which were compared with the extensive ground measured data for validation. Kelbe & Romanczyk, 2012, have worked on automatic extraction of tree stem from single TLS scan, using algorithms as for DTM extraction morphological filtration and triangulation, for line fitting Principle Component Analysis (PCA), and for cylinder fitting via initial estimation (point

projection onto the vector orthogonal to the both eigenvector and vector to the origin) and optimization. The completeness and correctness of the estimated information is missing in the study, though from single scan tree parameter estimation is beneficial in cost-limited applications.

Schilling et al., 2012, have used principal curve computation method for retrieving trunk and branch curves for the obtaining the tree skeleton. The process is fast and robust to the noise also fills the data gaps, but during prior segmentation of the 3D points, large outliers caused for the improper segmentation with higher distance errors. Another study was carried out by (Hongyu Huang et al., 2015) wherein they have extracted the individual tree skeleton from a point cloud and estimated the different radii of the hierarchical skeleton of the individual tree, then using OpenGL rendering and bump texture mapping techniques they modelled the tree. In this project the authors have addressed a robust method to reconstruct the tree model which is useful when the sample is less. On the other hand the branches of the tree are not determined from the fitting of point data, the estimation was based on the child nodes of the main branches which may not be the true case.

2.3.5. Surface Reconstruction

Reconstruction of a surface needs to be matched with the original geometric and topological properties of the same object. The reconstruction output depends on the sampling of the data. The point cloud obtained through TLS usually has redundancies, noisiness especially in forestry inventories. Therefore, exact or even optimal surface reconstruction of the trees along the original curves of the shape is challenging (Cazals & Giesen, 2004). There are many surface reconstruction techniques as explained by Lim & Haron, 2012, wherein the methods are categorized in explicit surface which includes parametric surfaces methods such as B-spline surfaces, Triangulated surfaces then in implicit surface techniques such as least square, Poisson surface reconstruction etc., then computer vision techniques etc. In conclusion authors have suggested neural network as suitable for dealing with unorganized and non-uniform density data for surface reconstruction but in case of 3D surface reconstruction it is under question.

In case of Hough transform if the no. of parameters are more than three then the detection of primitives other than lines or circles needs to be done with care because if the parameters is large then the accumulator cell or bin containing more parameters in Hough space compare to its neighbouring bin is hard to find ("Hough Transform," 2015). Similar case is with RANSAC algorithm, the samples with even moderate outliers or noise, it performs inadequately (Hast & Nysjö, 2013). In a study by Moskal & Zheng, 2011, which was based on voxel data structure derived from TLS PCD showed an underestimate result in DBH and tree height when compared with the field based measurements. Another study was carried out by (Hongyu Huang et al., 2015) wherein they have extracted the individual tree skeleton from a point cloud and estimated the different radii of the hierarchical skeleton of the individual tree, then using OpenGL rendering and bump texture mapping techniques they modelled the tree. In this project the authors have addressed a robust method to reconstruct the tree model which is useful when the sample is less. On the

other hand the branches of the tree are not determined from the fitting of point data, the estimation was based on the child nodes of the main branches which may not be the true case. For detecting cylinders and its orientation in a point cloud Hough transform algorithm has been used by various authors. Su & Bethel, 2010, have used the same and concluded that if sample size is large, more will be the accuracy but at the cost of speed in terms of run time. Similar findings were highlighted by Rabbani & Heuvel, 2005, the geometric fitting problems in 3D the time and space complexity which could be represented as $sp-1n$ and sp respectively where n is the number of points, p is number of parameters and s is number of samples in Hough transform. As per Stewart, 1997, the RANSAC which is a robust algorithm for modelling gets limited to substantially discontinuous and irregular large datasets as it deals with neighbouring inliers proximity, which is usually handled by Hough transform but still the bin size adjustment is delicate to the noisy data, as cited in (Labatut et al., 2009). Therefore, to extract the tree parameters from point cloud obtained from TLS using defined primitives with higher parameters and redundancies in the data is a challenge. For some trees with variable shape Poisson's Surface Reconstruction approach has been used in this project. The Poisson Surface Reconstruction algorithm follows three steps mainly ("Poisson Surface Reconstruction," 2016):

1. Finding the tangential planes for approximation of the local planes, which is done by computing the centroid of the vertexes as the average of all the nearest neighbours. Then the eigenvector computes the corresponding normal.
2. Building Riemannian graph which required to include every nearest neighbours by creating structure for every vertex and edges.
3. Uses the minimum spanning tree algorithm which connects all the vertices together with the minimal total weighting for its edges.

3. STUDY AREA

In this chapter the significance of choosing the study area, an insight of the locational information is provided. Sections of this chapter explained about the geographical, topological information along with the details of the species of forest flora. The project has been carried out with the data acquired from Barkot forest area (78.160-78.280 E and 30.060-30.170 N) located at the Dehradun district of Uttarakhand state, India. It is a deciduous forest comprising Sal (*Shorea Robusta*), mixed forest and Teak plantations which are in dominance other than these the forest covers Chamror, Shagaun, Amaltash, Jamun etc. as well. It is located in subtropical region and covers around 11498.30 hectares with a reserved forest area of approximately 7120.40 Hectares. The study area is surrounded by Lachhiwala forest range from West, Thano range from North and Motichur range from South.

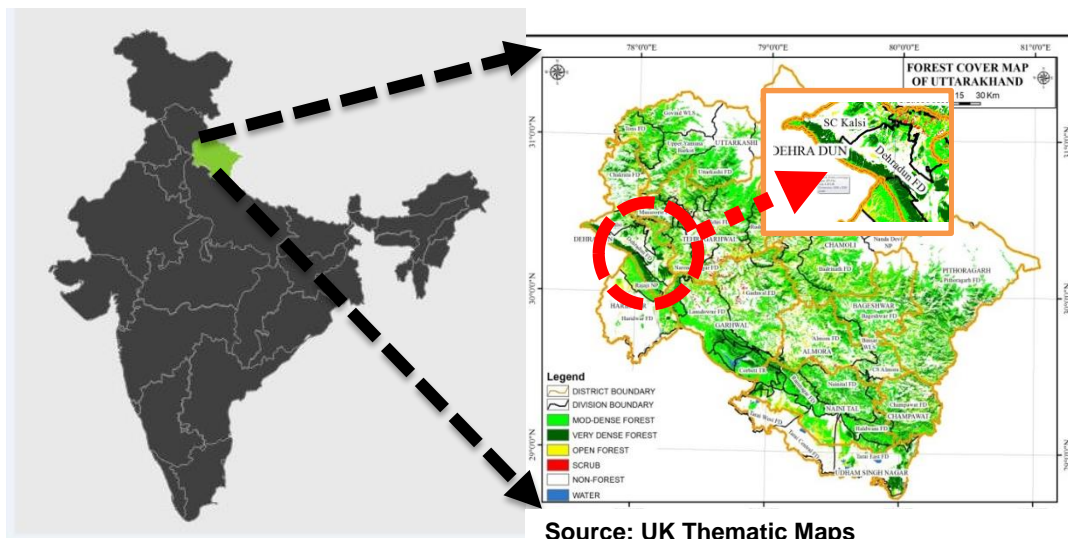


Figure 1: Study area location map

3.1. Significance of the study area

The location of the Barkot forest under the easy and accessible range makes it better choice for carrying the study. The principle objective of this study is to estimate tree parameters such as stem volume, basal area, diameter at breast height and tree height automatically using TLS based modelling. Therefore, the prime concern before data acquisition was to select the plot with minimal variation in terms of shape of the tree stems and species of the trees and sparse density. The site selected was comparatively with sparse tree density and is dominated with Sal (*Shorea Robusta*) trees which have stem shape more likely to the straight cylindrical shape. This provided an opportunity to get the adequate point cloud of the trees on the plots with minimal outlier and redundancies. At the initial stage in order to get the result two sites were selected. One at the IIRS campus in front of the guest house to get the point cloud of trees with varying shapes and

another plot was selected for data acquisition in the Barkot forest range in Doon valley. Since at the plot in Barkot forest there is an abundance of Sal (*Shorea Robusta*) trees, and the shape of the almost all trees were homogeneous, the automatic retrieval of tree height is less complicated compared to the plot at the IIRS campus.

3.2. Topography

The Barkot forest area is located at the foot hills of the lower Himalayan range in Uttarakhand state of India. It is bounded by the lesser Himalayan rocks in the north and Shivaliks in the west. Therefore most of the study area is relatively flat with gentle elevated topography with an average altitude of 340 m above the mean sea level. Hence, in the project the filtration for DTM extraction has been done using local thresholding.

4. METHODOLOGY

As per the objective of the project for retrieving the tree parameters, the data were acquired at three sites Barkot forest range and Thano forest range and one plot at the IIRS campus. Four datasets were acquired at said sites by using Terrestrial Laser Scanner (TLS). The post processing part of the methodology comprises the registration of the scans at each site individually followed by the removal of DTM and individual tree extractions. The retrieval of the tree parameters were carried out using algorithms based on mathematical explanations and derivations. In Figure:2 the flow of the whole project is mentioned, which have been elaborated in further sections.

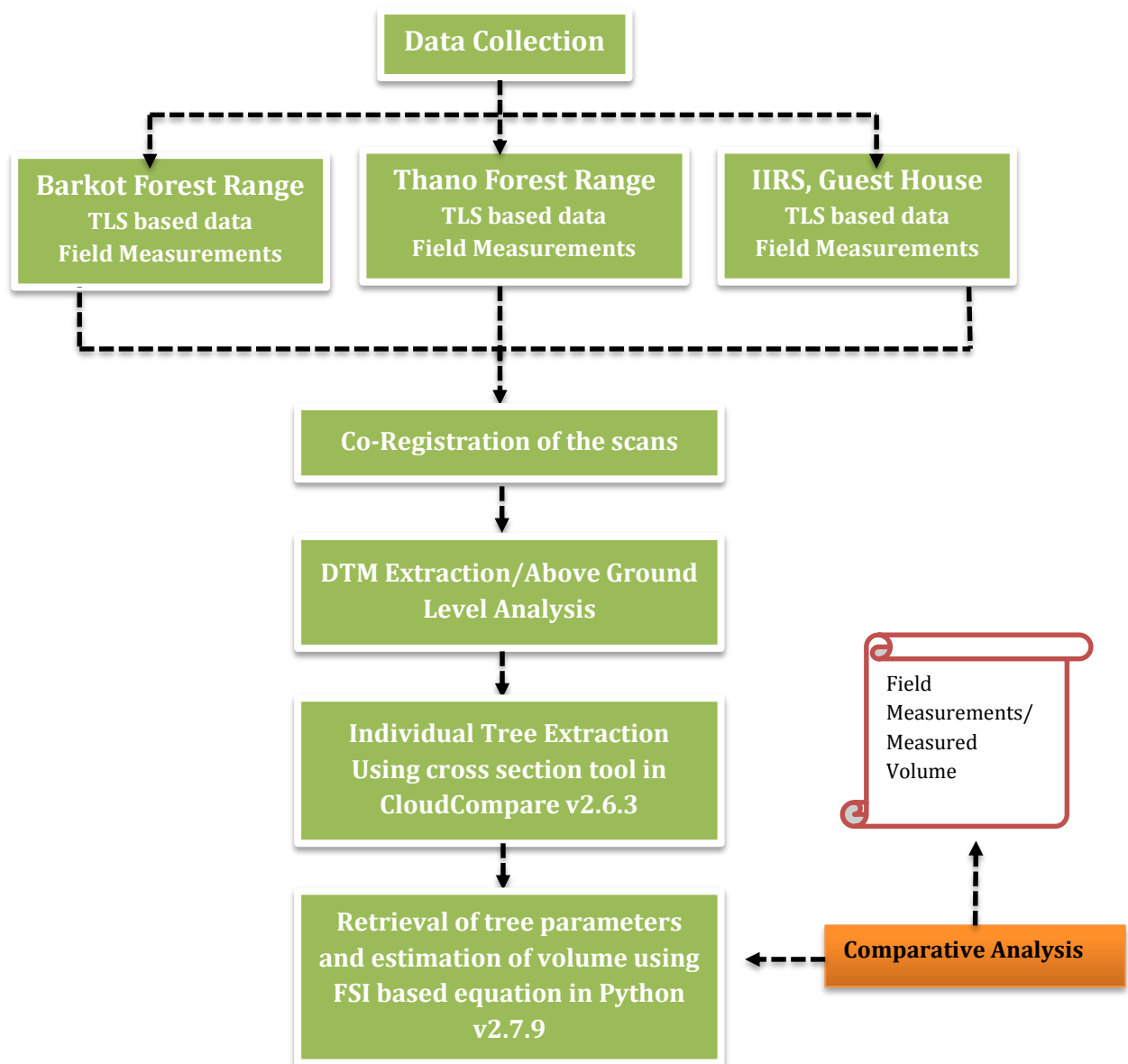


Figure 2: Methodology flowchart

4.1. Site Planning

To retrieve the tree parameters like tree height, DBH and then estimation of the volume, plot wise and individual tree wise is the main objective of the project. At the initial stage the site selected at the Barkot forest area near the flux tower in Dehradun. The plot was dominating with the straight Sal (*Shorea Robusta*) trees with very less variation in terms of shape and size. Another plot was taken at the IIRS campus, where in front of the Guest house few trees are located with variations in tree stems. The idea behind considering the tree shape variation is to check the potential of the algorithm in order to retrieve the tree parameters and its validation. Later stage two more data sets from Thano forest range were acquired, which are comparatively denser including low lying shrubs at the sites. The data was acquired using Terrestrial laser scanner (TLS) and field measurements using Forestry pro – range finder for height measurement and measuring tape for the DBH measurement. The whole process was divided into four phases, first phase was to acquire the data from multiple scanning position on each plot in order to get the completeness of the tree point cloud, second phase was to register the point clouds, third phase to determine the tree parameters automatically and the last phase was to do the comparative analysis among the automatically obtained and field measured parameters.

4.2. TLS Based Data Acquisition

As mentioned above the data acquisition was carried out in the Barkot forest area, IIRS Campus in front of the guest house and Thano Forest range in the month of November 2015 and January 2016. The plot size of 31.6mX31.6m at Barkot and Thano forest ranges and 16.85m X 16m at IIRS were selected for data acquisition. As in the first step the demarcation of the plot was done using the magnetic compass. The intension was to mark the first side at the north direction and accordingly the other sides were demarcated. Another deliberate intension was to take at least one side along the road side. The second step was to locate and fix the circular reflector position within the plot in such a way so that it could be visible from all five scanner positions marked at the corners and centre and well distributed at the plot. In this project only three circular reflectors were available which were used, strip reflectors at least on four corner trees. To validate the modelled tree parameters field measurements were taken using Laser range finder (Forest Pro – Range Finder) for height estimation and measuring tapes for DBH measurements. For identification of the trees the maximum trees were labelled with numbers made up of retro-reflectors. The scanning positions were decided on the basis of field observation considering optimum visual ranges with minimum occlusion. The plot descriptions for the plots are shown below:

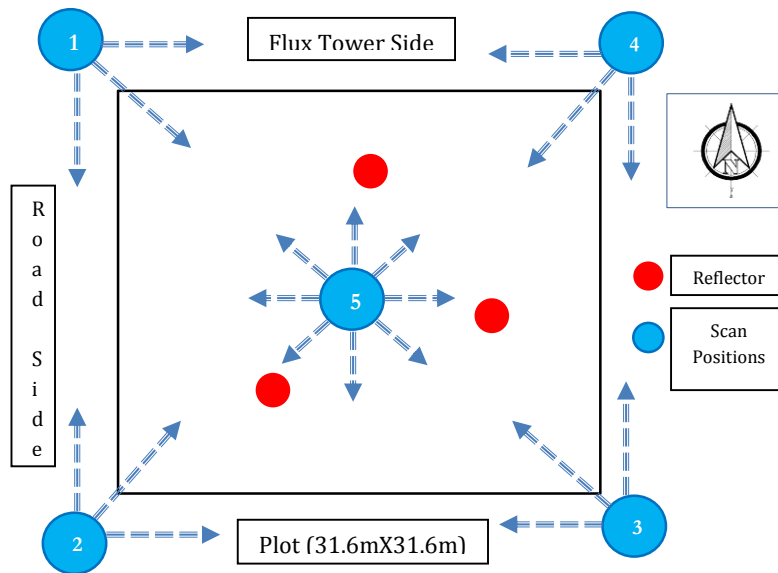


Figure 3: Plot measurements and data acquisition plan – Barkot forest area, Dehradun

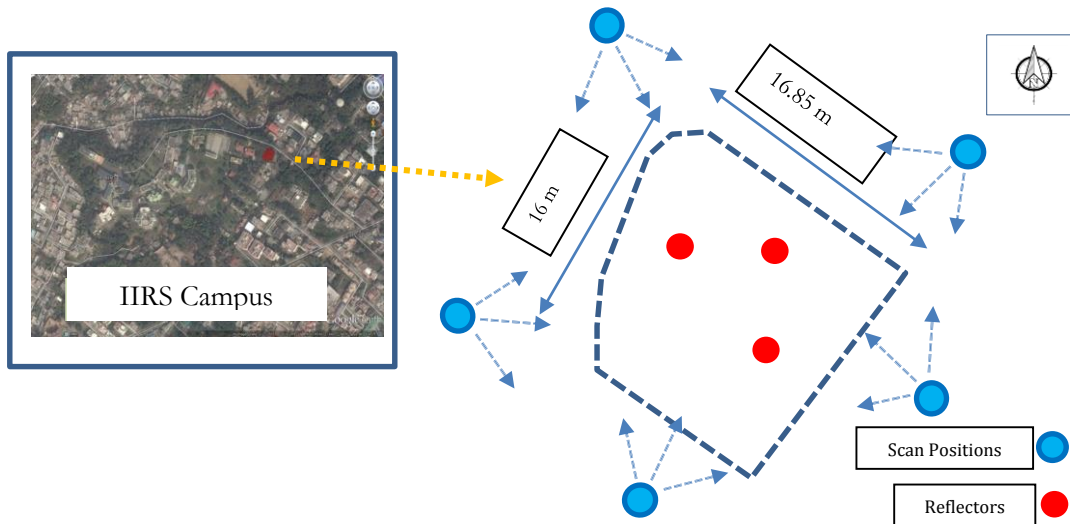


Figure 4: Plot measurements and data acquisition plan – Guest house garden, IIRS Campus, Dehradun

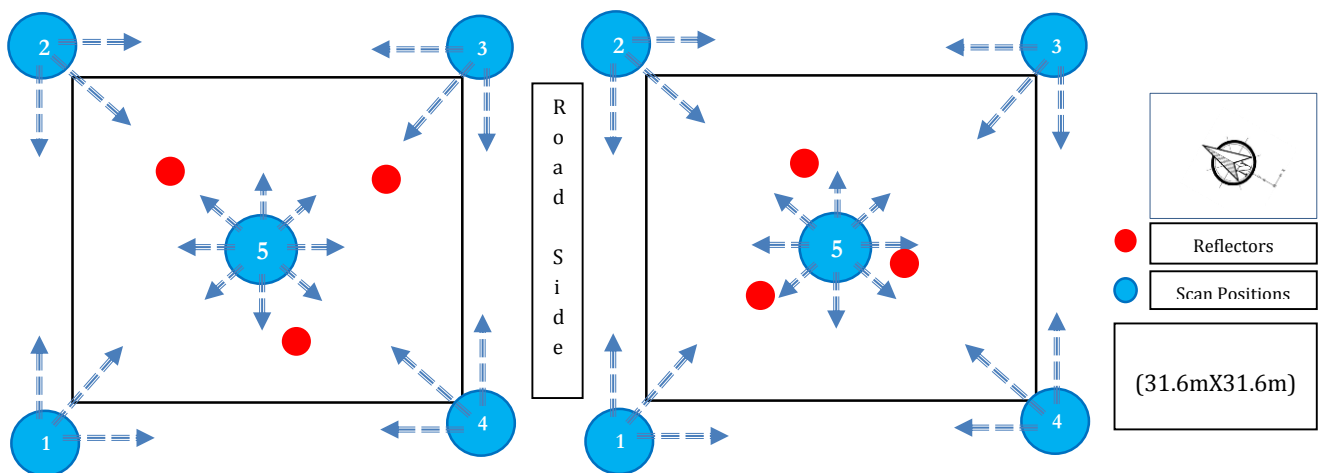


Figure 5: Plot measurements and data acquisition plan – Thano Forest Range, Dehradun

4.2.1. Terrestrial Laser Scanner settings

In this project RIEGL VZ-400 V-Line 3D Terrestrial Laser Scanner (TLS) was used. It provides the data acquisition with 5 mm accuracy/3 mm repeatability. The range is up to 600 m with an efficient measurement rate up to 122,000 measurements/Sec. The field of view range varies from 0° to 100° vertically and 0° to 360° horizontally. The vertical and horizontal resolution range provided from 0.0024 to 0.288 and 0.0024 to 0.50 respectively. For this project the angular resolution was set up to 0.03 mrad for both vertical and horizontal direction because the point density for each scan is coming around 4-5 points/cm² if the range of the scanner is set up to the 5 m from the first object. The field of view was set 30° to 130° vertically and 0° to 90° - 110° at the corners and 0° to 360° horizontally at the centres at both Barkot and Thano forest range. At IIRS campus the angular resolution and vertical field of view was same but the horizontal field of view was set up to 0° to 100° at all five positions around the plot. The scanner positions were decided as per the variation and field of view at each site. The intention was to set up the scanner at such position from where the minimum distance from the first object is 3-5 m at least.

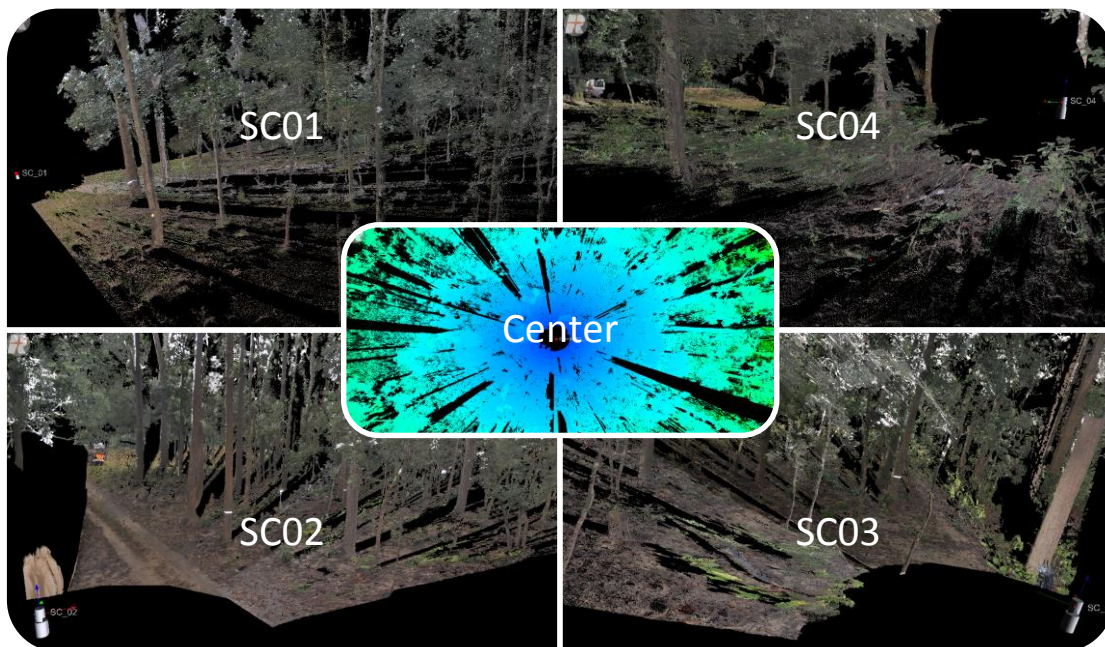


Figure 6: Views of all five scans on the plot in Barkot forest area



Figure 7: Views of all five scans along the plot at Guest House, IIRS Campus

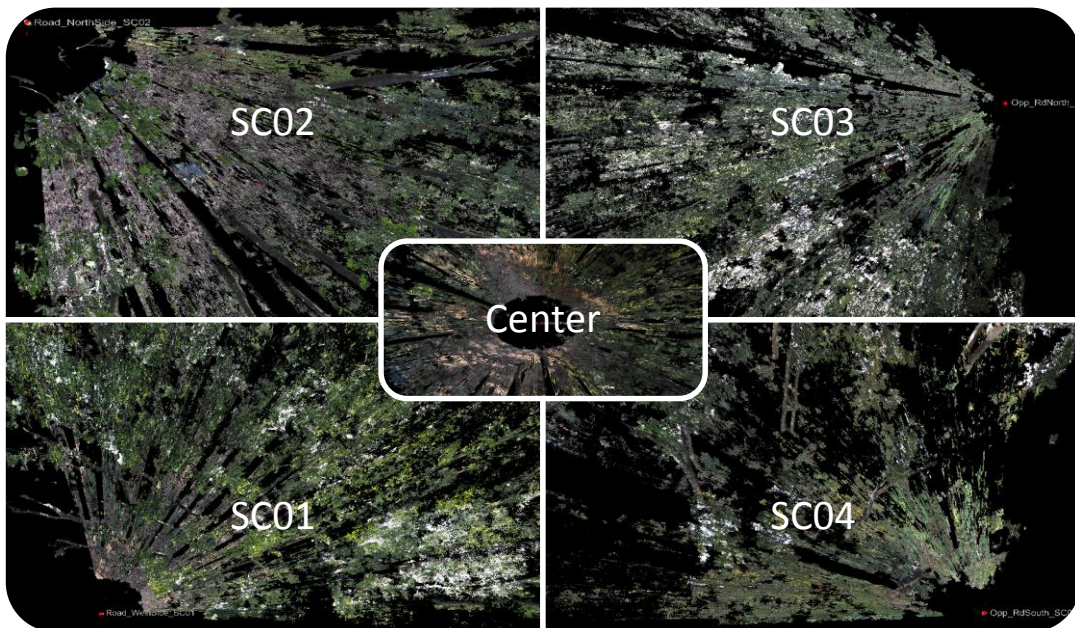


Figure 8: Views of all five scans on the plot in Thano forest area-1

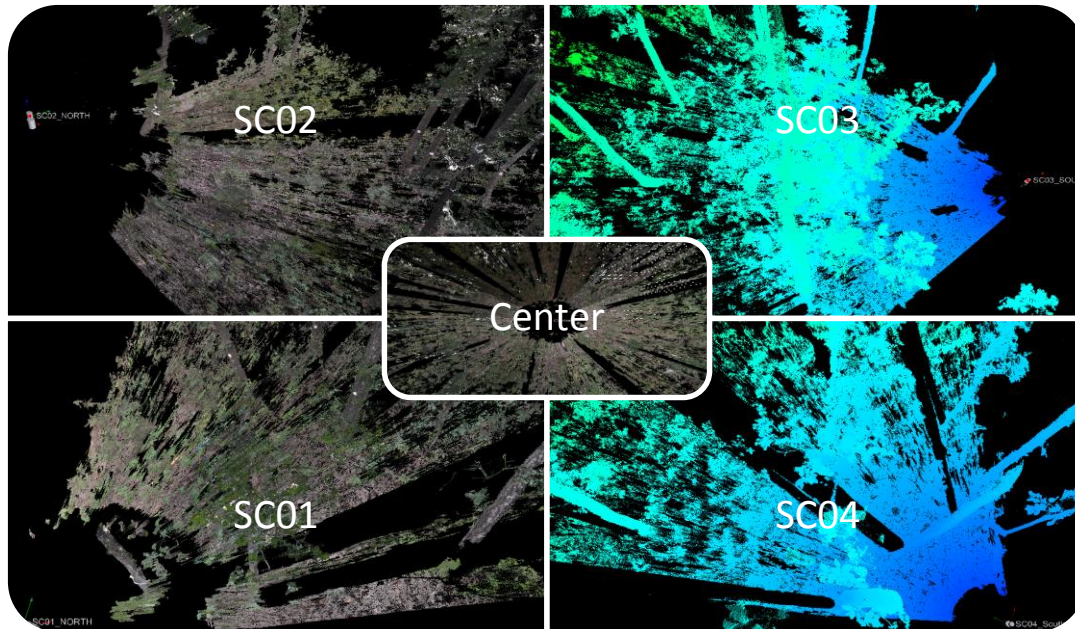


Figure 9: Views of all five scans on the plot in Thano forest area-2

4.3. Field Based Measurements:

During the TLS based data acquisition the field measurements took place. For measuring the height of the trees Nikon Forestry Pro Laser Rangefinder was used and simple measuring tape was used to measure the circumference of the trees. The Forestry Pro can measure the actual distance from the object under observation. It can act as a clinometer to give us the measurements of height, angle, and vertical separation. In this project the vertical separation mode was used to measure the tree height (Figure 10). In the height mode we have to target at the bottom of the tree and then at the top of the canopy which gives the distance between these two targeted points. The photographs of field inventory are provided in Appendix E.

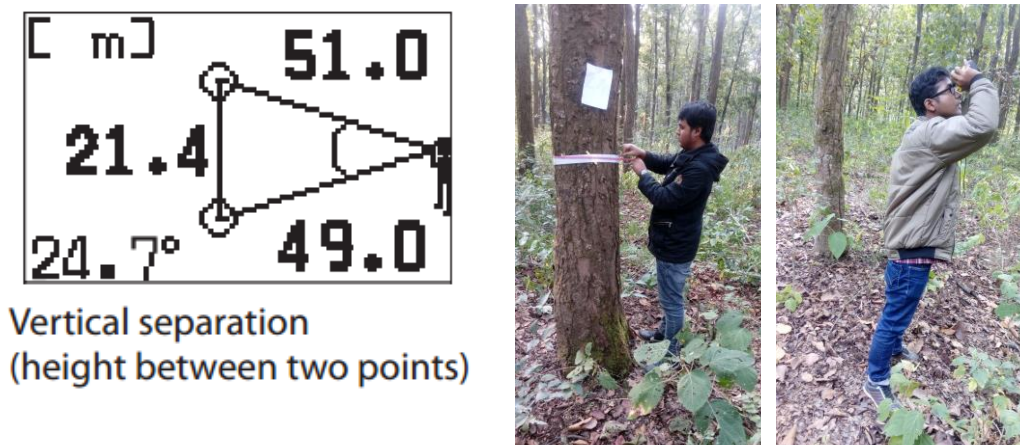


Figure 10: Vertical Separation mode as explained in (Forestry-Suppliers, 2016) and field measurements using Forestry Pro and measuring tape.

4.3.1. Multiple Measurements:

For each and every tree parameter 10-10 measurements were taken in order to get the idea about the uncertainty in the field measurements. In the next chapter a comparative analysis has been done between the error in the field based measurements and the error between modelled and measured parameters. A Performa for data entry has been filled during the survey as shown below:

		Field measurements at Thano Forest Range: Plot-I										
		Measurements										
S. No.	Tree Name	Parameters	M1	M2	M3	M4	M5	M6	M7	M8	M9	M10
270	TT1-1	Height	10	10.6	10.6	10.5	10.5	11	10.5	10.6	10.6	10.6
		Circumference	67	68	68.5	68	69	68	68	68.5	68.5	68
223	TT1-2	Height	16	17	16.8	16.8	16.5	16	16	16.5	16.8	16.5
		Circumference	100.5	101	100.5	100.5	100.5	100.5	100.5	101	100.5	100.5
472	TT1-3	Height	7.6	7.6	7.6	7.6	7.6	7.6	7.6	7.6	7.6	7.6
		Circumference	100.5	100	100	100	100	100	100	100.5	100	100.5
35	TT1-4	Height	19	19	19.0	19.0	19.0	19.0	19	19.0	19.0	19.0
		Circumference	137	137.5	136	137	138	137	136	136	136	136
44	TT1-5	Height	15	15	15.0	15.0	15.0	15.0	15.0	15.0	15.0	15.0
		Circumference	130	129.5	130	130	130	130	130	130	130	130
89	TT1-6	Height	17	18	17.8	18.5	18	18	17.8	17.8	18	17.6
		Circumference	96	96.5	92.5	92	92	91.5	92	92.5	92	91.1

Figure 11: Survey Performa

These measurements were taken for calculating the standard error and then the uncertainty in the measurements. Uncertainty in the measurements could be estimated by calculating the standard error in the sampling, which is as follows: $StandardError = \frac{StandardDeviation}{\sqrt{No.ofSamples}}$ and the mean values of all the measurements.

$$Uncertaintyinsampling = \left(\frac{StandardError}{Meanofthesamples} \right) 100$$

4.4. Post processing the data

The acquisition process was carried out with the package software of the RIEGL VZ-400 which is called as the RiSCAN PRO. It has the property of creating a project in which it stores all the scans along with the images taken during the scans and fine scans of the tie points. In RiSCAN PRO it uses different coordinate systems. Scanner's Own Coordinate System (SOCS) which delivers the raw data and generates a coordinate system with respect to each and every scanner positions to get geometric information. Project Coordinate System (PRCS) which generated after the registration a common coordinate system of the whole project. Global Coordinate System (GLCS) is used when the Ground Control Points (GCP's) are obtained through GPS and imported to the project, but in this project GLCS has not been used because the GCP's were not collected at the field. The registration process can be done by two main process, coarser and fine registration. In this project the registration has been done by considering SOCS of one scan as reference coordinate system and finding out the corresponding points which are tie points on the other consecutive scans. Once the points from different scans are found a new tie point in the PRCS is generated. All affected SOCS of different scans linked with the newly generated PRCS and the coordinates of the PRCS are the calculated or averaged of all SOCS tie points. The same step has been repeated for all other scans to acquire one final

coordinate system which is called as PRCS. The scans were exported as per the supporting format for Cloud Compare freeware software, where merging, clipping, filtration, individual tree extraction and quality assessment has been carried out.

4.4.1. Co-Registration of the point clouds

Each scan position has its SOCS, which are to be transformed in one common reference system. To do so the tie points (circular reflectors) which were static during all scanning process, obtained from fine scans were taken into the account. Since, the centroid of the circular reflectors remains at one position even if the direction of the reflectors been changed during scans, three centroids of the circular reflector were the basis for co-registration of all the scans. The first step is to open TPL (Tie Point List) SOCS of the two scans, the tie points other than circular reflectors have been removed from the list. Finding corresponding points of one scan by keeping it as unregistered, with respect to the referenced scan, gives the linked points as PRCS. Before, finding corresponding points the three available fine scan tie points were renamed into same in both the scans manually. The same process was carried out for remaining scans as well for co-registration of the project scans. This could be done manually as well, using coarse registration/GCP's/multi-station adjustment etc. (3D Laser Mapping Ltd., 2016). But in our case picking common points in a forest area other than known points is difficult. Therefore, only three tie points obtained from fine scans were used to do coarser registration in order to prepare for multi-station adjustment in the next stage for improving the registration quality. These registered scans were exported in ASCII format for the Cloud Compare application for further processing. The individual tree extractions etc. were done in CloudCompare v2.6.3 beta version. The 3D view of the registered point cloud is shown as below (Figure 12):



Figure 12: A 3D view of the plot at Barkot forest areas after registration

4.4.1.1. Registration quality

Since the ground control points are not available in the project, tie points from the circular reflector which were obtained from the fine scans, were used for the registration of the scans. The central scan position was considered as the reference scan, selected as the registered and other scans were co-registered by identifying the corresponding tie points in the referenced scan. The algorithm tries to find corresponding points between the current TPL SOCS and the selected coordinate systems. If correspondences between points of different scan positions are found, a new tie point in the TPL PRCS is created and all affected SOCS tie points are linked to this PRCS tie point. The coordinates of the PRCS tie point are calculated (averaged) from all linked SOCS tie points. The tolerance value which is the search radius within which points are to be recognized as corresponding was fixed with 0.2 m and minimum point pairs were fixed as 3 as only three tie points were available. RiSCAN PRO gives a standard registration process based on the finding corresponding tie-points obtained via fine scans. Though the tie points considered are from the centroid of the circular reflectors only, but misalignment in the scans might occur in the project as each scan is been registered with respect to the direct predecessor, so at the end of the registration process the propagated error may be huge. Therefore, the process of Multi Station Adjustment (MSA) is essentially required to check the registration quality along with the alignment of the scans. For doing so two main methods are there:

- ✓ Manual definition of corresponding plane surface patches: It comprises the corresponding planes and overlapping part of the surface of the point clouds which are to be registered together. MSA tries to minimize the distance between the defined planes
- ✓ Automatic search for corresponding points using Iterated Closet Points (ICP) algorithm: The automatic determination of the corresponding points by detecting the closest point in one point cloud with respect to the other.

In this project Iterated Closest Points (ICP) algorithm (Mitra et al., 2004) has been used to do the MSA. For filtration the Plane path filter option was used, it searches for plane patches in the point cloud. The algorithm behind the process is as followed:

- ✓ Divides point cloud into several equal sized cubes of certain size.
- ✓ Estimates the best fit plane inside the cube
- ✓ Standard deviation of the normal distances between all points and the plane is less than "Maximum plane error" then the plane is added to the resulting list of plane patches.
- ✓ If the above condition is not fulfilled, the cube's points are divided into 8 smaller cubes, each having the half edge length of the current cube.
- ✓ For each sub cube the plane estimation as described above is repeated.
- ✓ The repetition is stopped when either a valid plane was found, the number of points inside a cube drops below "Minimum number of points per plane" or the cube size (edge length) drops below "Minimum search cube size".

- ✓ For each plane patch found, the centre of gravity of its points and the normal vector are stored in a new point cloud in the "POLYDATA" folder of the scan position.

The plane patch filter settings such as maximum plane error were 0.02, minimum numbers of points per plane were 5 and minimum search cube was fixed as 0.128. These settings are good enough in terms of time and accuracy (C. R. Kennedy, 2015a). The MSA has been carried out for all the scans for each site. The central scans have been considered as the reference point cloud. The adjustment iteratively modifies the position and orientation of the scans with reference to the scan which is locked, in our case it is the central scan. The description of the parameters and process definitions are taken from the documentation of the RiSCAN PRO help which are explained below:

- ✓ Adjustments Parameters:

1. **Using tie points, tie objects and polydata:** Since in the project no GCP's were taken, so instead of using GCP's as tie points, the created polydata for all scans, obtained after applying plane patch filter were used.
2. **Nearest point search:** It searches for nearest points of a point in other datasets, and the search radius is defined before searching corresponding points, along with adjusting Max. tilt angle in order to restrict wrong pairing. As explained above the filtration process, each point represents a plane has its surface normal, if the angle between surface normal of two planes are smaller than the max tilt angle then both planes will be considered as the corresponding planes.
3. **Adjustment:** The iteration process for the adjustment stops when the change in the error is less than the set minimum error which was 0.01 m for the first iteration (C. R. Kennedy, 2015b). As below this range the computing time is uncertain as the pairs of polydata objects would be higher. After reaching minimum change of error, the outliers are removed from the list of corresponding points. The distances higher than the threshold outlier distance are removed from the list of polydata objects which is needed in order to reduce computation time in the next iteration.
4. **Error:** The standard deviation of the distances between all tie-points, polydata, tie-objects. In this project polydata has been used whereas the distance between pairs of polydata objects is the average distance of the normal distance from the corresponding planes.

Three iterations were carried out in MSA. Initially the search radius was large with min change in error as 10 cm. Then the values for next iterations were narrowed down in order to reduce error. After first iteration the corresponding point pairs were considered for next iteration by removing the the point pairs with larger distances than the threshold distance which was 2 m for first iterations (Figure 12) and 1 in the last iteration (Figure 14). All mentioned parameters were taken as per the suggestion given by C. R. Kennedy, 2015c, as the parameters were reduced in a trial but the computation time was uncertain, then it was cancelled and suggested parameters were chosen. 63 million points were there after clipping and merging the scans at the Barkot forest area, out of which 0.6 million polydata were taken in first iteration with an error of 0.39 m. In

the second iteration the 0.47 million polydata with an error of 0.37 m and in the last iteration 0.08 million polydata with an error of 0.06 m, which is quite good adjustments of the scans. In below figures the histogram shows the normal distribution of errors and the up there is the polar plot which shows the distribution of the overlapped planes. Polar plot basically shows, how spreaded the overlapping planes are in the point clouds and in the histogram the dark red colours shows the best align or overlapped planes. So if we look at the result of 1st and 2nd iterations in both Barkot (Figure 13, 14) and Thano datasets (Figure 16, 17) the overlapped planes are not very well distributed but in 3rd iteration for Barkot (Figure 15) it took around 78 thousand overlapping planes with the St. Deviation (Error) of 0.065 m and for Thano (Figure 18) it is the overlapping planes around 73 thousand with an error of 0.063 m, which is quite good adjustment in the registration of the point clouds. The polar plots for other two datasets are attached in Appendix-F

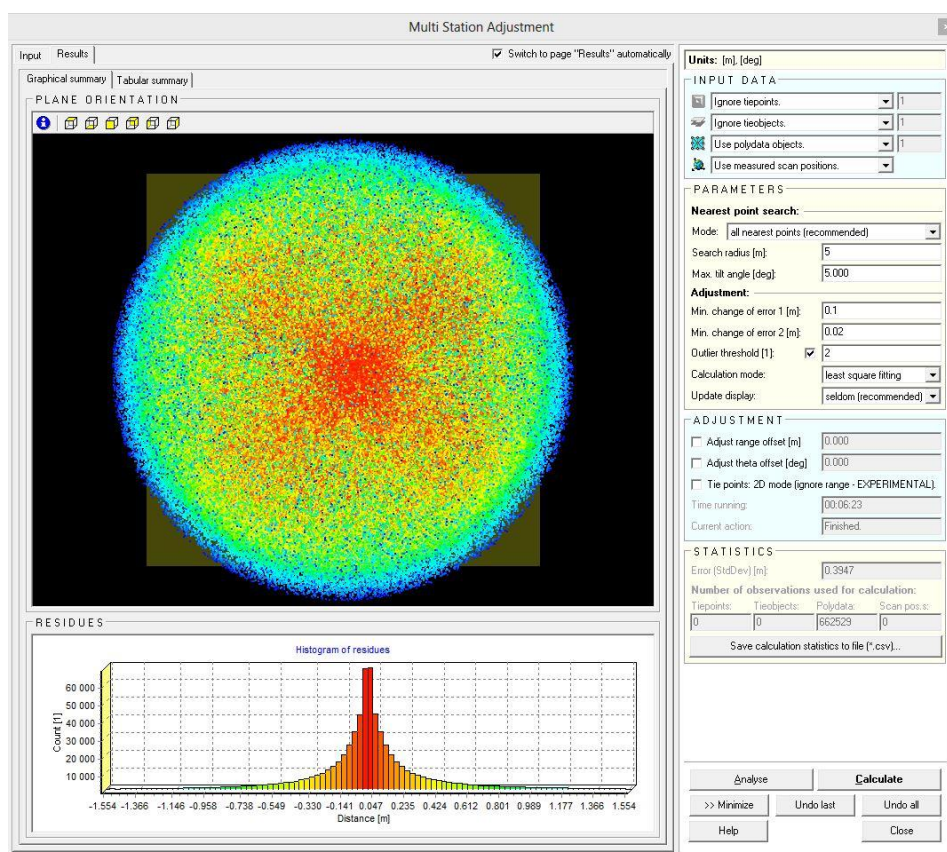


Figure 13: Adjustment after first Iteration: Barkot Forest

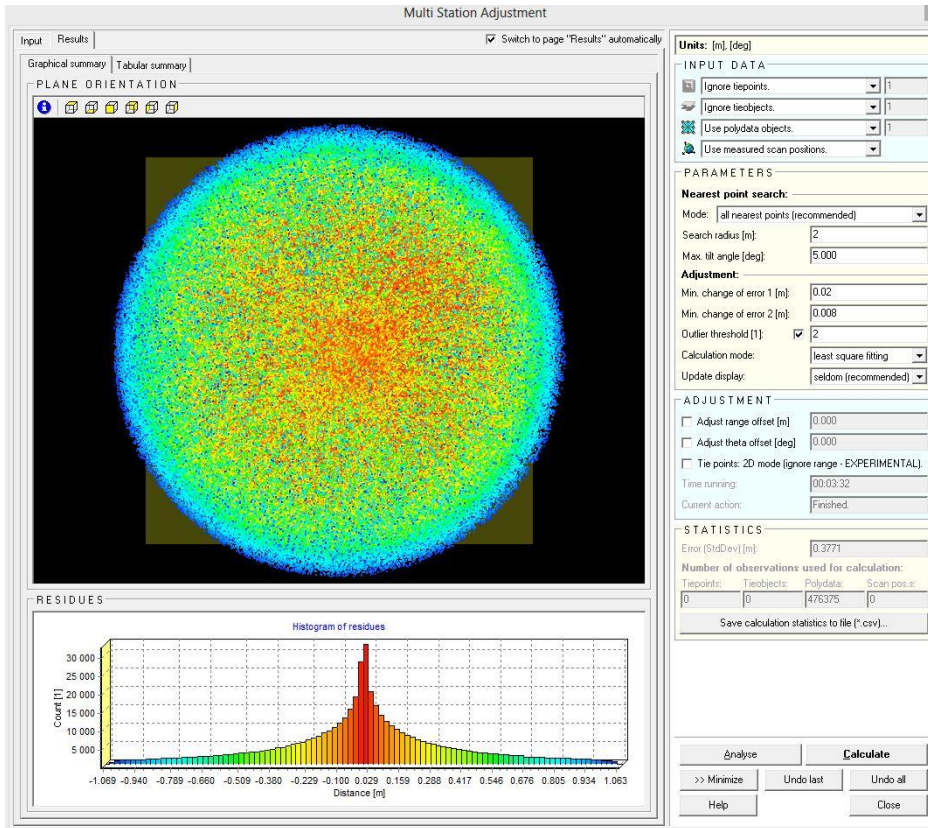


Figure 14: Adjustment after second Iteration: Barkot Forest

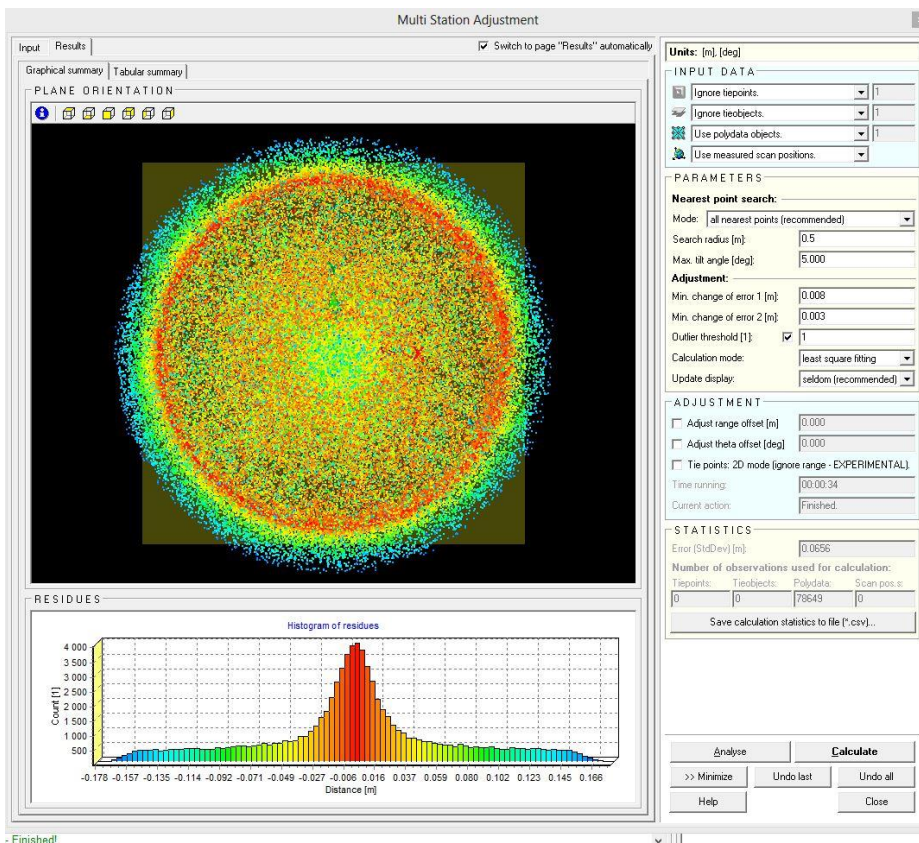


Figure 15: Adjustment after third Iteration: Barkot Forest

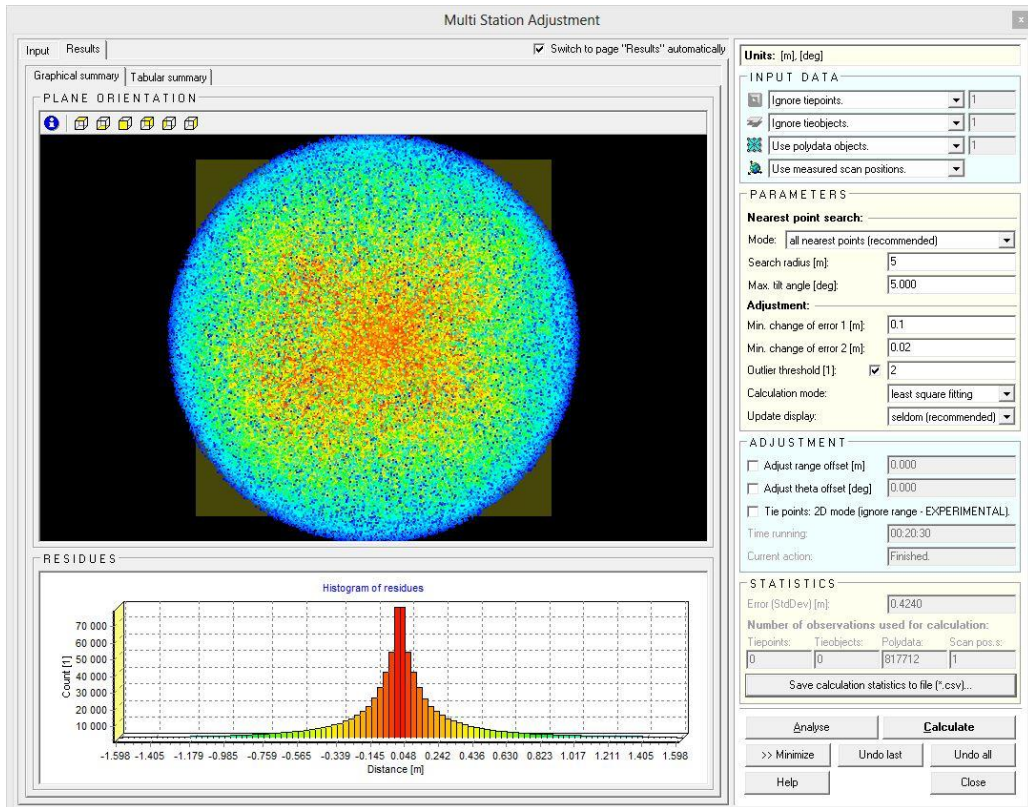


Figure 16: Adjustment after first Iteration: Thano Forest (Dataset-1)

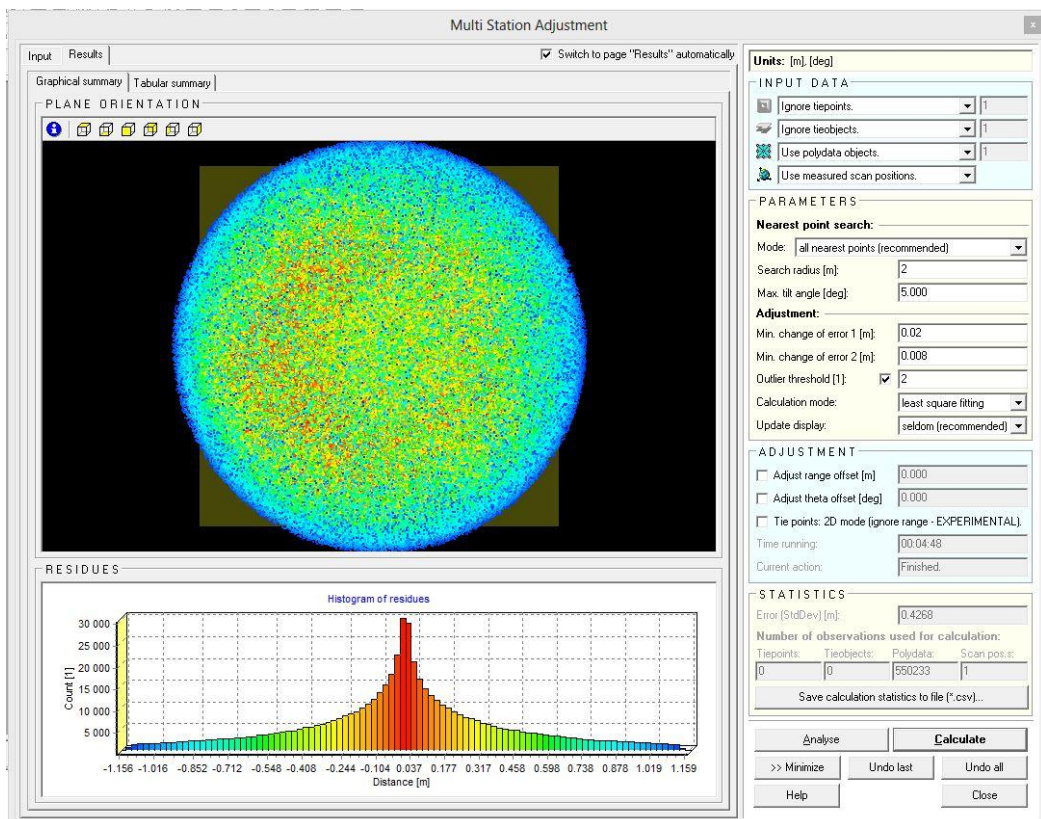


Figure 17: Adjustment after second Iteration: Thano Forest (Dataset-1)

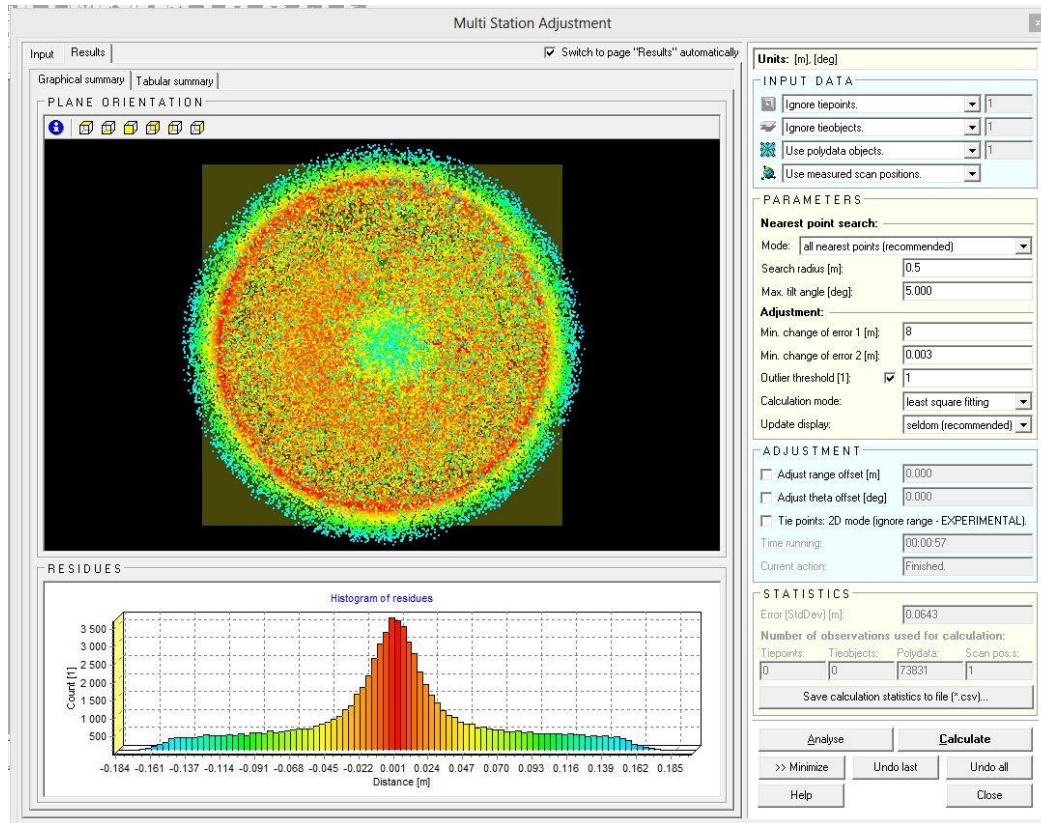


Figure 18: Adjustment after third Iteration: Thano Forest (Dataset-1)

Similarly in case of first dataset in the Thano forest area the considered polydata varied from 0.8 million to 0.07 million with error reduction from 0.42 m to 0.06 m. In second dataset it was 0.5 million to 0.04 million and error reduction from 0.5 m to 0.06 m. The polydata variation in case of IIRS site was from 0.3 million to 0.04 million and reduction in error was from 0.27 m to 0.07 m. The red colour in the polar plot and normal distribution shows the most overlapping planes at each and every iteration. Some 3D views of the trees and process has been attached in Appendix D.

4.4.2. Individual tree extraction

The extraction of the Digital Terrain Model (DTM) and point cloud of the individual tree was carried out manually using cross-section tool available in the CloudCompare v2.6.3 beta version. The sites were chosen at the Barkot and Thano forest range, located in the valleys of Dehradun as explained in Chapter-2. The topography here is varying comparatively with plane areas. The bushes and shrubs especially in Thano forest was found abundantly. Therefore, the filtration algorithms as used by Guarnieri et al., 2009 or Lau et al., 2015, and many other as in (Sithole, 2005) were not used. The first step was to divide whole plot into several patches using cross-section tool in CloudCompare, then by manually identifying tree were extracted. Once the tree point cloud was obtained the above ground tree point clouds were segmented out individually using cross section and segment tools available in the CloudCompare (Figure 19). The outliers such as from the bushes canopies of neighbouring trees etc. were removed using Octree filtration at the later stage.

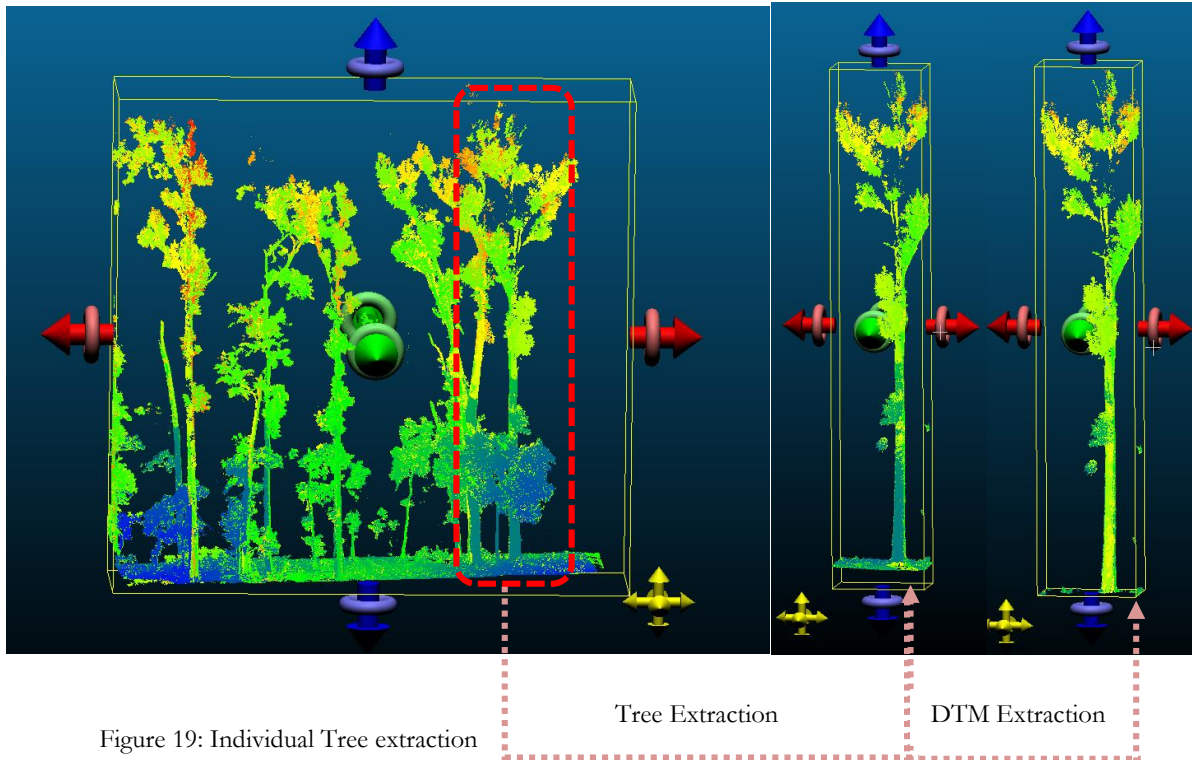


Figure 19: Individual Tree extraction

4.4.3. Removal of outliers

As explained earlier the plot at the Barkot forest was comparatively cleaner than the plots at Thano forest range. Due to the presence of the long and dense bushes the point cloud has the outliers, which were removed using filtration tool available in the CloudCompare application.

4.4.3.1. Connected Component:

For connecting the neighbouring points along with assigning the segment number is the main aim of using connected component analysis. It starts with selecting the seed point inside the object point cloud, then the set of points which are connected to this seed point with a distance smaller than some fixed threshold value are labelled as one connected component (Figure 20). This approach of analysis gives a better result when the object density is higher and the clusters are well separated from each other (Barbakh et al., 2009). But the problem occurs while establishing a global threshold value for a wide range of objects with varying point densities because the adequate distance threshold is hard to take, which results unwanted connected components sometimes (Pratihast, 2010).

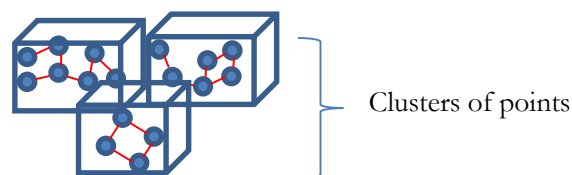


Figure 20: Three components example

4.4.3.2. Octree 3-D grid

The octree is a 3D data structure which has eight children, which are responsible for subdivision of the 3D dimensional space into eight octants recursively. The octree depth levels generates further eight octants from each and every node, wherever the node satisfies the threshold (Su et al., 2016) as shown in figure 21. The threshold value represents the minimum no. of points that a child node comprises. In this project the octree level was set up to the 8 and minimum number of points under each subgroup was set up to 10 that means the data structure will continue the search until all the subgroups contains minimum 10 points in it and will stops when it is lesser than the threshold (Figure 22).

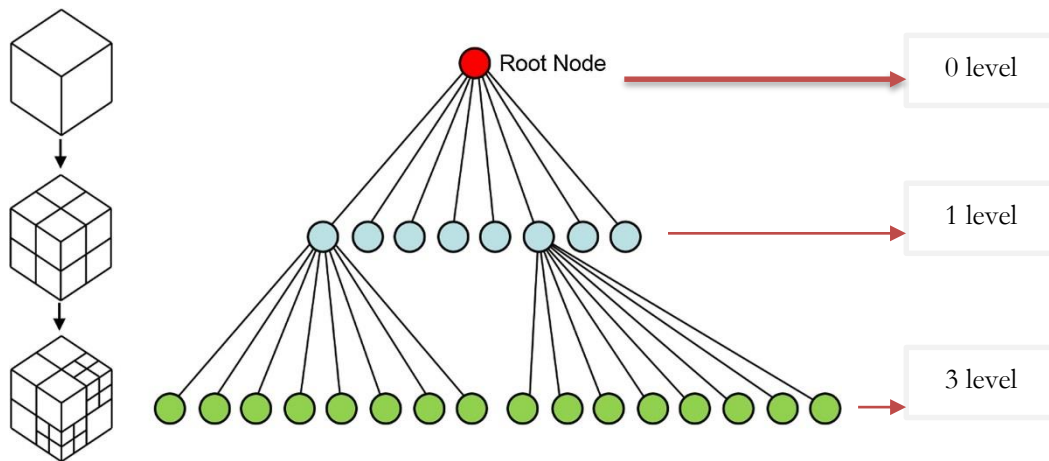


Figure 21: Octree illustration

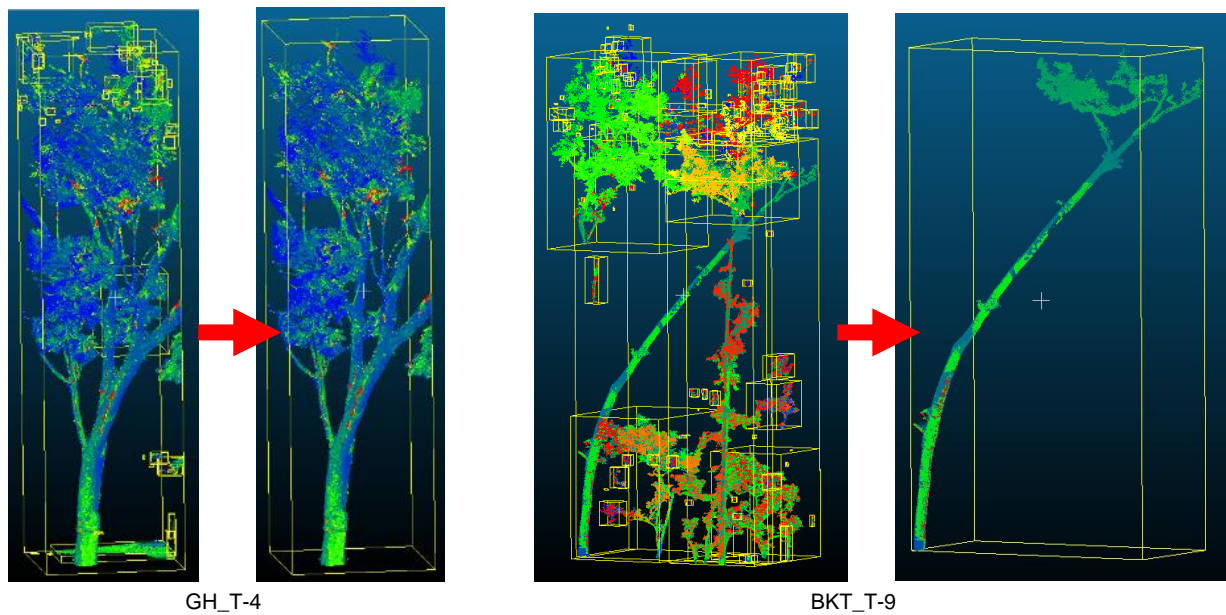


Figure 22: The removal of outliers using connected component analysis

4.5. Modelling of tree for parameters retrieval

The individual tree was extracted from the plot and exported into the ASCII format wherein, the locational information of each and every points are there. An algorithm was developed and implemented to retrieve the tree parameters. The estimation of height could be easier if trees are straight without any tilt vertically. The difference between the points with highest and lowest 'z' coordinate value (as per PRCS) could be the height and similarly a list of points around the cross section at breast height could give us the diameter. But if trees are tilted then the said method would not be the appropriate. Therefore, in order to get the length of the tree also the exact breast height length along the tree stem the retrieval of tilt angle of the trees was considered. The Steps that were followed for obtaining the tilt angle along with the tree parameters are as follows with respect to the Figure 24 (a, b):

- | | |
|----------------------|--|
| Initial Steps | 1. Input point cloud files
2. Get coordinates list from point cloud file |
| Tree Height | 3. Get the two points with maximum and minimum 'z' coordinate.
4. Calculate the distance between these two points which will be the length/height of the tree.
5. Assume breast height = 1.37m
6. Taking list of points at 'z'min+1m to determine the midpoint of the cross section bounded by the listed points (the list could be extracted at any height in our case it is 1 m).
7. Calculate the midpoint of the farthest points on this cross section say A(x1, y1, 'z'min+1)
8. Taking the list of points with 'z'min coordinates (cross section of the bottom of tree stem).
9. Calculate midpoint of the farthest points on this cross section say B having (x2, y2, 'z'min)
10. Calculate distance AB
11. In ΔABC Get tilted angle of tree with $\sin(\Theta) = 1/AB$ (C is the point on the ground so that AC is perpendicular on the horizontal plane (Figure 23 a) |
| Tree DBH | 12. Assume another point(P) on line AB of the tree at 1.37m from point A and O is the point on the ground such that PO is perpendicular to horizontal plane.
13. Calculate the perpendicular distance PO from this point with same eq.. $\sin(\Theta) = PO/1.37$ this gives us 'z'min+PO which is 'z' coordinate at breast height.
14. Taking the list of points on the cross section of the stem at breast height.
15. Calculate distance between all the points from one point.
16. Get the points coordinates which is giving maximum distance.
17. This maximum distance is the gives us the diameter of the tree 'D=DBH' |
| Tree Volume | 18. Use diameter calculated in previous step to calculate volume
19. Volume= $0.0308585 - 0.77794D + 8.42051D^2 + 5.91067D^3$ |

4.5.1. Tree Height

At Barkot forest area Sal (*Shorea Robusta*) trees are dominance in the area. It is found that the shape of the Sal (*Shorea Robusta*) trees in the study are not very much varying. However, some of the trees are tilted (Figure 23) and bended. Usually if trees are straight then the height of the tree could be measures as $H = \text{distance}(\text{Point with } Z_{\max} - \text{Point with } Z_{\min})$, where H is tree height and Z is the vertical coordinates of the points. But in case of tilted or bended trees this will not work. Therefore, for this project the height of the trees are estimated by using the distance formula.

$$H = \sqrt{(X_2 - X_1)^2 + (Y_2 - Y_1)^2 + (Z_2 - Z_1)^2}$$

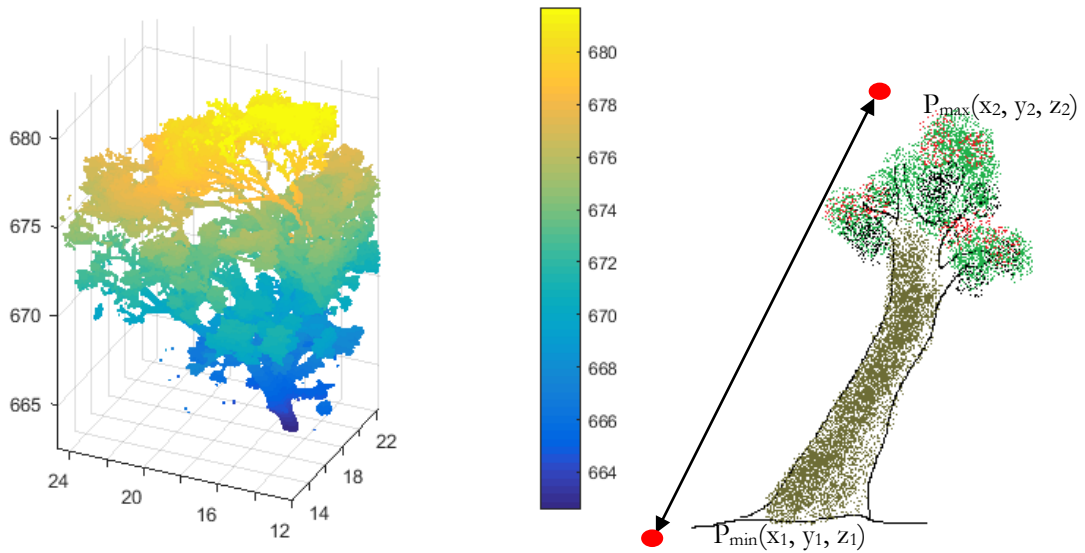


Figure 23: Tilted tree height calculation

4.5.2. Diameter at Breast Height (DBH)

Measuring diameter at breast height is a real challenge. If tree is straight then again using the same algorithm the point cloud above 1.37 m could be removed to identify the circular point cloud on the cross section of the remaining stem point cloud. But what if the tree is tilted? In order to resolve this as per the field observation and on the basis of few measurements of the circumference of the tree stem at different heights, it has been found that within the length of 50 cm of stem log, there is negligible variation in the shape. Therefore, the assumption has been made that the cross section of the log within this range would not change much. However, if any significant difference comes up then even, the impact on overall uncertainty in the volume at the plot level will not be significant.

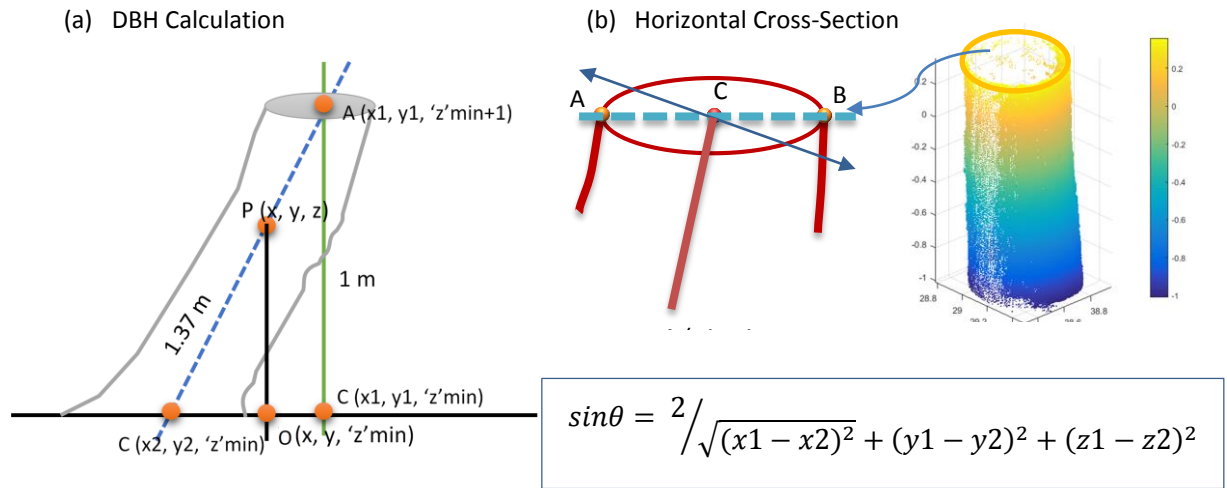


Figure 24: (a, b) Diameter estimation

Let (x, y, z) be the coordinate of the point 'P' of the cross section on the axis at 1.37 m

In triangle AOP

$$\sin\theta = \frac{z - 'z'min}{1.37}$$

$$z - 'z'min = 1.37 * \sin\theta \Rightarrow z = 1.37 * \sin\theta + 'z'min$$

Now we know the 'z' coordinate of the point on the cross section of the stem at which the length is measuring as 1.37. Therefore, the surrounding points on the periphery of the same point could be listed out for obtaining DBH by using farthest distance algorithm.

4.5.3. Volume Estimation using Forest Survey of India (FSI) based volumetric equations

As per the FSI, 1996, the capital of the forest which is termed as the growing stock in the forest, essentially required in efficient forest management. The quantification of the growing stock actually helps us to get an idea about the harvesting limit. The estimation of the forest capital requires the retrieval of the forest stand parameters, which are being used for the volume estimation of the stock. For obtaining such information the Forest Survey of India (FSI) developed a total number of 753 volume equation for 198 species in India. These volume equations are based on the data collection through field inventories during last 30 years. These equation varies as per the local ecological conditions and species, even trees on same site with identical diameters and other parameters may have different volume. Three types of volume equations were developed:

- Local Volume Equations
- Regional Volume Equations
- General or Standard Volume Equations

The local volume equations uses only one parameter i.e. DBH by assuming that the trees with same DBH will have same height and form. Regional equation comprises two parameters with wide range of species and the standard or the general volume equations covers full distribution of the species. By using the equation we can estimate the biomass plot wise for different tree species by multiplying it with the specific gravity and biomass expansion factor which are species specific. This obtained volume further used to estimate the carbon by using conversion factor of 0.47 as given by (IPCC 2006) (Singh, 2014). In this project the same FSI based volumetric equation was used to estimate the individual tree volume, using field based measured parameters and modelled parameters using TLS. The best fit regression equation is used for estimating the growing stock in the forest. FSI based volume equation for Sal tree (*Shorea robusta*) in the areas like Landsdowne forest division and part of Yamuna, Tehri and Garhwal forest divisions, the same local volume equation is being used for the hill region as well such as Almora, Nainital, Pithauragarh and part of Chamoli, Fehradun and Tehridistricts of Uttarakhand state of India.

Local Volume Equation (FSI, 1996a):

$$V = 0.0308585 - 0.77794D + 8.42051D^2 + 5.91067D^3 \quad (n = 710, R^2 = 0.96135)$$

'n' is the total no. sample trees on which regression equations were based whereas 'R²' is the co-efficient of determination. The coefficients in the equations are empirically defined values for different forest species appearing in the different geographical condition in different locations (FSI, 1996b). In this project the DBH measured in the field and TLS based estimated DBH were used in the aforesaid volumetric equation to do a comparative analysis. This has to be more reliable and non-destructive method to estimate the woody biomass using the TLS based retrieved parameters. A study was carried out by Yu et al., 2013, they used destructive sampling method to investigate two biomass estimation models based on DBH and sum of the stem section volume. Both were determined from the automatic reconstruction of the stem curves, then the results were compared with the field based measurements of 30 trees. The DBH based estimation gave the correlation coefficient [r] as 0.93 and RMSE as 21.5% whereas the stem section volume approach gave [r] as 0.98 and RMSE as 12.5%. Therefore, the result obtained through the approach adopted in this project needs to be validated with some ground data and for that R² obtained by FSI may be considered as the parameter for the validation.

5. RESULT AND DISCUSSION

As per the methodology mentioned in the previous chapter, the acquired data was processed. This chapter covers the how obtained tree parameters are accurate or varying from the field measurements. If uncertainty is there, then why and how it can be mitigated, what will be the overall impact on the volume estimation using FSI based volumetric equation. It also covers the alternative methods for obtaining the tree shape and stem modelling using various freeware applications.

5.1. Field measurements and it's uncertainty

The field measurements were taken using Nikon Forestry Pro Laser Rangefinder for tree height measurement and ordinary measuring tape for measuring the circumference of the tree at breast height. The total length of the circumference was then considered as the circumference of a circle irrespective of the stem size and shape variation to obtain the diameter. For each tree approximately 10 measurements were taken in order to check the uncertainty in field measurements as well. The uncertainty in the tree parameters obtained via In-situ measurement for selected trees was obtained in order to do a comparative analysis with the uncertainty in the modelled parameters. Uncertainty in the measurements could be estimated by calculating the standard error in the sampling, which is as follows:

$StandardError = \frac{StandardDeviation}{\sqrt{No.ofSamples}}$ and the mean values of all the measurements.

$$Uncertaintyinsampling = \left(\frac{StandardError}{Meanofthesamples} \right) 100$$

5.1.1. Regression Statistics

In this project the FSI based volumetric equation comprising only two variables DBH and volume, has been used by taking DBH as the independent variables and volume as dependent. In statistics the regression analysis is a tool to seek the information about the effect of dependent variables w.r.t. the independent variable (Sykes, 2016). For the analysis ANOVA which stands for Analysis of Variance was carried out. This is basically to testify how much variance is there in the population. There are two ways to do so first is one way which comprises the comparison of two groups based on one factor the second one is comparison of the two groups based on two factors. In this project Two-way ANOVA was carried out as we have four plots as groups wherein the estimation of volume needs to be done on the basis of field based and TLS based DBH. For the data analysis regression model was used in Microsoft Excel. The regression statistics gives various parameters which are required to check the appropriateness or the accuracy in our model. 'R' is the correlation it measures how two variable moves in relation to each other, R square which is the coefficient of determination or the covariance, is the proportion of variability in Y (y axis) that is explained by the independent variable X (x axis) in the model. So in this case the dependent variable is the estimated volume (Figure 25) at y axis whereas the independent variables are field and TLS based DBH along x axis.

The adjusted R square is more reliable statistics because it takes the total sample cases in account. Standard Error (St. Error) measures the variability of the actual Y values from the predicted Y values same as Standard Deviation. In the analysis of the variance statistics or ANOVA which gives the degree of freedom (d.f), square sum (SS), mean square (MS) F test and P values/levels in the regression and residual. Degree of freedom, which affects t-test, f-test and adjusted R square, it takes into account the sample size, adjusting normal distribution with lower sample sizes to have fatter tails which increases the statistical probability of the unlikely events. The SS and MS are essentially used to calculate the t-test or f-test. The f-test value is to determine the significance of the regression analysis, and the p-value is the probability of occurring the results randomly. The p value basically look for the predictors with a significance less than 0.05, meaning there is at least 95% chance there is a true relationship between the variables. Then the coefficients of the intercept and slope of the regression line, then the St. Error in the coefficients. Lower and upper confident limits (LCL and UCL) which is the range of the obtained coefficients. The t-tests determines the probability of the p-values randomly as in Table 5. The residuals as shown in the Table 6 is basically the difference between the predicted Y values and the actual Y values and the Standard Residuals (St. Res) are the no. of Standard Deviations that the actual Y value deviates from the actual Y values. In our case the predicted and actual Y values are the predicted volume from the line of regression and the actual volume obtained from FSI based volumetric equation using measured and modelled DBH in the plot.

5.2. The regression analysis of the data acquired at Barkot forest area

Total ten trees were taken to do the analysis from the plot of Barkot forest area. For each tree 10 measurements were taken in order to get the idea about the uncertainty in the manual measurements at the field.

Table 1: Field based measured parameters and TLS based modelled parameters

S. No.	Tree Name	Measured Parameters			Modelled Parameters		
		Height	DBH	Volume	Height'	DBH'	Volume'
1	BKT_1	32.88	0.34	1.27	29.17	0.40	1.41
2	BKT_3	32.90	0.43	2.05	30.82	0.48	2.26
3	BKT_5	30.27	0.50	2.76	27.76	0.54	3.01
4	BKT_7	31.22	0.36	1.29	27.23	0.39	1.40
5	BKT_12	30.05	0.40	1.57	27.33	0.44	1.77
6	BKT_13	33.80	0.53	3.19	30.27	0.57	3.43
7	BKT_15	30.72	0.37	1.27	27.02	0.40	1.45
8	BKT_25	31.14	0.44	2.19	27.01	0.49	2.33
9	BKT_27	32.86	0.79	8.36	29.24	0.85	9.13
10	BKT_28	33.06	0.69	5.47	31.72	0.73	6.29

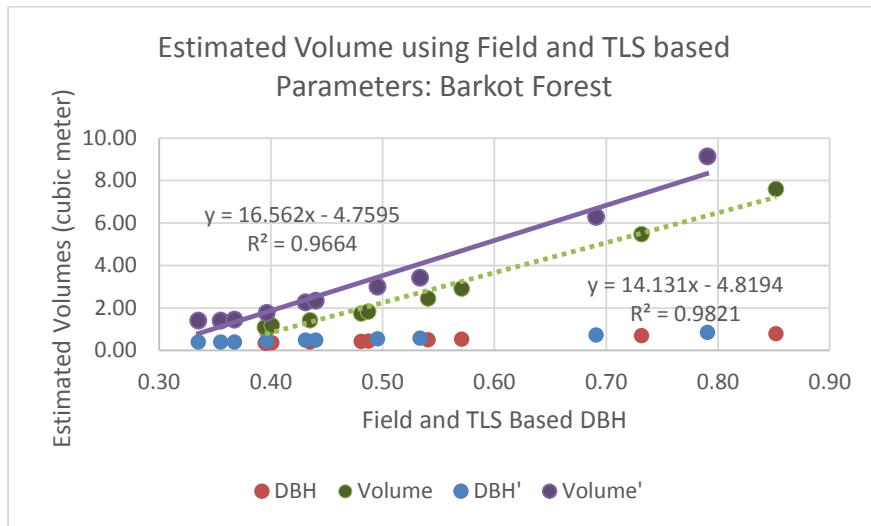


Figure 25: The estimation of the volume w.r.t. modelled DBH at Barkot Forest

The field measurements were taken 10 times for each tree in order to obtain uncertainty (Appendix A.1). The obtained tree parameters from field measurement and TLS based estimation are shown in Table 1. The average relative error in the DBH and estimated volume found as 0.10 m and 0.26 m³ at Barkot Forest (Appendix C.1). This can be clearly seen in the above (Figure 25) which shows a systematic error between the estimated volumes using field based DBH and TLS based DBH'. The estimated TLS based DBH' using the developed algorithm was more than the field based DBH and in FSI based volumetric equation only DBH is being used. The violet colour regression line shows the predicted volume w.r.t the TLS based DBH and the green one is with the field based DBH. However, when it is compared with the coefficient of determination (R^2) of the FSI based equation which has considered 710 samples is around 0.96. In this case the R^2 of the estimated volume is coming around 0.97 which satisfies the aim of this project.

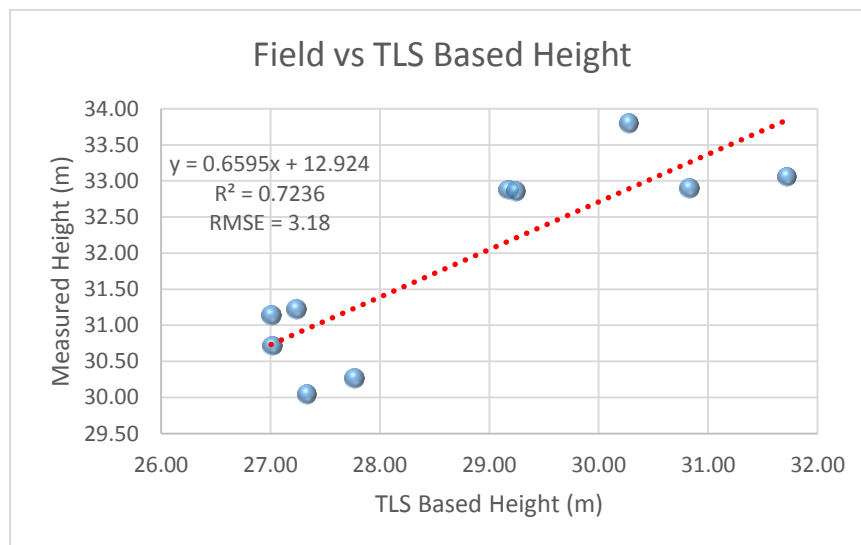


Figure 26: RMSE assessment in both field measured and TLS based Height

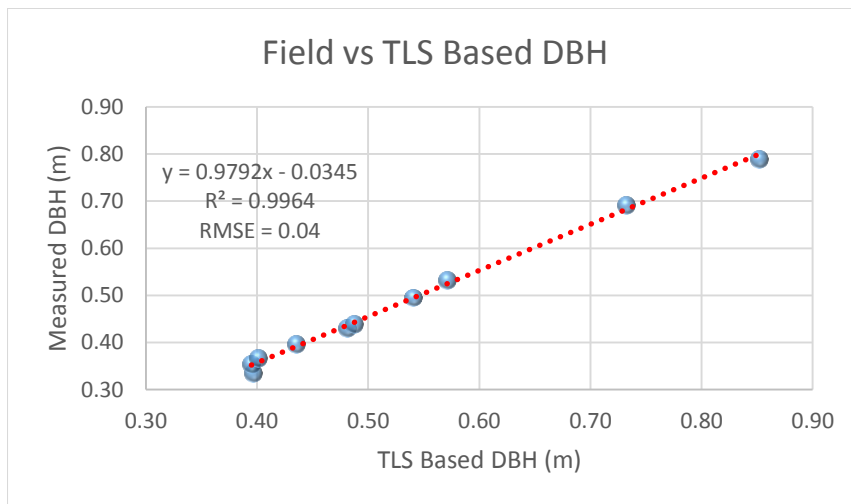


Figure 27: RMSE assessment in both field measured and TLS based Height

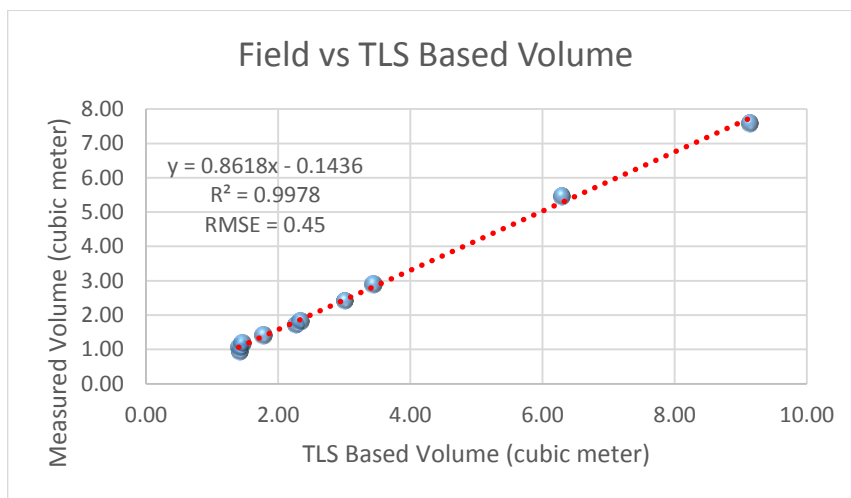


Figure 28: RMSE assessment in both field measured and TLS based Height

In above graphs (Figure 26, 27, 28) shows the line of regression between measured and modelled parameters. The line of regression has been used for predicting the respective parameters by using TLS based parameters as the independent variables in the equation. The R^2 for measured vs. TLS based height is less which is 0.72 but in case of DBH and volume it coming 0.99 which shows high correlation among them. The coefficient of Determination (R^2) is 0.98 for both measured and modelled volume prediction respectively (Table 2). Which shows the goodness of the best fitting line. The average relative error for height and DBH is 10% whereas the volume has 26% relative error. This implies that in through modelling of height and DBH it is giving 90% accuracy whereas in overall volume estimation the accuracy is 74% (Appendix C.1).

From Table 3 the F value is coming around 348.55 to check the significance of the correlation critical point has been calculated using function available in the excel which is as follows:

Critical Point = F.INV.RT(significance level, d.f.1, d.f.2) where sig. level is 0.05 and d.f.1 and d.f.2 are 1 and 8 in our case (Table 3).

The estimated critical point comes around 5.32. The F value is coming 348.33 and 325.37 (Table 3) for both modelled and measured parameters which is far away from the assessed critical value in the F distribution. This signifies that we pass the F test and there is a nice correlation (95%) between the independent and dependent variables. Similarly, t-test has been carried out for the same by estimating the critical points, but in this case need to evaluate the degree of freedom first which is:

Degree of freedom = $n - k - 1$ where n is the total observations and k is the no. of coefficient of the variable, therefore $d.f = 10 - 1 - 1 \Rightarrow 8$

Critical Points = T.INV.2T(5%,8) $\Rightarrow 2.3$

Cut-off Value = T.DIST.2T(Critical Point, 8) $\Rightarrow 0.0504 = 5\%$

Since it is two tail test therefore the critical values would be from -2.3 to +2.3 in the normal distribution. From Table 3 the t-stat for independent variable is 18.66 which is lying far beyond the critical point on the tail, so we pass the test. The p-value is the probability is 1×10^{-6} which lesser than the 5% and out of the cut off value, which means it is not falling between our lower and upper level confidence interval (95%). t-test was used for regression of independent variable and the R square was used for f-test in order to check the regression quality.

Table 2: Regression Statistics by using modelled Volume and DBH

	Modelled	Measured
R Square	0.98	0.98
Adjusted R Square	0.97	0.97
St. Error	0.40	0.36
Observations	10	10

Table 3: ANOVA

Modelled						
	df	SS	MS	F	F Sig	
Regression	1	56.65	56.65	348.33	7.01E-08	
Residual	8	1.30	0.16			
Total	9	57.95				
Measured						
Regression	1	42.10	42.10	325.37	9.16E-08	
Residual	8	1.04	0.13			
Total	9	43.14				
Modelled						
	Coeff.	St. Error	t Stat	P-value	Lower 95%	Upper 95%

Intercept	-5.40	0.48	-11.23	0.0000035	-6.50	-4.29
DBH	16.34	0.88	18.66	0.0000001	14.32	18.36
Measured						
Intercept	-4.29	0.40	-10.68	0.00	-5.21	-3.36
DBH	14.36	0.80	18.04	0.00	12.52	16.20

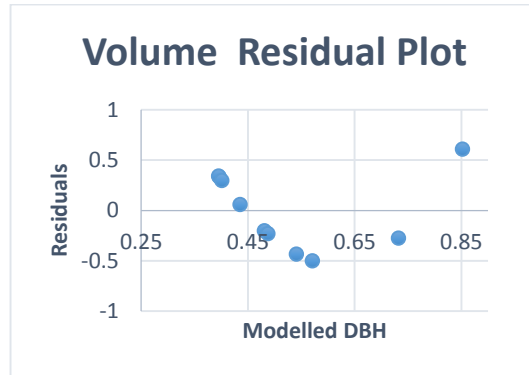


Figure 29: The volume residual plot w.r.t. TLS based DBH

In figure 29 which is the residual plot of the estimated volumes using both field based and TLS based DBH it shows a smooth pattern in the plot. Residual plot basically shows the distribution of the residuals on the vertical axis w.r.t the independent variable which is DBH here. Residual here means the difference between the estimated volume and the predicted volume using the regression line. If the distribution is random that means that means the linear regression line is appropriate for the data. But in above case it is not scattered, it follows a “U” pattern that means a non-linear model is required for the prediction of the volume. In order to tackle this situation a non-linear transformation is required. This FSI based volumetric equation ($V = 0.0308585 - 0.77794D + 8.42051D^2 + 5.91067D^3$ ($n = 710, R^2 = 0.96135$), is of 3rd order, therefore, the linear equation for justifying the correlation in volume would not be the appropriate method. Therefore, the linear equation has been transformed into the non-linear regression (Figure 30) which is of 3rd order polynomial for best fit regression with $R^2 = 1$.

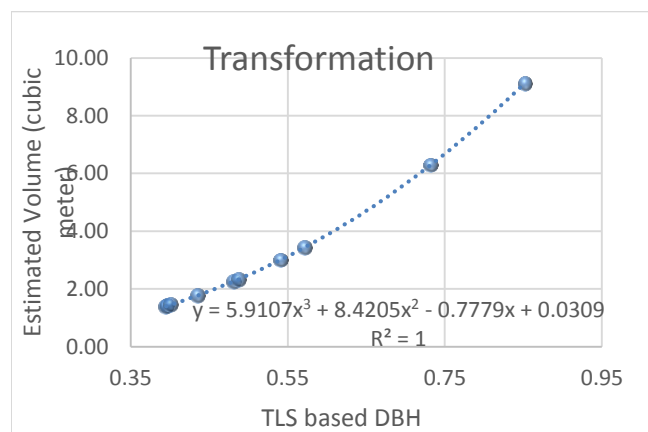


Figure 30: The non-linear regression after transformation

5.3. The regression analysis of the data acquired at IIRS Campus

The site at IIRS was taken to get the point cloud of some variable tree shapes for the modelling to check the accuracy. Total seven trees were taken to do the analysis and for each tree 10 measurements were taken in order to get the idea about the uncertainty in the manual measurements at the field (Appendix A.2). The field based and TLS based parameters along with the obtained respective volumes are shown in the table below:

Table 4: Measured and modelled parameters:

S. No	Tree Name	Measured Parameters			Modelled Parameters		
		Height	DBH	Volume	Height'	DBH'	Volume'
1	GT-1	15.14	0.71	1.15	13.21	1.03	14.76
2	GT-2	16.76	0.31	6.66	14.46	0.34	0.99
3	GT-3	22.6	0.36	0.85	19.52	0.38	1.25
4	GT-4	22.28	0.75	4.96	20.24	0.82	8.40
5	GT-5	23.86	0.32	1.92	21.08	0.35	1.02
6	GT-6	26.16	0.66	0.03	21.33	0.72	6.05
7	GT-7	23.66	0.45	0.03	21.34	0.50	2.53

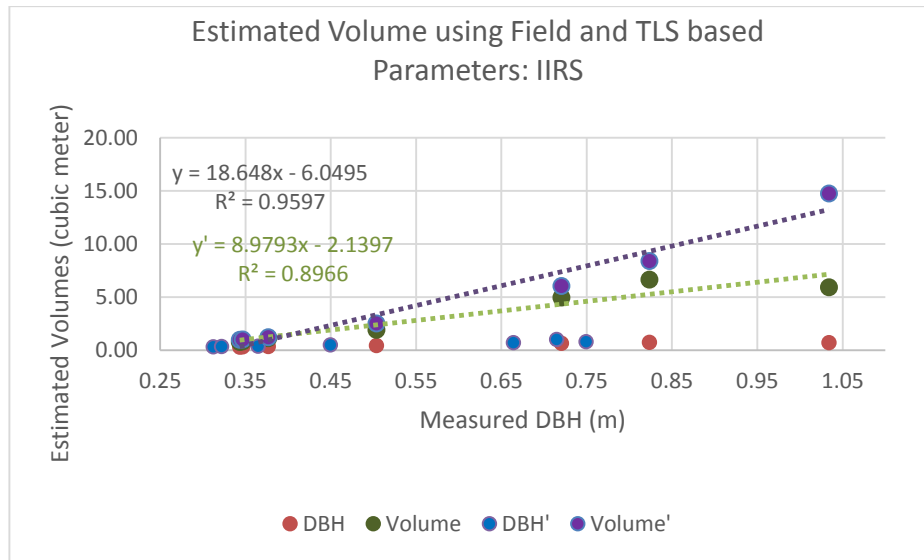


Figure 31: The estimation of the volume w.r.t. modelled DBH at IIRS Campus

The field measurements were taken 10 times for each tree in order to obtain uncertainty (Appendix A.2). The Standard error in the measurements of DBH measurement was in the range of 0.001 m to 0.01m similarly in height. The obtained tree parameters from field measurement and TLS based estimation are shown in Table 5 which shows R^2 for modelled as 0.96 and 0.98 for field based parameters. The average relative error in the DBH and estimated volume found as 0.14 m and 0.40 m³ at IIRS (Appendix C.2). A systematic error between the estimated volumes using field based DBH and TLS based DBH' can be seen

in Figure 31. Here also the estimated 'TLS based DBH' using the developed algorithm was more than the field based DBH and in FSI based volumetric equation only DBH is being used. The violet colour regression line shows the predicted volume w.r.t the TLS based DBH and the green one is with the field based DBH with an R^2 of 0.96 approximately whereas the R^2 for field based measurement is coming 0.90. However, when it is compared with the coefficient of determination (R^2) of the FSI based equation which has considered 710 samples is around 0.96, the TLS based estimation seems satisfied in this case.

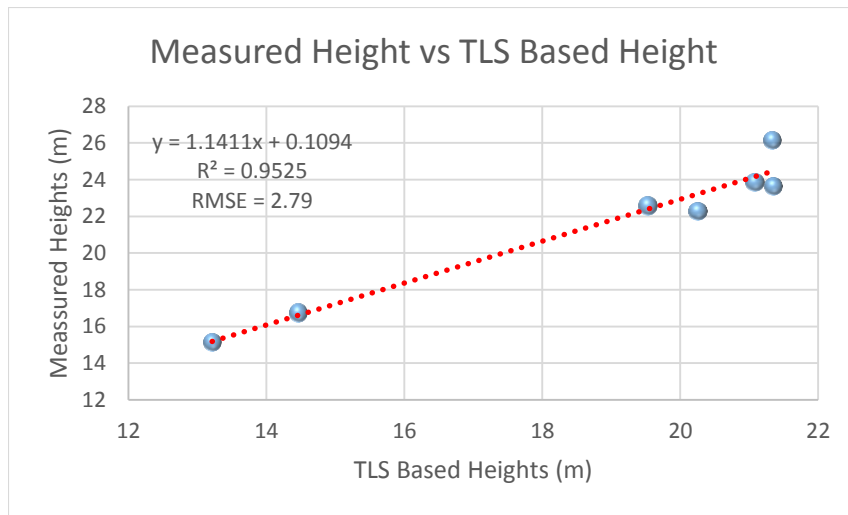


Figure 32: RMSE assessment in both field measured and TLS based Height

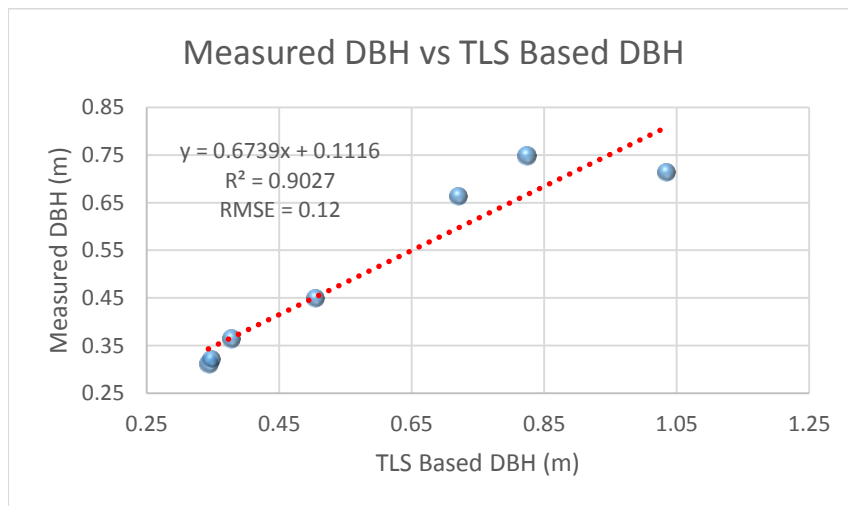


Figure 33: RMSE assessment in both field measured and TLS based Height

In figure 32 shows the most of the height estimation in the field is above 22 m whereas the height obtained from the algorithm is lesser than that though it is showing a good correlation with R^2 as 0.95. The reason already has been mentioned as there is a limitation of the instrument in the field. The TLS based height estimation is more accurate because the scanner takes the point cloud of from 30^0 to 130^0 vertically which covers the whole tree length and the height has been estimated from the point at the bottom of the height

to the top of the tree which has been validated with manual measurement as well in the CloudCompare application.

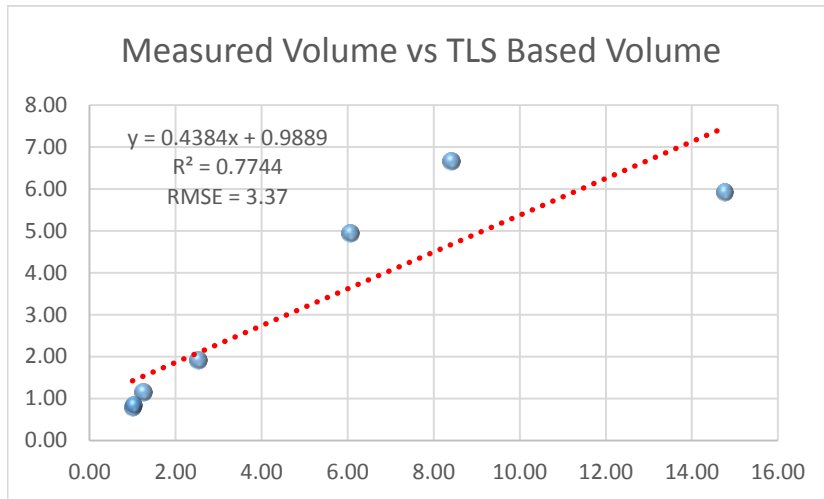


Figure 34: RMSE assessment in both field measured and TLS based Height

Figure 34, shows the overestimated volume using modelled DBH compared to the volume estimated via measured DBH. The measured and predicted volume with the measured vs modelled DBH follows a positive correlation with coefficient of determination of 0.98 and 0.95 respectively. The RMSE in the height, DBH and volume are 0.80, 0.05 and 0.08 respectively. The standard deviation in measured and modelled heights are 4.01 and 3.43 respectively and similarly in DBH its 0.19 and 0.27 respectively, which implies that there is not much variation in terms of the measurement. Below Table shows the statistics of the measurements at IIRS.

For F test the estimated critical point comes around 6.61. The F value is coming 118.97 and 419.65 (Table 6) for both modelled and measured parameters which is far away from the assessed critical value in the F distribution. This signifies that we pass the F test and there is a nice correlation (95%) between the independent and dependent variables. Similarly, t-test has been carried out for the same by estimating the critical points, but in this case need to evaluate the degree of freedom first which is:

$$\text{Degree of freedom} = n - k - 1 \text{ where } n \text{ is the total observations and } k \text{ is the no. of coefficient of the variable, therefore } d.f = 7 - 1 - 1 \Rightarrow 5$$

$$\text{Critical Points} = T.INV.2T(5\%,5) \Rightarrow 2.57$$

$$\text{Cut-off Value} = T.DIST.2T(\text{Critical Point}, 5) \Rightarrow 0.050 = 5\%$$

Since it is two tail test therefore the critical values would be from -2.57 to +2.57 in the normal distribution. From Table 11 the t-stat for independent variable is 10.91 for modelled and 20.49 for measured, which are lying far beyond the critical point on the tail, so we pass the t-test. The p-value is the probability with value 1×10^{-4} and 1×10^{-5} for both modelled and measured respectively, which is lesser than the 5% which is our cut off value, which means it is not falling between our lower and upper level confidence interval (95%). t-test

was used for regression of independent variable and the R square was used for f-test in order to check the regression quality.

Table 5: Regression Statistics by using modelled Volume and DBH

	Modelled	Measured
R Square	0.96	0.988
Adjusted R Square	0.95	0.986
St. Error	1.14	0.306
Observations	7	7

Table 6: ANOVA

Modelled						
	df	SS	MS	F	F-Sig	
Regression	1	153.56	153.56	118.97	0.00011256	
Residual	5	6.45	1.29			
Total	6	160.02				
Measured						
Regression	1	39.24	39.24453	419.65	5.12946E-06	
Residual	5	0.47	0.093518			
Total	6	39.71				
Modelled						
	Coeff.	St. Error	t Stat	P-value	Lower 95%	Upper 95%
Intercept	-6.05	1.10	-5.50	0.0027	-8.88	-3.22
WIDTH	18.65	1.71	10.91	0.0001	14.25	23.04
Measured						
Intercept	-3.61	0.35	-10.28	0.00015	-4.51	-2.71
DBH	13.29	0.65	20.49	0.00001	11.62	14.96

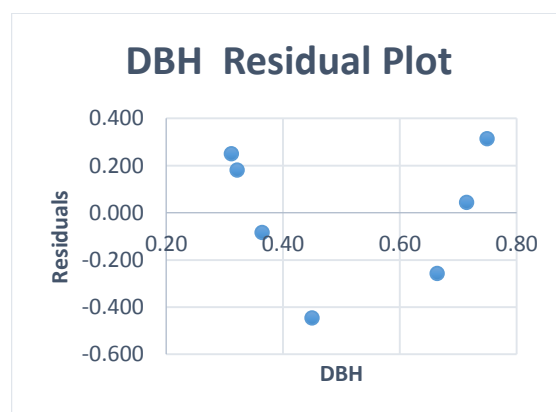


Figure 35: The volume residual plot w.r.t. TLS based DBH

In this case also residual plot (Figure 35) showing a pattern which needs to be transformed to get the better non-linear relation as done for Barkot plot. In case of site at the IIRS as shown in (Appendix C.2) the relative error with respect to the modelled values. The average relative error for height and DBH is 13% and 14% respectively, whereas the volume has 40% relative error. Here in height and DBH has 87% and 86% accuracy but the accuracy in volume is 60% which is comparatively less. The reason behind this may be the varying shapes of the trees; the detailed explanation is there in the discussion section of the chapter.

5.4. The regression analysis of the data acquired at Thano forest range: Plot-I

Thano forest range is denser in comparison to the Barkot forest. Therefore, no. of trees under the considered plot sizes, were more. Out of around 53 trees only 25 trees could be identified for which field measurements were available. The tables for uncertainty in the manual measurements at the field are attached in Appendix A.3. Below tables shows the field based and TLS based parameters along with the obtained respective volumes

Table 7: Measured and modelled parameters

S. No.	Tree Name	Measured Parameters			Modelled Parameters		
		Height	DBH	Volume	Height	DBH	Volume
1	TT1_2	24.86	0.21	6.58	22.92	0.24	0.43
2	TT1_7	20.40	0.39	22.44	17.40	0.43	1.68
3	TT1_13	25.38	0.33	15.06	23.88	0.35	1.02
4	TT1_17	25.81	0.36	18.89	23.42	0.41	1.51
5	TT1_19	26.49	0.45	32.01	24.47	0.50	2.46
6	TT1_21	21.01	0.24	8.93	19.92	0.27	0.58
7	TT1_22	26.41	0.27	11.78	23.93	0.31	0.78
8	TT1_23	19.94	0.27	11.62	16.59	0.30	0.74
9	TT1_24	26.85	0.28	13.26	24.06	0.33	0.88
10	TT1_25	27.43	0.33	14.54	25.68	0.41	1.54
11	TT1_27	30.26	0.33	20.29	27.43	0.39	1.37
12	TT1_28	27.29	0.37	25.80	24.45	0.42	1.65
13	TT1_29	26.96	0.32	13.30	24.53	0.36	1.08
14	TT1_30	28.18	0.47	35.49	26.49	0.54	3.01
15	TT1_31	18.93	0.22	6.65	15.47	0.25	0.45
16	TT1_32	32.17	0.39	13.24	28.85	0.42	1.66
17	TT1_33	29.00	0.31	13.21	26.63	0.38	1.31
18	TT1_34	21.06	0.25	8.62	18.00	0.28	0.58
19	TT1_35	27.11	0.36	21.89	24.34	0.40	1.43

20	TT1_36	25.89	0.30	13.09	22.53	0.32	0.83
21	TT1_38	30.29	0.39	28.65	27.52	0.44	1.83
22	TT1_39	17.26	0.28	11.96	13.80	0.31	0.79
23	TT1_42	28.76	0.35	17.03	26.26	0.42	1.66
24	TT1_43	26.22	0.28	12.21	22.48	0.32	0.81
25	TT1_45	15.41	0.29	13.23	11.32	0.32	0.85

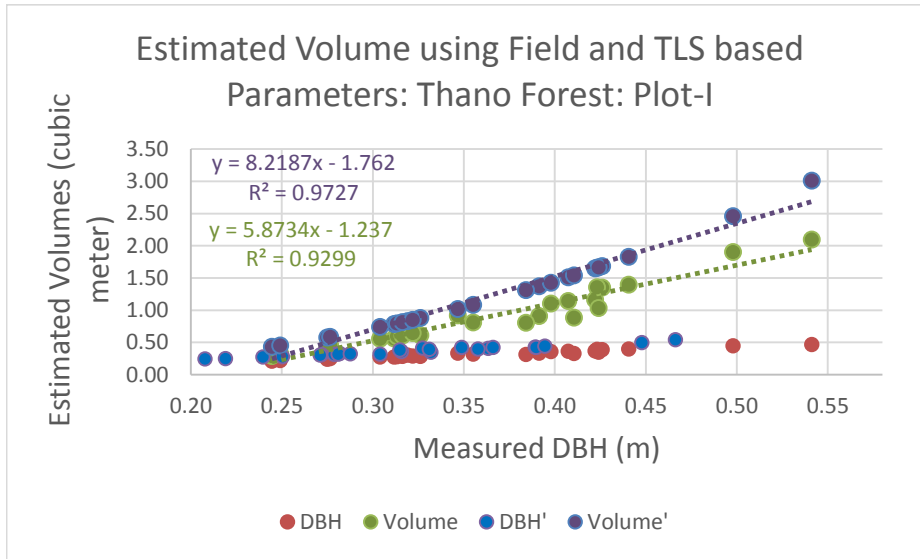


Figure 36: The estimation of the volume w.r.t. modelled DBH at Thano Range: Plot-I

The field measurements were taken 10 times for each tree in order to obtain uncertainty (Appendix A.3). The Standard error in the measurements of DBH measurement was in the range of 0.001 m to 0.01m similarly in height. The obtained tree parameters from field measurement and TLS based estimation are shown in Table 7. The average relative errors for height and DBH are 12% and 14% respectively, whereas the volume has 37% relative error. This implies that in through modelling of height and DBH it is giving 88% and 86% accuracy whereas in overall volume estimation the accuracy is 63% (Appendix C.3). A systematic error between the estimated volumes using field based DBH and TLS based DBH' can be seen in Figure 36. Here also the estimated TLS based DBH' using the developed algorithm was more than the field based DBH and in FSI based volumetric equation only DBH is being used. The violet colour regression line shows the predicted volume w.r.t the TLS based DBH and the green one is with the field based DBH. However, when it is compared with the coefficient of determination (R^2) of the FSI based equation which has considered 710 samples is around 0.96. In this case the R^2 of the estimated volume is coming around 0.97 which satisfies the aim of this project.

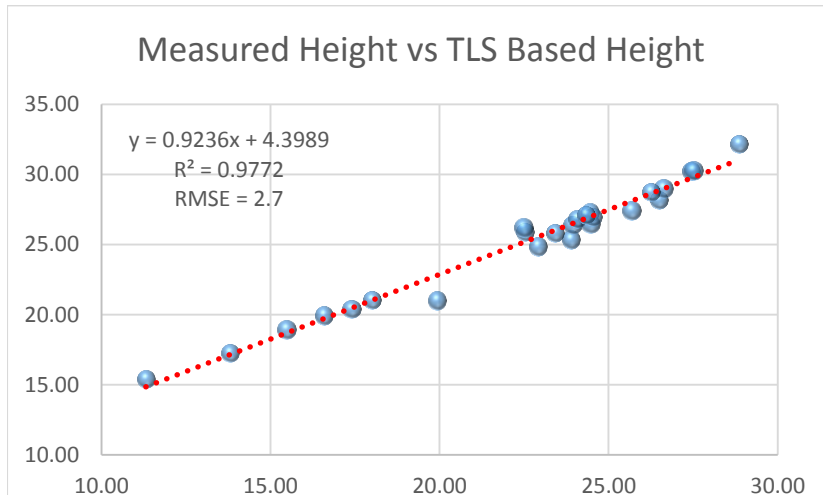


Figure 37: RMSE assessment in both field measured and TLS based Height

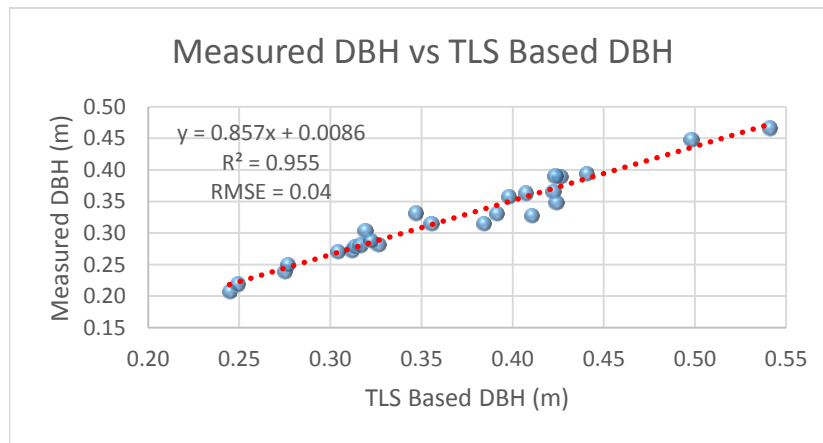


Figure 38: RMSE assessment in both field measured and TLS based Height

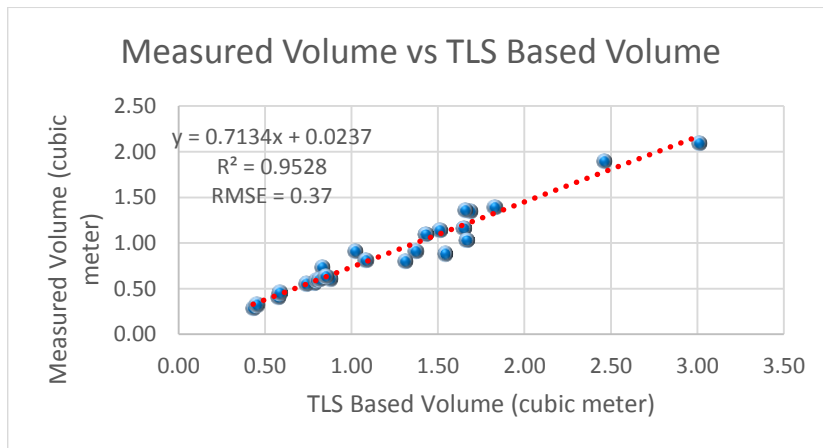


Figure 39: RMSE assessment in both field measured and TLS based Height

In above graphs (Figure 37, 38, 39) shows the line of regression between measured and modelled parameters with R^2 greater than 0.95. The line of regression has been used for predicting the respective parameters by

using TLS based parameters as the independent variables in the equation. Using predicted and TLS based parameters residuals were calculated to estimate the RMSE.

The measured and predicted volume with the measured vs modelled DBH follows a positive correlation with coefficient of determination of 0.97. The standard deviation in measured and modelled heights are 4.29 and 4.6 respectively and similarly in DBH its 0.065 and 0.075 respectively, which implies that there is not much variation in terms of the measurement in case of DBH.

For F test the estimated critical point comes around 4.27. The F value is coming 818.81 and 828.08 (Table 9) for both modelled and measured parameters which is far away from the assessed critical value in the F distribution. This signifies that we pass the F test and there is a nice correlation (95%) between the independent and dependent variables. Similarly, t-test has been carried out for the same by estimating the critical points, but in this case need to evaluate the degree of freedom first which is:

Degree of freedom = $n - k - 1$ where n is the total observations and k is the no. of coefficient of the variable, therefore $d.f = 25 - 1 - 1 \Rightarrow 23$

Critical Points = $T.INV.2T(5\%,23) \Rightarrow 2.06$

Cut-off Value = $T.DIST.2T(\text{Critical Point}, 5) \Rightarrow 0.050 = 5\%$

Since it is two tail test therefore the critical values would be from -2.06 to +2.06 in the normal distribution. From Table 9 the t-stat for independent variable is 28.61 for modelled and 28.78 for measured, which are lying far beyond the critical point on the tail, so we pass the t-test. The p-value is lesser than the 5% (cut-off) for both measured and modelled, which means it is not falling between our lower and upper level confidence interval (95%). t-test was used for regression of independent variable and the R square was used for f-test in order to check the regression quality. The residual is estimated from the difference of the volume (Y value) and predicted volume (from regression line), the residual plot (Figure 40) has been shown for both measured and modelled DBH, wherein, the distribution of the residuals is again following a pattern which requires the transformation to get the linearity using non-collinear equation.

Table 8: Regression Statistics by using modelled Volume and DBH

	Modelled	Measured
R Square	0.97	0.97
Adjusted R Square	0.97	0.97
St. Error	0.11	0.08
Observations	25	25

Table 9: ANOVA

Modelled						
	df	SS	MS	F	Sig. F	
Regression	1	9.16	9.16	818.81	1.74E-19	
Residual	23	0.26	0.01			
Total	24	9.42				
Measured						
Regression	1	4.90	4.90	828.08	1.54E-19	
Residual	23	0.14	0.01			
Total	24	5.03				
Modelled						
	Coeff.	St. Error	t Stat	P-value	Lower 95%	Upper 95%
Intercept	-1.76	0.11	-16.48	0.00	-1.98	-1.54
DBH	8.22	0.29	28.61	0.00	7.62	8.81
Measured						
Intercept	-1.30	0.08	-16.60	0.00	-1.46	-1.13
DBH	6.85	0.24	28.78	0.00	6.36	7.34

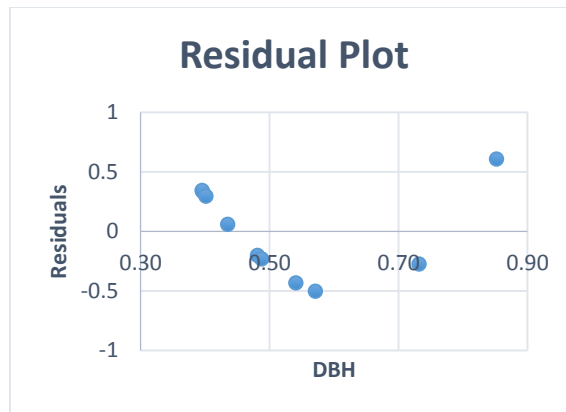


Figure 40: Volume residual plot w.r.t. TLS based DBH

In this case also the distribution is following a pattern which needs to be transformed as per the 3rd order polynomial regression equation in order to achieve the linear relation in the parameters. The table comprising Residuals are attached in (Appendix B.3).

5.5. The regression analysis of the data acquired at Thano forest range: Plot-II

A second plot was taken at the Thano forest range. Out of around 67 trees only 30 trees could be identified for which field measurements were taken. The uncertainty in the manual measurements at the field from

multiple measurements of the tree parameters is shown in (Appendix C.4). Below tables shows the field based and TLS based parameters along with the obtained respective volumes.

Table 10: Measured and modelled parameters

S. No.	Tree Name	Measured Parameters			Modelled Parameters		
		Height	DBH	Volume	Height'	DBH'	Volume'
1	TT2_5	24.89	0.35	1.38	22.21	0.41	1.50
2	TT2-6	18.66	0.21	0.37	17.75	0.26	0.51
3	TT2-8	21.86	0.24	0.61	18.57	0.29	0.65
4	TT2-10	25.49	0.32	1.03	23.29	0.38	1.27
5	TT2-13	16.64	0.28	0.75	13.79	0.31	0.78
6	TT2-15	25.82	0.30	0.84	23.86	0.33	0.87
7	TT2-16	26.75	0.35	1.42	24.54	0.42	1.63
8	TT2-17	27.55	0.35	1.20	26.92	0.38	1.28
9	TT2-18	28.30	0.48	2.29	26.67	0.51	2.65
10	TT2-20	30.50	0.39	1.55	27.27	0.42	1.59
11	TT2-21	25.83	0.28	0.73	22.47	0.33	0.91
12	TT2-22	30.64	0.39	1.66	27.35	0.43	1.74
13	TT2-23	19.67	0.45	2.29	17.47	0.49	2.31
14	TT2-25	25.70	0.30	0.99	23.17	0.33	0.92
15	TT2-26	28.10	0.37	1.53	26.65	0.42	1.60
16	TT2-27	28.74	0.39	1.32	26.37	0.41	1.55
17	TT2-29	19.67	0.21	0.32	15.65	0.23	0.39
18	TT2-30	30.78	0.43	1.74	28.18	0.46	2.08
19	TT2-31	27.50	0.32	1.16	24.04	0.39	1.32
20	TT2-33	20.54	0.10	0.11	17.05	0.16	0.14
21	TT2-34	28.64	0.30	0.96	27.93	0.35	1.01
22	TT2-35	31.66	0.45	1.93	28.77	0.49	2.33
23	TT2-36	30.57	0.53	2.91	28.28	0.58	3.52
24	TT2-37	30.56	0.22	0.43	28.86	0.25	0.47
25	TT2-38	25.02	0.29	0.67	27.13	0.37	1.23
26	TT2-40	29.15	0.35	1.19	27.54	0.40	1.42
27	TT2-41	19.54	0.25	0.48	16.49	0.28	0.60
28	TT2-42	28.92	0.26	0.61	26.18	0.30	0.74
29	TT2-43	17.99	0.18	0.24	14.70	0.21	0.29
30	TT2-44	31.68	0.31	0.83	28.53	0.34	0.97

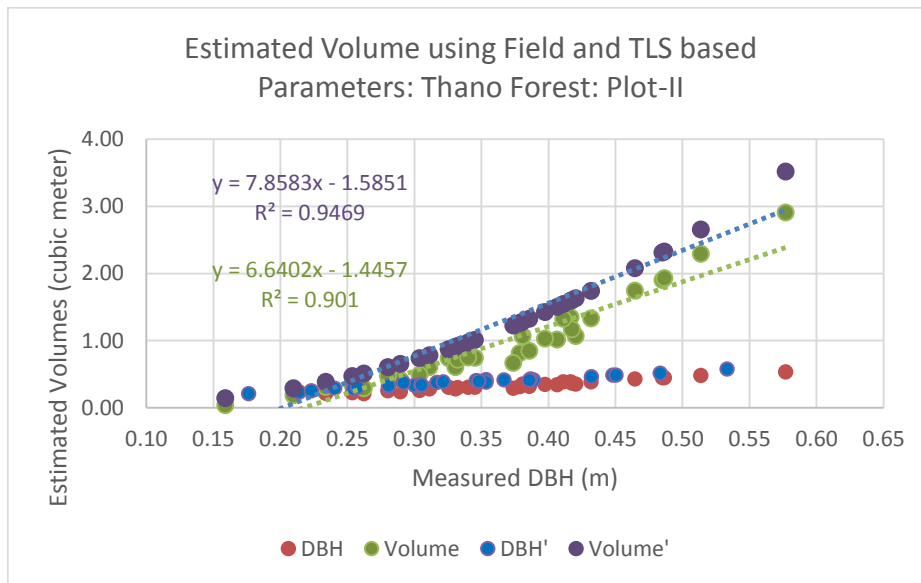


Figure 41: The estimation of the volume w.r.t. modelled DBH at Thano Range: Plot-II

The field measurements were taken 10 times for each tree in order to obtain uncertainty (Appendix A.3). The Standard error in the measurements of DBH measurement was in the range of 0.001 m to 0.01m similarly in height. The obtained tree parameters from field measurement and TLS based estimation are shown in Table 10. The average relative errors for height and DBH are 13% and 15% respectively, whereas the volume has 44% relative error. This implies that in through modelling of height and DBH it is giving 87% and 85% accuracy whereas in overall volume estimation the accuracy is 66% (Appendix C.3). A systematic error between the estimated volumes using field based DBH and TLS based DBH' can be seen in Figure 41. Here also the estimated TLS based DBH' using the developed algorithm was more than the field based DBH and in FSI based volumetric equation only DBH is being used. The violet colour regression line shows the predicted volume w.r.t the TLS based DBH and the green one is with the field based DBH. However, when it is compared with the coefficient of determination (R^2) of the FSI based equation which has considered 710 samples is around 0.96. In this case the R^2 of the estimated volume is coming around 0.95 which satisfies the aim of this project. One observation here is the DBH between 0.35 m to 0.40 in the same measurement the estimation of the volume is almost same or nearby. This proves that in FSI based equation only one parameter is being used which would not be true for all case. The considered homogeneity vanishes here in this particular case. Therefore, the assumption we are carrying this far that the Tarai area of Uttarakhand forest with Sal trees would have similar height is under question, because it is possible that the trees with same DBH may have height variation and similarly variation in the volume.

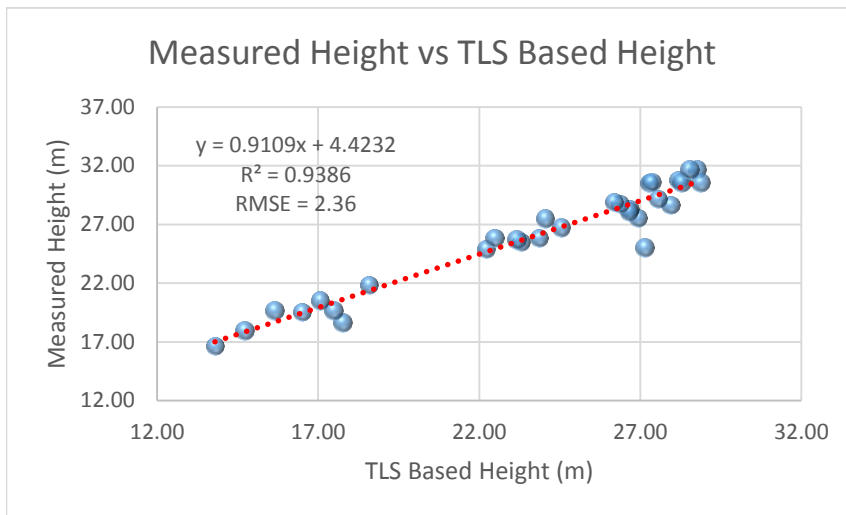


Figure 42: RMSE assessment in both field measured and TLS based Height

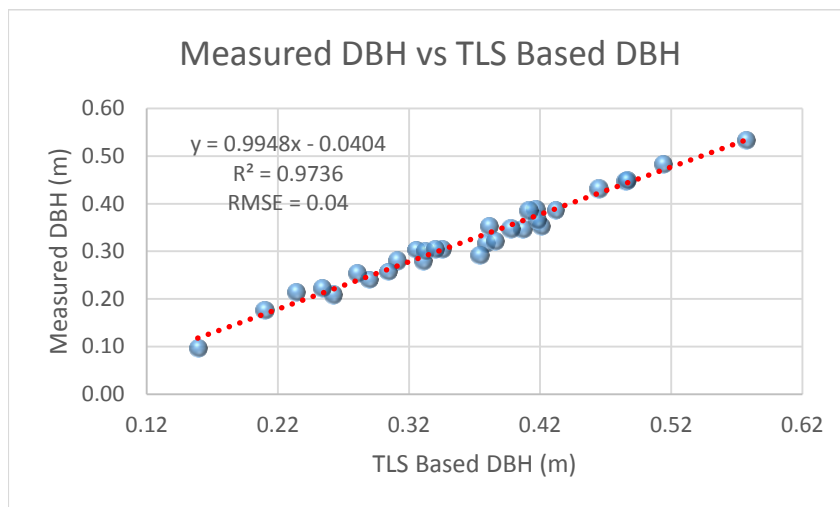


Figure 43: RMSE assessment in both field measured and TLS based DBH

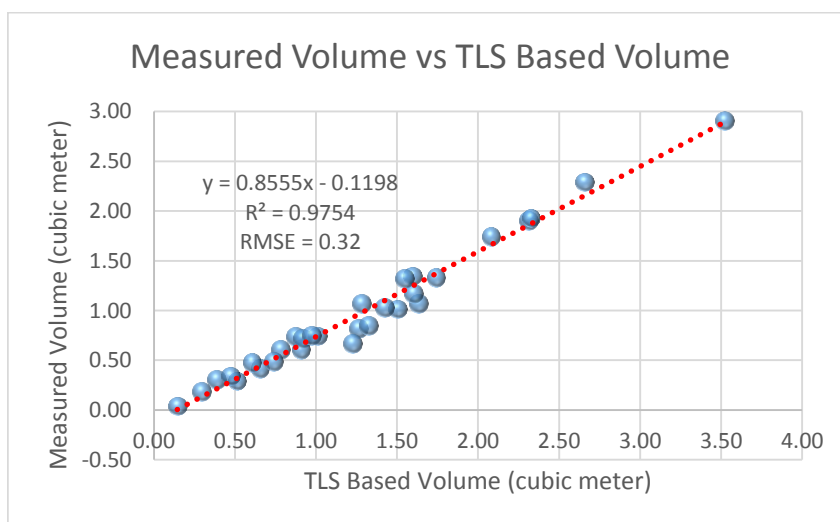


Figure 44: RMSE assessment in both field measured and TLS based volume

In above graphs (Figure 42, 43, 44) shows the line of regression between field based and TLS based parameters. The line of regression has been used for predicting the respective parameters by using TLS based parameters as the independent variables in the equation. Using predicted and TLS based parameters residuals were calculated to estimate the RMSE.

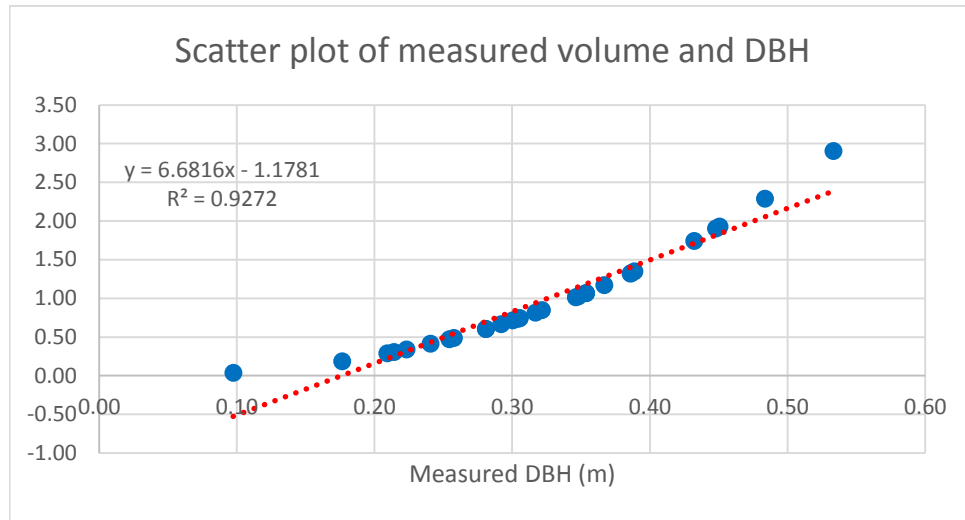


Figure 45: Scatter Plot of Measured Volume and Measured DBH at Thano Forest: Plot-2

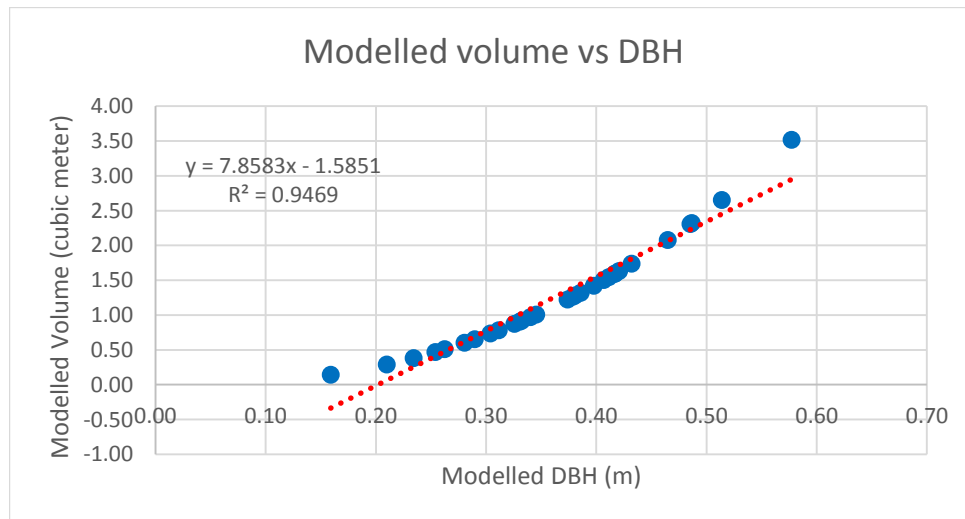


Figure 46: Scatter Plot of Modelled Volume and Modelled DBH at Thano Forest: Plot-2

The measured and predicted volume with respect to the measured and modelled DBH follows a positive correlation with coefficient of determination of 0.93 and 0.95 respectively (Figure 45, 46). The standard deviation in measured and modelled heights are 4.5 and 4.8 respectively and similarly in both DBH its 0.09, which implies that there is not much variation in terms of the measurement in case of DBH.

For F test the estimated critical point comes around 4.2. The F value is coming 499.5 and 356.7 (Table 12) for both modelled and measured parameters which is far away from the assessed critical value in the F

distribution. This signifies that we pass the F test and there is a nice correlation (95%) between the independent and dependent variables. Similarly, t-test has been carried out for the same by estimating the critical points, but in this case need to evaluate the degree of freedom first which is:

Degree of freedom = $n - k - 1$ where n is the total observations and k is the no. of coefficient of the variable, therefore $d.f = 30 - 1 - 1 \Rightarrow 28$

Critical Points = $T.INV.2T(5\%,28) \Rightarrow 2.05$

Cut-off Value = $T.DIST.2T(\text{Critical Point}, 28) \Rightarrow 0.0498 = 5\%$

Since it is two tail test therefore the critical values would be from -2.05 to +2.05 in the normal distribution. From Table 12 the t-stat for independent variable is 22.35 for modelled and 18.89 for measured, which are lying far beyond the critical point on the tail, so we pass the t-test. The p-value is lesser than the 5% (cut-off) for both measured and modelled, which means it is not falling between our lower and upper level confidence interval (95%). t-test was used for regression of independent variable and the R square was used for f-test in order to check the regression quality. The residual is estimated from the difference of the volume (Y value) and predicted volume (from regression line), the residual plot (Figure 47) has been shown for both measured and modelled DBH, wherein, the distribution of the residuals is following similar pattern as in other plots therefore in this case as well the transformation of the equation is required using non-collinear equation for the best fit.

Table 11: Regression Statistics by using modelled Volume and DBH

	Modelled	Measured
R Square	0.95	0.93
Adjusted R Square	0.95	0.92
St. Error	0.18	0.18
Observations	30	30

Table 12: ANOVA

Modelled						
	df	SS	MS	F	Significance F	
Regression	1	15.80	15.80	499.50	2.16E-19	
Residual	28	0.89	0.03			
Total	29	16.68				
Measured						
Regression	1	11.61	11.61	356.71	1.81E-17	
Residual	28	0.91	0.03			
Total	29	12.52				

Modelled						
	Coeff.	St. Error	t Stat	P-value	Lower 95%	Upper 95%
Intercept	-1.59	0.13	-12.00	1.49E-12	-1.86	-1.31
DBH'	7.86	0.35	22.35	2.16E-19	7.14	8.58
Measured						
Intercept	-1.18	0.12	-9.94	1.1E-10	-1.42	-0.94
DBH	6.68	0.35	18.89	1.81E-17	5.96	7.41

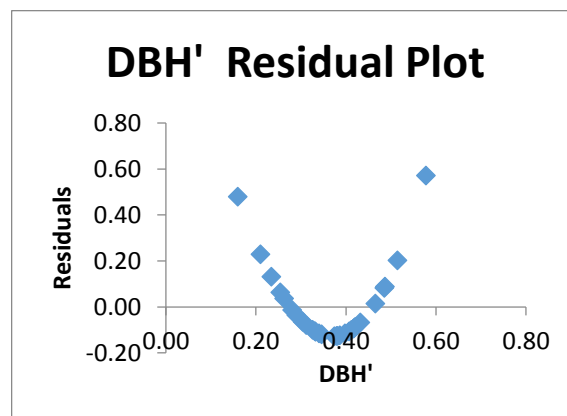


Figure 47: Volume residual plot w.r.t TLS based DBH

In this case also the transformation of the regression is required. For all the plots it is coming same and since the FSI based equation is of 3rd order equation the transformation has to be done using a 3rd order polynomial equation which would be the best fit curve w.r.t. the correlation.

5.6. Comparative analysis of DBH vs Height

As per the derived parameters using the model, the obtained DBH and height were compared as shown in the below figures (48 – 50). It has been found that the heights of the trees with the almost same DBH are varying. This means the assumption that was made during formulation of the FSI based volumetric equation, that in Tarai region the heights of the Sal Tree (*Shorea Robusta*) are homogeneous. That is why only DBH was considered in the formulated volumetric equation.

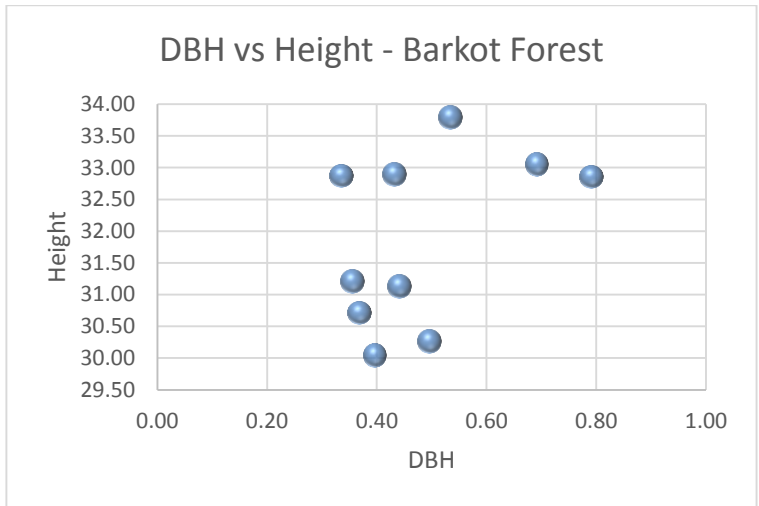


Figure 48: DBH vs Height, Barkot

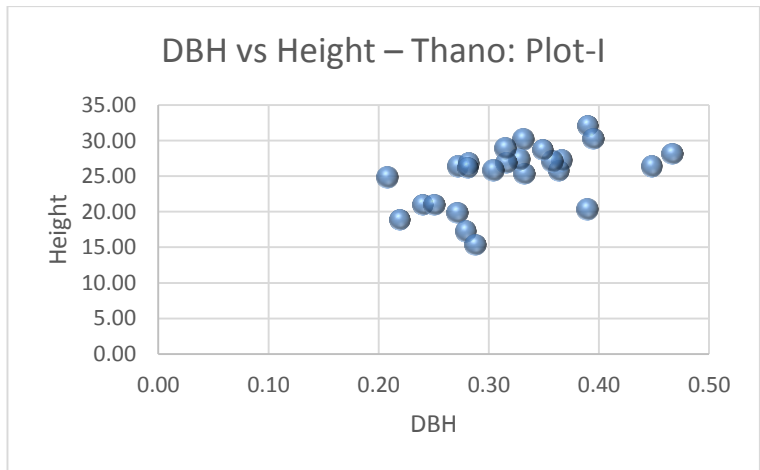


Figure 49: DBH vs Height, Thano-Plot-I

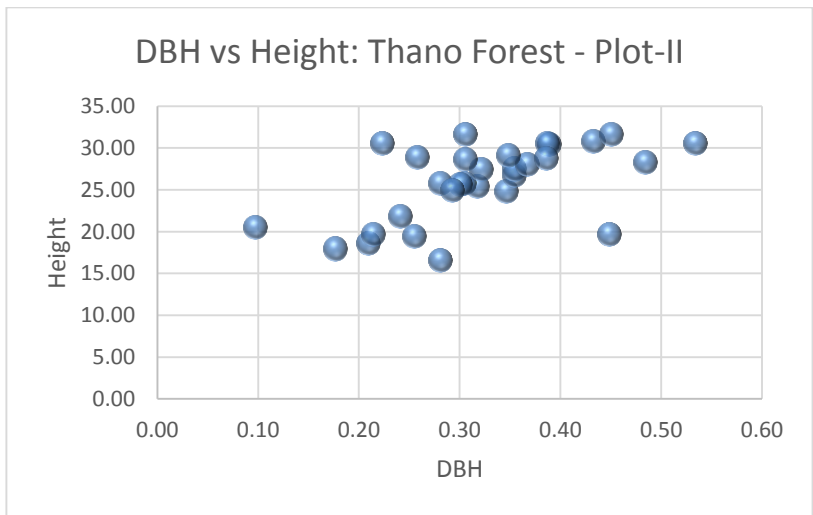


Figure 50: DBH vs Height Thano-Plot-II

5.7. Discussion

As per the yielded results in this study a positive correlation has been detected in both measured and modelled height and DBH. Though there is significant variation in the heights of trees in all four plots. For measuring tree heights Nikon Laser Range finder was used. As per the manual of the equipment for proper measurement the user need to stand at least 20 m away from the object under observation. In forest area the trees are densely located, along with the low lying bushes on the site, which restricts the clear vision on the base of the trunk. Apart from this it is also hard find a clear line of sight on the top of the canopy due to occlusion. However, the height estimation using point cloud of the trees manually in CloudCompare applications is giving almost same result as the modelled one (Figure 34). The variation in the diameter is due to the shape variation, which could be measured more accurately using best fit curve along the circumference of the trees (Figure 33). But in this project diameter was obtained using maximum distanced point in the list of points around cross section of the tree at the breast height. Therefore, for most of the trees the DBH is varying from 3-6 m approximately with a RMSE varying from 0.04 m to 0.12 m.

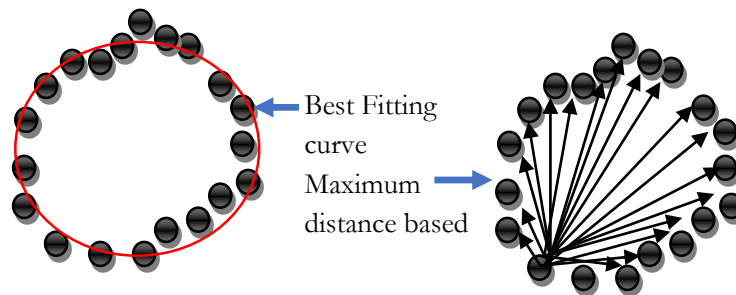


Figure 51: Methods to estimate the tree diameter

5.7.1. Limitation of the Nikon Forestry Pro Laser Rangefinder:

Measurement may result in inaccuracy or failure in the following cases(Forestry-Suppliers, 2016):

- Slender or small target
- Target has diffusing reflective surface
- Target does not reflect the laser beam to the rangefinder (glass, a mirror, etc.)
- Black target
- Target has varying depths
- In snow, rain or fog
- Target measured through glass
- Reflective surface measured from diagonal direction
- Moving target
- Obstacle moving in front of the target
- When targeting the surface of water

In case of tilted trees the measured tree heights are significantly varying with comparison to the modelled values. It is the limitation of the laser range finder. The measurements get affected due to the tilt and also

the position from where the measurements are being taken. If tree is leaning towards particular direction then the measurements comprises significant errors (“Tree Height Measurement,” 2015):

Table 13: Uncertainties in height measurements using Laser Rangefinder

100' Tree Leaning towards you			100' Tree Leaning away from you		
Degree of Lean	50' Away	100' Away	Degree of Lean	50' Away	100' Away
1 Degree	3.6%	1.8%	1 Degree	-3.4%	-1.7%
5 Degree	33.3%	9.5%	5 Degree	-14.8%	-8.0%
10 Degree	53.2%	21.0%	10 Degree	-25.8%	-14.8%
15 Degree	107.3%	34.9%	15 Degree	-34.1%	-20.6%

The heights were verified with the obtained point cloud by manual measurements, it is found the modelled heights for tilted trees are accurate.

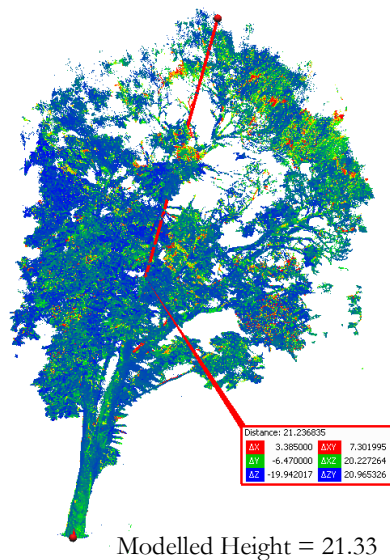
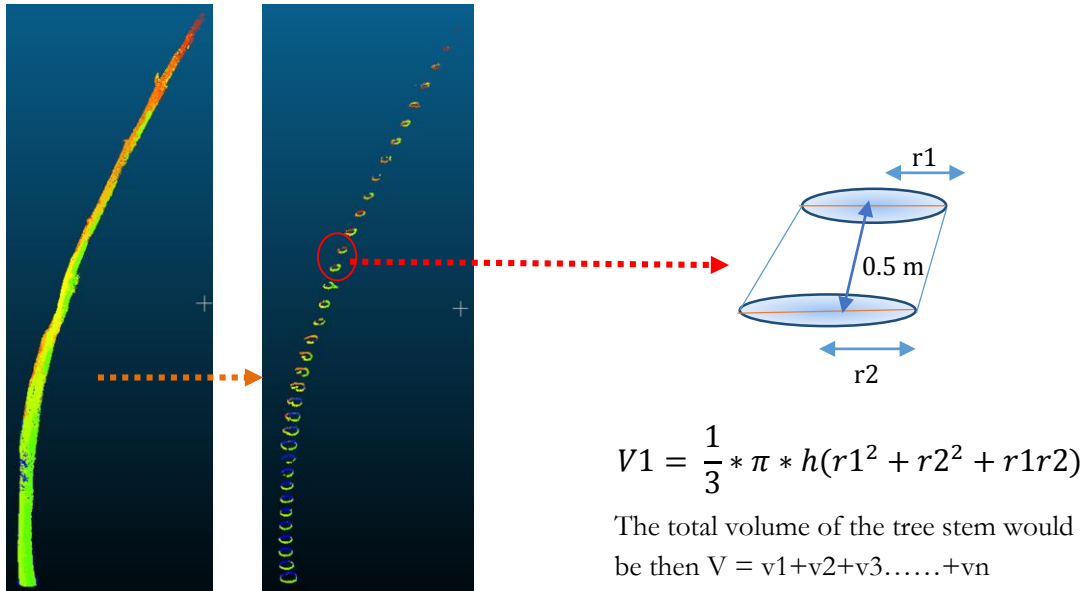


Figure 52: The measured height through the distance measurement tool in CloudCompare

5.8. Volume of the bent trees

The estimation of the heights of the bent trees were not accurate neither with the Forestry Pro equipment along with the uncertainties nor with the model. The model takes the coordinates at the minimum and maximum height on the tree point cloud. Therefore, the estimated vertical height for the bent trees would not be the accurate value. As per the field observation and manual measurement using the CloudCompare application the shape of the trees at every section of 50 cm of the tree stem is not varying much. In order to estimate the volume of such trees the whole tree could be divided into many sections at the length of each 50 cm along tree stem (Figure 50). The shape of the hollow section could be considered as the cylinder but more appropriate estimation of volume could be done using truncated cone volume equation, as tree stem becomes narrower with respect to the height. The addition of volume of all sections of the stem then added to get the volume of three. The modelling has been done by considering the stem point cloud only. The point cloud with outliers, which includes canopy, branches would not give output through this model.



BKT_9 Figure 53: The method adopted for the bending trees

The diameters are obtained using the same algorithm as explained in the Chapter-4, but instead of measuring at 1.37 m an iterative function was used to obtain the diameter at each section. The estimation starts from the cross section with the minimum z value then the list of all the points at every height such as Zmin_0.5 m then Zmin+1 m and so on, were listed out from where diameters were taken into the equation mentioned above to estimate the volume of each section. The addition of the all volumes of the section gives the total volume of the stem. The pre-requirement to use this model is to refine the point cloud before using. Since it is using list of points on the circumference vertically any outlier may affect the result. Therefore, all the branches and outliers were removed using filtration and segment tool available in the CloudCompare application. Few trees (Figure 52) from all sites which are bent or have variable shapes were taken to estimate the volume with the said algorithm. Since the field measurements were not taken especially for this case, as measuring diameter at different height on the tree was not feasible in this project. Therefore, the volume has been compared with the estimated volume using DBH only (Table 14).

Table 14: Estimated volume using algorithm for different sections at different heights and DBH

S. No.	FILE	Volume using (Eq-1) (m3)	Volume using DBH (m3)
1	T-6.txt	3.67	6.05
2	TT1_10.txt	1.13	0.71
3	TT1_2.txt	0.73	0.43
4	TT1_4.txt	1.28	0.98
5	TT1_5.txt	0.99	0.59
6	TT1_6.txt	0.50	0.31
7	TT2_5.txt	2.14	1.5

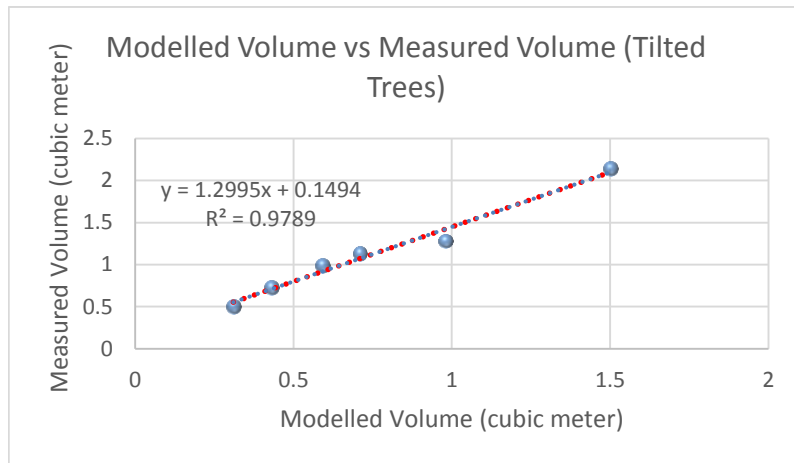


Figure 54: Correlation between modelled and measured volumes of tilted trees

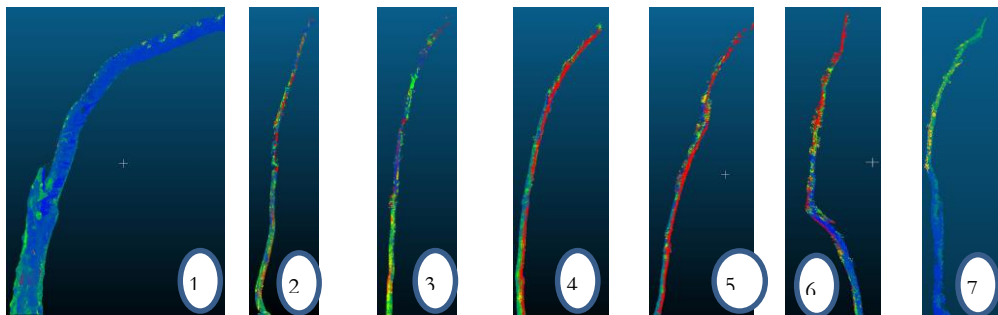


Figure 55: Bent Trees as listed in Table 27

The regression plot between modelled and measured volume for tilted trees has been shown in Figure 51, after removing T-1 as it was acting extreme outlier, which true because it is one of the most variable tree in the plot with twin stems and multiple branches and removed during filtration. The R^2 is for the volumes is coming around 0.98 which shows a positive correlation. Relative errors for each tree as listed in Table 14 are as per serial no. 65%, 37%, 41%, 23%, 40%, 38% and 30%. So it is clear from the Figure 52 that the trees with gradual bending (TT1_4) has lesser relative error (23%) with compare to others. The limitation of this algorithm is it does not consider the multiple stems or the tree with branches as in case of T-6 the branches were removed which results lesser estimation than the estimated value with DBH. A tree stem has to be freed from branches and multiple stems if any before using the algorithm. However, for addressing more variation and then estimation of the volume meshed modelling could be the solution. Therefore, for similar varying trees, surface reconstruction using triangulation was considered which is explained in the next point.

5.9. Trees with varying shapes

The site at the IIRS was taken in order to get the trees with variable shape. Few trees such as T-1 and T-6 and few trees at Thano sites as well have trees with multiple branches (Figure 53). Since the FSI based equation doesn't contain the parameters other than DBH even for the tree with the variations, the estimation of the true volume on the basis of DBH wouldn't be sufficient. Therefore, the major findings of the project are to verify and validate the retrieved tree parameters for every individual tree by considering its shape and size. Point cloud of the trees were filtered before applying the Poisson Surface Reconstruction, this plugin is available in CloudCompare to do the triangular mesh generation which was proposed by (Kazhdan & Hoppe, 2013). The octree depth was taken as 8 more the level better would be result, but the computation time increases. Some of the examples are shown below:

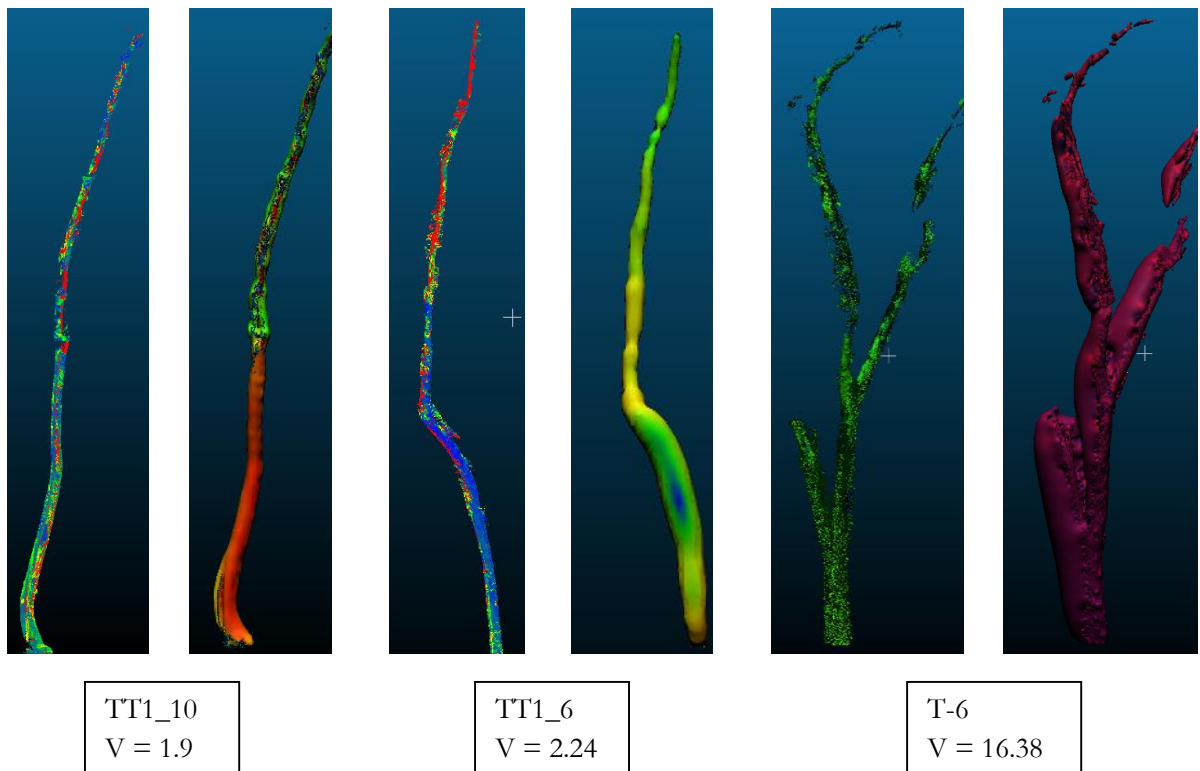


Figure 56: Meshed models of few variable trees

The volume of TT1_10 from truncated cone volume formula is 1.13 m^3 whereas by meshed model is 1.9 m^3 for TT1_6 it is 0.5 m^3 and 2.24 m^3 respectively and for T-6 it is highly varying from 3.67 m^3 to 16.38 m^3 . Because the in meshed modelling the multiple stem and branches are also considered. The overestimation is due to the over modelling of the tree shape which depends upon the parameters we are taking in the aforesaid surface reconstruction algorithm, which needs to be explored in further studies, especially in case of varying trees with multiple stems or branches.

6. CONCLUSION AND RECOMMENDATION

This research mainly aimed to retrieve the tree parameters automatically using TLS based modelling. Using obtained parameters through modelling in FSI based volumetric equation a comparative analysis has been done with the estimated volume with field measurements. The model has successfully obtained the tree parameters for both individual tree and plot wise by addressing the trees with any tilt angle vertically. The summary of the RMSE's and coefficient of determination for all four plots are mentioned in the table below:

Table 15: Summarization of the results.

S. No.	Plot	No. of Trees	Parameters (Measured/Modelled)	RMSE (m)	R ²
1	Barkot Forest Area	10	Height	3.18	0.72
			DBH	0.04	0.99
			Volume	0.45	0.99
2	IIRS Campus	7	Height	2.79	0.95
			DBH	0.12	0.90
			Volume	3.37	0.77
3	Thano Forest Range: Dataset-I	25	Height	2.7	0.97
			DBH	0.04	0.95
			Volume	0.37	0.95
4	Thano Forest Range: Dataset-II	30	Height	2.36	0.93
			DBH	0.04	0.97
			Volume	0.32	0.97

6.1. Conclusion

As per the FSI based volumetric equation the total R² for 710 sample trees was coming as 0.96. In this project the large difference is in case of the plot of IIRS which comprises the trees with variable shapes. In the result of dataset-I of Thano range is also lesser than the same because this plot also comprises many variable trees. In order to overcome this situation the bent trees and relatively less variable trees were taken and the diameters at every 0.5 m were estimated. Assuming that the considered trees are well filtered, means which has single stem, without any branches and has significant bending shape but not very irregular. In this case the obtained slices for each tree were considered as the truncated cone and using its volume formula the volume of whole tree was estimated as shown in Table 27. The obtained R² is coming around 0.98 which is again more than the R² from FSI based volumetric equation as stated before. Apart from the trees from IIRS plot many trees on other plots were found which has variable shape. This situation has been addressed using the Poisson's Surface Reconstruction method, but the trees with branches again giving drastic result.

This could be mitigate using the appropriate parameters in the tool which was used in CloudCompare application.

6.1.1. Answers of Research Questions

- **How the modelling of stem diameter can be ensured in case of data gaps due to occlusion and extreme tree shape variation?**

The scanning has been carried out from the five position on each and every plot of size 31.6 mx31.6 m. One position was at the center and rest four at the corners of the plot in order to minimize occlusion. However, very few trees along the edges and which were covered with long bushes were ignored in the project. Some trees with covered bushes however were filtered in order to get the tree point cloud. The most of the trees including trees with variable shape has more than 200 thousand points and the point cloud at the breast height also was sufficient. The bent trees and trees with variable shaped were addressed using the algorithm for obtaining diameters at different heights and by triangulation to do surface reconstruction for volume estimation.

- **Identification of the appropriate linear or polynomial function of the interpolation of the irregularities of stem circumference?**

The interpolation has not been done in this project. Instead of using best fit curve along the circumference in order to estimate DBH, the algorithm addresses the farthest distance method among the points on the cross section of stem at 1.37m. The algorithm gives overestimated DBH as per individual measurement but overall RMSE is coming 0.04 m for all the plots with R^2 varying from 0.90 to 0.99 which may consider as a good result.

- **The projection of the underestimated or overestimated measurement could be mitigated via using correction factor in appropriate function but how can the obtained values will be validated?**

Taking one plot as an example the average uncertainty in the field measured DBH is coming around 0.003 m and the average relative error between field based and TLS based DBH is 0.1 m. Therefore, there is no true data available for the validation in this project. However, as per this project objective if TLS based parameters are considered as the nearer to the true value the residual between predicted volume and TLS based volume is coming 0.33 m^3 (Figure 54). May this could be taken as the uncertainty during estimation of the volume using linear equation of the predicted volume.

6.2. Recommendations

Extracting individual trees and removing outliers were the major tasks in this project to use in the algorithm to retrieve parameters. After removing the ground point cloud there is need to find a way with which automatically tree stem could be detected and extracted. Srinivasan et al., 2015, have created a ‘Map Trees’ tool in Python to map the trees using map centre and a height bin varying from 1 m to 1.6 m, which was used to get the DBH of the trees. For woody biomass estimation it is necessary to segment out the tree stem along with the branches. Similar research has been carried out by Hackenberg et al., 2014, wherein, for describing the branching and stem structure they have used fitting cylinder as a hierarchical tree-like data structure, it detects as per the tree’s direction of growth, which was the initial approach in this project but couldn’t be implemented. For plot wise estimation of tree volume especially when we are considering that the plot has trees with homogeneous height, after extraction of DTM, the A slice of point cloud at breast height could be segmented out and converted into raster image by fixing the full extent scale. Projected raster image in grey scale the operators for gradient detection or algorithms like Hough Transformation for circle detection could be used to detect the circumference of the stem in order to get the DBH for each and every tree in the plot (Huabing Huang et al., 2011)(Olofsson et al., 2014b). The field measurements specially height measurement comprises significant errors as the laser range finder are sensitive to the range as well the site condition such as high density, low lying bushes, merged canopies, tilted and bent trees, occlusion etc. Therefore, the validation of the height measurements shall be done with the available measurements from airborne datasets which may have precise and close to the accurate parameters (Leitold et al., 2015).

Some of the open sources applications are very useful especially for the forest inventories. SimpleTree is one of them, which is capable of modelling the cylindrical tree models accurately. The segmentation of the stems and branches as per the required parameters then canopy segmentation along with the estimation of stem volume are just the click away in the SimpleTree interface. Hackenberg et al., 2015, have validated the same using 101 point cloud datasets of six species. The obtained parameters were validated with the ground truth and the coefficient of determination (R^2) was coming around 0.92 with maximum 8% of relative error. Another open source platform is Computree which is also capable of DTM extraction on a plot level, the detection of stem using circle fittings comprising Hough Transformation algorithm along with the DBH estimator, stem skeleton and the height of the detected trees (Computree, 2016). PypeTree(Delagrang, Jauvin, & Rochon, 2014), is another open-source for visual modelling of the environment, PCL (pcl, 2016), Meshlab(MeshLab, 2016), Paraview(Paraview, 2016) are some of the useful open-sources are also available for dealing with the point clouds. The difficulty comes in aforesaid open-source applications is the compatibility, the required dependencies are highly sensitive or specific to the environment.

REFERENCES:

- 3D Laser Mapping Ltd. (2016). RiSCAN PRO Data Registration Guide. Retrieved from https://s3-eu-west-1.amazonaws.com/3dlmsitecontent/police/documents/RiSCAN_PRO_DataRegistrationGuide_v2_low-res.pdf
- Adhikari, M. (2005). *A Non-destructive Approach for Quantitative Assessment of Tree Resources Outside the Forest*. Retrieved from https://www.itc.nl/library/papers_2005/msc/nrm/adhikari.pdf
- Bae, K. H., & Lichti, D. D. (2004). Automated registration of unorganised point clouds from terrestrial laser scanners. *Update*, 35, 222–227. Retrieved from <http://citeseerx.ist.psu.edu/viewdoc/download?doi=10.1.1.2.3606&rep=rep1&type=pdf>
- Barbakh, W. A., Wu, Y., & Fyfe, C. (2009). Review of Clustering Algorithms, Non-Standard Parameter Adaptation for Exploratory Data Analysis (p. 223). Springer Science & Business Media. Retrieved from https://books.google.com/books?id=4GshTn_SuGYC&pgis=1
- Beguet, B., Guyon, D., Boukir, S., & Chehata, N. (2014). Automated retrieval of forest structure variables based on multi-scale texture analysis of VHR satellite imagery. *ISPRS Journal of Photogrammetry and Remote Sensing*, 96, 164–178. <http://doi.org/10.1016/j.isprsjprs.2014.07.008>
- C. R. Kennedy. (2015). *C.R. Kennedy Training Program for Riegl RiScan Pro - Multi Station Adjustment Using the Plane Patch Filter*. Retrieved from <https://www.youtube.com/watch?v=MDnqP5KV5eA>
- Cazals, F., & Giesen, J. (2004). *Delaunay Triangulation Based Surface Reconstruction*. Retrieved from <http://www.cs.jhu.edu/~misha/Fall13b/Papers/Cazals06.pdf>
- Charles. (2011). Top 10 countries interested in biomass energy. Retrieved July 30, 2015, from <http://www.biomass-energy.org/2011/09/top-10-countries-interested-in-biomass-energy/>
- Computree. (2016). Computree : Forest inventory with Lidar (ONF). Retrieved March 1, 2016, from <http://computree.onf.fr/?lang=en>
- Dassot, M., Constant, T., & Fournier, M. (2011a). The use of terrestrial LiDAR technology in forest science: application fields, benefits and challenges. *Annals of Forest Science*, 68(5), 959–974. <http://doi.org/10.1007/s13595-011-0102-2>
- Dassot, M., Constant, T., & Fournier, M. (2011b). The use of terrestrial LiDAR technology in forest science: application fields, benefits and challenges. *Annals of Forest Science*, 68(5), 959–974. <http://doi.org/10.1007/s13595-011-0102-2>
- Delagrangé, S., Jauvin, C., & Rochon, P. (2014). PypeTree: a tool for reconstructing tree perennial tissues from point clouds. *Sensors (Basel, Switzerland)*, 14(3), 4271–89. <http://doi.org/10.3390/s140304271>
- Ferretti, M. (2013). Forest Monitoring: Methods for terrestrial investigations in Europe with an overview of North America and Asia (p. 536). Newnes. Retrieved from <https://books.google.com/books?id=x7RsgxYjXNgC&pgis=1>

- Forestry-Suppliers. (2016). Forestry Pro: Instruction Manual. Retrieved from http://www.forestry-suppliers.com/Documents/1345_msds.pdf
- FSI. (1996). *Volume Equations for Forests of India, Nepal, and Bhutan*. Forest Survey of India, Ministry of Environment & Forests, Government of India. Retrieved from https://books.google.co.in/books/about/Volume_Equations_for_Forests_of_India_Ne.html?id=k5jztgAACAAJ&pgis=1
- Gibbs, H. K., Brown, S., Niles, J. O., & Foley, J. A. (2007). Monitoring and estimating tropical forest carbon stocks: making REDD a reality. *Environmental Research Letters*, 2(4), 045023. <http://doi.org/10.1088/1748-9326/2/4/045023>
- Giri, N., & Rawat, L. (2013). Assessment of biomass carbon stock in an *Ailanthus excelsa* Roxb. plantation Uttarakhand, India. Retrieved from [http://www.academicjournals.org/article/article1385119288_Giri and Rawat.pdf](http://www.academicjournals.org/article/article1385119288_Giri%20and%20Rawat.pdf)
- Guarnieri, a, Vettore, A., Pirotti, F., & Marani, M. (2009). Filtering of TLS point clouds for the generation of DTM in salt-marsh areas. *Laser Scanning*, XXXVIII(Part 3/W8), 293–298.
- Hackenberg, J., Morhart, C., Sheppard, J., Spiecker, H., & Disney, M. (2014). Highly accurate tree models derived from terrestrial laser scan data: A method description. *Forests*, 5, 1069–1105. <http://doi.org/10.3390/f5051069>
- Hackenberg, J., Spiecker, H., Calders, K., Disney, M., & Raunonen, P. (2015). SimpleTree —An Efficient Open Source Tool to Build Tree Models from TLS Clouds. *Forests*, 6(11), 4245–4294. <http://doi.org/10.3390/f6114245>
- Hast, A., & Nysjö, J. (2013). Optimal RANSAC - Towards a Repeatable Algorithm for Finding the Optimal Set. *Journal of WSCG*, 21(1), 21–30. Retrieved from <http://uu.diva-portal.org/smash/record.jsf?pid=diva2:624363&cdswid=7948>
- Hough Transform. (2015). Retrieved November 2, 2015, from https://en.wikipedia.org/wiki/Hough_transform
- Huang, H., Li, Z., Gong, P., Cheng, X., Clinton, N., Cao, C., ... Wang, L. (2011). Automated Methods for Measuring DBH and Tree Heights with a Commercial Scanning Lidar. *Photogrammetric Engineering and Remote Sensing*, 77(3), 219–227. Retrieved from http://apps.webofknowledge.com/full_record.do?product=UA&search_mode=GeneralSearch&qid=1&SID=V1aRdc1dNfc4BYqPOUS&page=1&doc=1
- Huang, H., Tang, L., & Chen, C. (2015). A 3D individual tree modeling technique based on terrestrial LiDAR point cloud data. In *2015 2nd IEEE International Conference on Spatial Data Mining and Geographical Knowledge Services (ICSDM)* (pp. 152–156). IEEE. <http://doi.org/10.1109/ICSDM.2015.7298043>
- Hyyppä, J., & Hallikainen, M. (1996). Applicability of airborne profiling radar to forest inventory. *Remote Sensing of Environment*, 57(1), 39–57. [http://doi.org/10.1016/0034-4257\(95\)00254-5](http://doi.org/10.1016/0034-4257(95)00254-5)
- Johansen, K., Coops, N. C., Gergel, S. E., & Stange, Y. (2007). Application of high spatial resolution satellite imagery for riparian and forest ecosystem classification. *Remote Sensing of Environment*, 110(1), 29–44.

- <http://doi.org/10.1016/j.rse.2007.02.014>
- Joseph, G. (2005). *Fundamentals of Remote Sensing*. Universities Press. Retrieved from <https://books.google.com/books?id=peUFLCy4zLYC&pgis=1>
- Jung, S.-E., Kwak, D.-A., Park, T., W.-K., L., & Yoo, S. (2011). Estimating Crown Variables of Individual Trees Using Airborne and Terrestrial Laser Scanners. *Remote Sens*, 3, 2346–2363. Retrieved from <http://www.mdpi.com/2072-4292/3/11/2346/>
- Kato, A., Moskal, L. M., Schiess, P., Swanson, M. E., Calhoun, D., & Stuetzle, W. (2009). Capturing tree crown formation through implicit surface reconstruction using airborne lidar data. *Remote Sensing of Environment*, 113(6), 1148–1162. <http://doi.org/10.1016/j.rse.2009.02.010>
- Kazhdan, M., & Hoppe, H. (2013). Screened poisson surface reconstruction. *ACM Transactions on Graphics*, 32(3), 1–13. <http://doi.org/10.1145/2487228.2487237>
- Kelbe, D., & Romanczyk, P. (2012). Automatic extraction of tree stem models from single terrestrial lidar scans in structurally heterogeneous forest environments. *Proceedings of ...*, (September), 1–8. Retrieved from http://www.researchgate.net/publication/257196149_Automatic_extraction_of_tree_stem_models_from_single_terrestrial_lidar_scans_in_structurally_heterogeneous_forest_environments/file/9c9605249c53a7eed3.pdf
- Koch, B. (n.d.). Remote Sensing supporting national forest inventories NFA, 1–18.
- Labatut, P., Pons, J.-P., & Keriven, R. (2009). Hierarchical shape-based surface reconstruction for dense multi-view stereo. *IEEE 12th International Conference on Computer Vision Workshops (ICCV Workshops)*, 1598–1605. <http://doi.org/10.1109/ICCVW.2009.5457421>
- Latifi, H., Fassnacht, F. E., Müller, J., Tharani, A., Dech, S., & Heurich, M. (2015). Forest inventories by LiDAR data: A comparison of single tree segmentation and metric-based methods for inventories of a heterogeneous temperate forest. *International Journal of Applied Earth Observation and Geoinformation*, 42, 162–174. <http://doi.org/10.1016/j.jag.2015.06.008>
- Lau, C. L., Halim, S., Zulkepli, M., Azwan, A. M., Tang, W. L., & Chong, A. K. (2015). Terrain Extraction By Integrating Terrestrial Laser Scanner Data and Spectral Information. *ISPRS - International Archives of the Photogrammetry, Remote Sensing and Spatial Information Sciences*, XL-2/W4(October), 45–51. <http://doi.org/10.5194/isprsarchives-XL-2-W4-45-2015>
- Launchbaugh, K. (2009). Why Measure Biomass or Production? Retrieved November 28, 2015, from [http://www.webpages.uidaho.edu/veg_measure/Modules/Lessons/Module7\(Biomass&Utilization\)/7_2_Why Measure Biomass.htm](http://www.webpages.uidaho.edu/veg_measure/Modules/Lessons/Module7(Biomass&Utilization)/7_2_Why Measure Biomass.htm)
- Leitold, V., Keller, M., Morton, D. C., Cook, B. D., & Shimabukuro, Y. E. (2015). Airborne lidar-based estimates of tropical forest structure in complex terrain: opportunities and trade-offs for REDD+. *Carbon Balance and Management*, 10(1), 3. <http://doi.org/10.1186/s13021-015-0013-x>
- Lim, S., & Haron, H. (2012). Surface reconstruction techniques: a review. *Artificial Intelligence Review*, (JUNE 2012). <http://doi.org/10.1007/s10462-012-9329-z>
- Maan, G. S., Singh, C. K., Singh, M. K., & Nagarajan, B. (2014). Tree species biomass and carbon stock

- measurement using ground based-LiDAR. *Geocarto International*, 6049(July), 1–18. <http://doi.org/10.1080/10106049.2014.925003>
- MeshLab. (2016). MeshLab. Retrieved March 1, 2016, from <http://meshlab.sourceforge.net/>
- Mitra, N. J., Gelfand, N., Pottmann, H., & Guibas, L. (2004). Registration of point cloud data from a geometric optimization perspective. *SGP '04: Proceedings of the 2004 Eurographics/ACM SIGGRAPH Symposium on Geometry Processing*, 22. <http://doi.org/10.1145/1057432.1057435>
- Mohren, G. M. J., Hasenauer, H., Köhl, M., & Nabuurs, G. J. (2012). Forest inventories for carbon change assessments. *Current Opinion in Environmental Sustainability*, 4, 686–695. <http://doi.org/10.1016/j.cosust.2012.10.002>
- Montagnoli, A., Fusco, S., Terzaghi, M., Kirschbaum, A., Pflugmacher, D., Cohen, W. B., ... Chiatante, D. (2015). Estimating forest aboveground biomass by low density lidar data in mixed broad-leaved forests in the Italian Pre-Alps. *Forest Ecosystems*, 2(1), 10. <http://doi.org/10.1186/s40663-015-0035-6>
- Morel, A. C., Saatchi, S. S., Malhi, Y., Berry, N. J., Banin, L., Burslem, D., ... Ong, R. C. (2011). Estimating aboveground biomass in forest and oil palm plantation in Sabah, Malaysian Borneo using ALOS PALSAR data. *Forest Ecology and Management*, 262(9), 1786–1798. <http://doi.org/10.1016/j.foreco.2011.07.008>
- Morgan, J. L., Gergel, S. E., & Coops, N. C. (2010). Aerial Photography : A Rapidly Evolving Tool for Ecological Management, 60(1), 47–59. <http://doi.org/10.1525/bio.2010.60.1.9>
- Moskal, L. M., & Zheng, G. (2011). Retrieving Forest Inventory Variables with Terrestrial Laser Scanning (TLS) in Urban Heterogeneous Forest. *Remote Sensing*, 4(12), 1–20. <http://doi.org/10.3390/rs4010001>
- Mursa, P. (2013). Forest Parameter Estimation by Lidar Data Processing. *RevCAD Journal of Geodesy and Cadastre*, 14, 27–36. Retrieved from http://www.uab.ro/geocad/upload/33_319_Paper5_RevCAD14_2013.pdf
- Olofsson, K., Holmgren, J., & Olsson, H. (2014a). Tree Stem and Height Measurements using Terrestrial Laser Scanning and the RANSAC Algorithm. *Remote Sensing*, 6(5), 4323–4344. <http://doi.org/10.3390/rs6054323>
- Olofsson, K., Holmgren, J., & Olsson, H. (2014b). Tree Stem and Height Measurements using Terrestrial Laser Scanning and the RANSAC Algorithm. *Remote Sensing*, 6(5), 4323–4344. <http://doi.org/10.3390/rs6054323>
- Otto, H.-J. (1998). *Écologie Forestière*. Paris: Institut pour le Développement Forestier.
- Pal, I. (2008). Measurements Of Forest Inventory Parameters On Terrestrial. Retrieved from http://www.isprs.org/proceedings/XXXVII/congress/3b_pdf/73.pdf
- Paraview. (2016). ParaView. Retrieved March 1, 2016, from <http://www.paraview.org/>
- Park, H., Lim, S., Trinder, J. C., & Turner, R. (2010). Voxel-based volume modelling of individual trees using terrestrial laser scanners. <http://doi.org/10.1016/j.compag.2012.09.017>
- Pasolli, L., Asam, S., Castelli, M., Bruzzone, L., Wohlfahrt, G., Zebisch, M., & Notarnicola, C. (2015). Retrieval of Leaf Area Index in mountain grasslands in the Alps from MODIS satellite imagery. *Remote*

- Sensing of Environment*, 165, 159–174. <http://doi.org/10.1016/j.rse.2015.04.027>
- pcl. (2016). Downloads - Point Cloud Library (PCL). Retrieved March 1, 2016, from <http://pointclouds.org/downloads/>
- Peregon, A., & Yamagata, Y. (2013). The use of ALOS/PALSAR backscatter to estimate above-ground forest biomass: A case study in Western Siberia. *Remote Sensing of Environment*, 137, 139–146. <http://doi.org/10.1016/j.rse.2013.06.012>
- Poisson Surface Reconstruction. (2016). Retrieved February 27, 2016, from http://vr.tu-freiberg.de/scivi/?page_id=365
- Pratihast, A. K. (2010). *3D tree modelling using mobile laser scanning data*. Retrieved from https://www.itc.nl/library/papers_2010/msc/gfm/pratihast.pdf
- Rabbani, T., & Heuvel, F. van den. (2005). Efficient Hough Transform For Automatic Detection Of Cylinders In Point Clouds. Retrieved from <http://www.isprs.org/proceedings/XXXVI/3-W19/papers/060.pdf>
- Romanczyk, P., van Aardt, J., Cawse-Nicholson, K., Kelbe, D., McGlinchy, J., & Krause, K. (2014). Assessing the impact of broadleaf tree structure on airborne full-waveform small-footprint LiDAR signals through simulation. *Canadian Journal of Remote Sensing*, 39(sup1), S60–S72. <http://doi.org/10.5589/m13-015>
- Rosette, J., North, P. R. J., Rubio-Gil, J., Cook, B., Los, S., Suarez, J., ... Blair, J. B. (2013). Evaluating Prospects for Improved Forest Parameter Retrieval From Satellite LiDAR Using a Physically-Based Radiative Transfer Model. *IEEE Journal of Selected Topics in Applied Earth Observations and Remote Sensing*, 6(1), 45–53. <http://doi.org/10.1109/JSTARS.2013.2244199>
- Rosillo-Calle, F., & Woods, J. (2012). *The Biomass Assessment Handbook* (Vol. 3). Taylor & Francis. Retrieved from <https://books.google.com/books?id=WvdcLmvt3Vkc&pgis=1>
- Schilling, A., Schmidt, A., & Maas, H.-G. (2012). Tree Topology Representation from TLS Point Clouds Using Depth-First Search in Voxel Space. *Photogrammetric Engineering & Remote Sensing*, 78(4), 383–392. <http://doi.org/10.14358/PERS.78.4.383>
- Sexton, J. O., Bax, T., Siqueira, P., Swenson, J. J., & Hensley, S. (2009). A comparison of lidar, radar, and field measurements of canopy height in pine and hardwood forests of southeastern North America. *Forest Ecology and Management*, 257(3), 1136–1147. <http://doi.org/10.1016/j.foreco.2008.11.022>
- Shaw, C. H., Bona, K. A., Kurz, W. A., & Fyles, J. W. (2015). The importance of tree species and soil taxonomy to modeling forest soil carbon stocks in Canada. *Geoderma Regional*, 4, 114–125. <http://doi.org/10.1016/j.geodrs.2015.01.001>
- Shi, J., Du, Y., Du, J., Jiang, L., Chai, L., Mao, K., ... Wang, Y. (2012). Progresses on microwave remote sensing of land surface parameters. *Science China Earth Sciences*, 55(7), 1052–1078. <http://doi.org/10.1007/s11430-012-4444-x>
- Sierra, C. A., del Valle, J. I., Orrego, S. A., Moreno, F. H., Harmon, M. E., Zapata, M., ... Benjumea, J. F. (2007). Total carbon stocks in a tropical forest landscape of the Porcè region, Colombia. *Forest Ecology*

- and Management*, 243(2-3), 299–309. <http://doi.org/10.1016/j.foreco.2007.03.026>
- Singh, N. (2014). *Impact of infestation of Sal Heartwood Borer (Hoplocerambyx spinicornis) on the carbon stock of Sal (Shorea robusta) forests of Doon valley*. Retrieved from http://www.iirs.gov.in/iirs/sites/default/files/StudentThesis/Singh_Neha_Thesis.pdf
- Sithole, P. T. (2005). *Segmentation and Classification of Airborne Laser Scanner data*. Delft University. Retrieved from http://repository.tudelft.nl/assets/uuid:64c82a6e-6db0-4457-9c4f-2446653e5b9d/ae_sithole_20050524.pdf
- Smith, A., Astrup, R., Raunonen, P., Liski, J., Krooks, A., Kaasalainen, S., ... Kaasalainen, M. (2014). Tree Root System Characterization and Volume Estimation by Terrestrial Laser Scanning and Quantitative Structure Modeling. *Forests*, 5(12), 3274–3294. <http://doi.org/10.3390/f5123274>
- Srinivasan, S., Popescu, S., Eriksson, M., Sheridan, R., & Ku, N.-W. (2015). Terrestrial Laser Scanning as an Effective Tool to Retrieve Tree Level Height, Crown Width, and Stem Diameter. *Remote Sensing*, 7(2), 1877–1896. <http://doi.org/10.3390/rs70201877>
- Stewart, C. V. (1997). Bias in robust estimation caused by discontinuities and multiple structures. *IEEE Transactions on Pattern Analysis and Machine Intelligence*, 19(8), 818–833. <http://doi.org/10.1109/34.608280>
- Su, Y.-T., & Bethel, J. (2010). Detection And Robust Estimation Of Cylinder Features In Point Clouds. *Asprs*. Retrieved from <http://www.asprs.org/a/publications/proceedings/sandiego2010/sandiego10/Su.pdf>
- Su, Y.-T., Bethel, J., & Hu, S. (2016). Octree-based segmentation for terrestrial LiDAR point cloud data in industrial applications. *ISPRS Journal of Photogrammetry and Remote Sensing*, 113, 59–74. <http://doi.org/10.1016/j.isprsjprs.2016.01.001>
- Suárez, J. C., Ontiveros, C., Smith, S., & Snape, S. (2005). Use of airborne LiDAR and aerial photography in the estimation of individual tree heights in forestry. *Computers & Geosciences*, 31(2), 253–262. <http://doi.org/10.1016/j.cageo.2004.09.015>
- Sun, G., Ni, W., Hall, F., Masek, J., Fatoyinbo, T., & Peddle, D. (2013). Retrieval Of Forest Biophysical Parameters Using Physically-Based Algorithms 1 . Department of Geographical Sciences , University of Maryland , College Park , MD 20742 , USA 2 . University of Maryland Baltimore County , 1000 Hilltop Cir , Baltimore , MD 2, (i), 2621–2624.
- Sykes, A. O. (2016). *An Introduction to Regression Analysis*. Retrieved from http://www.law.uchicago.edu/files/files/20.Sykes_.Regression.pdf
- T. Vashum, K. (2012). Methods to Estimate Above-Ground Biomass and Carbon Stock in Natural Forests - A Review. *Journal of Ecosystem & Ecography*, 02(04). <http://doi.org/10.4172/2157-7625.1000116>
- Tanase, M. A., Panciera, R., Lowell, K., Tian, S., Hacker, J. M., & Walker, J. P. (2014). Airborne multi-temporal L-band polarimetric SAR data for biomass estimation in semi-arid forests. *Remote Sensing of Environment*, 145, 93–104. <http://doi.org/10.1016/j.rse.2014.01.024>
- Tree Height Measurement.. Retrieved December 30, 2015, from <http://www.lasertech.com/Tree-Height->

Measurement.aspx

- van Leeuwen, M., & Nieuwenhuis, M. (2010). Retrieval of forest structural parameters using LiDAR remote sensing. *European Journal of Forest Research*, 129(4), 749–770. <http://doi.org/10.1007/s10342-010-0381-4>
- Vohland, M., Stoffels, J., Hau, C., & Schüler, G. (2007). Remote sensing techniques for forest parameter assessment: Multispectral classification and linear spectral mixture analysis. *Silva Fennica*, 41(3), 441–456.
- West, P. W. (2009). *Tree and Forest Measurement*. Berlin, Heidelberg: Springer Berlin Heidelberg. <http://doi.org/10.1007/978-3-540-95966-3>
- Why use BIOMASS? (2015). Retrieved July 29, 2015, from http://www.biomassenergycentre.org.uk/portal/page?_pageid=76,15068&_dad=portal&_schema=PORTAL
- Wimmer, A., Schardt, M., Ziegler, M., Ruppert, G., Granica, K., Schmitt, U., ... Hyypä, J. (2000). Forest inventory by means of satellite remote sensing and laser scanning. *International Archives of Photogrammetry and Remote Sensing*, XXXIII, Pa, 1316–1324.
- Wu, L. L., Feng, Z. K., Luo, X., & Deng, X. R. (2008). Study On Application Of Three-Dimensional Laser Scanning Imaging System In Tree Measuring. Retrieved from http://www.isprs.org/proceedings/XXXVII/congress/1_pdf/45.pdf
- Wulder, M. (1998). Optical remote-sensing techniques for the assessment of forest inventory and biophysical parameters. *Progress in Physical Geography*, 22(4), 449–476. <http://doi.org/10.1177/030913339802200402>
- Yao, T., Yang, X., Zhao, F., Wang, Z., Zhang, Q., Jupp, D., ... Strahler, A. (2011). Measuring forest structure and biomass in New England forest stands using Echidna ground-based lidar. *Remote Sensing of Environment*, 115(11), 2965–2974. <http://doi.org/10.1016/j.rse.2010.03.019>
- Yao, W., Krzystek, P., & Heurich, M. (2012). Tree species classification and estimation of stem volume and DBH based on single tree extraction by exploiting airborne full-waveform LiDAR data. *Remote Sensing of Environment*, 123, 368–380. <http://doi.org/10.1016/j.rse.2012.03.027>
- Yu, X., Liang, X., Hyypä, J., Kankare, V., Vastaranta, M., & Holopainen, M. (2013). Stem biomass estimation based on stem reconstruction from terrestrial laser scanning point clouds. *Remote Sensing Letters*, 4(4), 344–353. <http://doi.org/10.1080/2150704X.2012.734931>
- Zhang, X., & Ni-meister, W. (2014). Biophysical Applications of Satellite Remote Sensing. In J. M. Hanes (Ed.), (pp. 63–98). Berlin, Heidelberg: Springer Berlin Heidelberg. <http://doi.org/10.1007/978-3-642-25047-7>
- Zhao, K., García, M., Liu, S., Guo, Q., Chen, G., Zhang, X., ... Meng, X. (2015). Terrestrial lidar remote sensing of forests: Maximum likelihood estimates of canopy profile, leaf area index, and leaf angle distribution. *Agricultural and Forest Meteorology*, 209-210, 100–113. <http://doi.org/10.1016/j.agrformet.2015.03.008>

APPENDIX A: TABLES OF THE FIELD MEASUREMENTS AND ITS UNCERTAINTY

A.1 Uncertainty in Barkot Forest Area

S. No.	Tree Name	Height		Circumference	
		Average	Uncertainty	Average	Uncertainty
1	BKT_1	32.88	0.9	1.05	0.01
2	BKT_3	32.90	1	1.35	0.004
3	BKT_5	30.27	1.7	1.56	0.02
4	BKT_7	31.22	1.5	1.12	0.01
5	BKT_12	30.05	0.75	1.24	0.01
6	BKT_13	33.80	1.2	1.67	0.01
7	BKT_15	30.72	1.3	1.15	0.01
8	BKT_25	31.14	1.8	1.38	0.004
9	BKT_27	32.86	2.3	2.48	0.01
10	BKT_28	33.06	1.4	2.17	0.06
	Average	31.89	1.39	1.52	0.01

A.2 Uncertainty in IIRS

S. No.	Tree Name	Height		Circumference	
		Average	Uncertainty	Average	Uncertainty
1	GT-1	15.14	1	2.24	0.04
2	GT-2	16.76	0.3	0.98	0
3	GT-3	22.60	1.7	1.15	0.01
4	GT-4	22.28	1.2	2.35	0.035
5	GT-5	23.86	0.6	1.01	0.005
6	GT-6	26.16	2.2	2.09	0.1
7	GT-7	23.66	1	1.41	0.01
	Average	21.49	1.14	1.60	0.03

A.3 Uncertainty in Thano Forest Range: Plot-I

S. No.	Tree Name	Height		Circumference	
		Average	Uncertainty	Average	Uncertainty
1	TT1-2	24.86	1	0.65	0.004
2	TT1-7	20.40	0.62	1.22	0.075
3	TT1-13	25.38	1.02	1.04	0.13
4	TT1-17	25.81	1	1.14	0.1
5	TT1-19	26.49	0.8	1.41	0.01
6	TT1-21	21.01	1.1	0.75	0.006
7	TT1-22	26.41	0.62	0.85	0.004
8	TT1-23	19.94	1	0.85	0.005
9	TT1-24	26.85	0.7	0.88	0.005
10	TT1-25	27.43	1.025	1.03	0.06
11	TT1-27	30.26	1.35	1.04	0.04
12	TT1-28	27.29	0.62	1.15	0.0215
13	TT1-29	26.96	0.5	0.99	0.01
14	TT1-30	28.18	1	1.46	0.06
15	TT1-31	18.93	0.7	0.69	0.01
16	TT1-32	32.17	1.255	1.22	0.005
17	TT1-33	29.00	1.12	0.99	0.0155
18	TT1-34	21.06	1.6	0.79	0.005
19	TT1-35	27.11	0.82	1.12	0.005
20	TT1-36	25.89	0.7	0.95	0.009
21	TT1-38	30.29	1.3	1.24	0.01
22	TT1-39	17.26	0.85	0.88	0.005
23	TT1-42	28.76	1.11	1.09	0.02
24	TT1-43	26.22	0.62	0.88	0.003
25	TT1-45	15.41	0.5	0.90	0.005
Average		25.18	0.92	1.01	0.02

A.4 Uncertainty in Thano Forest Range: Plot-II

S. No.	Tree Name	Height		Circumference	
		Average	Uncertainty	Average	Uncertainty
1	TT2_5	24.89	1.11	1.09	0.025
2	TT2-6	18.66	0.7	0.66	0.005
3	TT2-8	21.86	1.7	0.76	0.005
4	TT2-10	25.49	1.18	0.99	0.015
5	TT2-13	26.56	0.8	0.96	0.001
6	TT2-15	16.64	0.6	0.88	0.005
7	TT2-16	25.83	1.12	0.95	0.004
8	TT2-17	26.75	1.12	1.11	0.02
9	TT2-18	27.55	0.825	1.11	0.02
10	TT2-20	28.29	0.82	1.52	0.015
11	TT2-21	30.53	1.62	1.22	0.02
12	TT2-22	25.83	1.3	0.88	0.006
13	TT2-23	30.65	1.3	1.21	0.015
14	TT2-25	19.67	1.48	1.41	0.01
15	TT2-26	25.70	0.7	0.94	0.004
16	TT2-27	28.07	1.01	1.15	0.004
17	TT2-29	28.74	0.9	1.21	0.005
18	TT2-30	19.67	0.7	0.67	0.004
19	TT2-31	30.78	1.1	1.36	0.005
20	TT2-33	27.50	0.8	1.01	0.01
21	TT2-34	20.50	1.3	0.31	0.005
22	TT2-35	28.64	0.85	0.96	0.006
23	TT2-36	31.66	1.3	31.66	1.3
24	TT2-37	30.57	0.82	1.41	0.005
25	TT2-38	30.57	1.6	1.67	0.013
26	TT2-40	25.02	1	0.70	0.01
27	TT2-41	29.15	1.05	0.92	0.008
28	TT2-42	19.54	1.2	1.09	0.01
29	TT2-43	28.92	1.7	0.80	0.004
30	TT2-44	17.99	0.75	0.81	0.006
Average		25.74	1.08	2.05	0.05

APPENDIX B: PREDICTED VOLUME RESIDUAL AND PROBABILITY TABLES

B.1 PV Residual and Probability Table: Barkot Forest Area

RESIDUAL OUTPUT				PROBABILITY OUTPUT	
Modelled					
Observation	PV	Res	St. Res	Percentile	Volume
1	1.08	0.33	0.88	5	1.40
2	2.46	-0.20	-0.53	15	1.41
3	3.44	-0.43	-1.14	25	1.45
4	1.06	0.34	0.90	35	1.77
5	1.71	0.06	0.16	45	2.26
6	3.93	-0.50	-1.32	55	2.33
7	1.16	0.30	0.78	65	3.01
8	2.57	-0.23	-0.61	75	3.43
9	8.53	0.61	1.60	85	6.29
10	6.56	-0.28	-0.72	95	9.13
Measured					
1	0.53	0.41	1.22	5	0.94
2	1.90	-0.17	-0.50	15	1.08
3	2.83	-0.40	-1.17	25	1.17
4	0.81	0.27	0.79	35	1.41
5	1.40	0.01	0.03	45	1.73
6	3.37	-0.46	-1.37	55	1.82
7	0.99	0.19	0.55	65	2.43
8	2.03	-0.21	-0.62	75	2.91
9	7.06	0.53	1.57	85	5.47
10	5.64	-0.17	-0.50	95	7.60

B.2 PV Residual and Probability Table – IIRS Plot

Modelled	RESIDUAL OUTPUT			PROBABILITY OUTPUT	
Observation	PV	Res	St. Res	Percentile	VOLUME
1	13.23	1.53	1.48	7.14	0.99
2	0.35	0.64	0.62	21.43	1.02
3	0.98	0.27	0.26	35.71	1.25
4	9.31	-0.91	-0.87	50.00	2.53
5	0.42	0.60	0.58	64.29	6.05
6	7.38	-1.33	-1.29	78.57	8.40
7	3.34	-0.81	-0.78	92.86	14.76
Measured					
1	5.889	0.044	0.158	7.14	0.79
2	0.539	0.249	0.893	21.43	0.85
3	1.237	-0.084	-0.299	35.71	1.15
4	6.350	0.314	1.123	50.00	1.92
5	0.670	0.181	0.648	64.29	4.96
6	5.216	-0.258	-0.925	78.57	5.93
7	2.367	-0.446	-1.597	92.86	6.66

B.3 PV Residual and Probability Table – Thano Forest Range: Plot-I

Modelled					
	RESIDUAL OUTPUT			PROBABILITY OUTPUT	
Observation	PV	Res.	St. Residuals	Percentile	Volume
1	0.25	0.18	1.77	2	0.43
2	1.74	-0.05	-0.53	6	0.45
3	1.09	-0.07	-0.65	10	0.58
4	1.59	-0.08	-0.73	14	0.58
5	2.33	0.13	1.26	18	0.74
6	0.50	0.08	0.76	22	0.78
7	0.80	-0.01	-0.14	26	0.79
8	0.74	0.00	0.02	30	0.81
9	0.92	-0.04	-0.39	34	0.83
10	1.61	-0.07	-0.70	38	0.85
11	1.45	-0.08	-0.81	42	0.88

12	1.71	-0.06	-0.58	46	1.02
13	1.16	-0.08	-0.73	50	1.08
14	2.69	0.33	3.15	54	1.31
15	0.28	0.17	1.60	58	1.37
16	1.72	-0.06	-0.57	62	1.43
17	1.39	-0.09	-0.83	66	1.51
18	0.51	0.07	0.71	70	1.54
19	1.51	-0.08	-0.79	74	1.65
20	0.86	-0.03	-0.27	78	1.66
21	1.86	-0.03	-0.30	82	1.66
22	0.81	-0.02	-0.17	86	1.68
23	1.72	-0.06	-0.55	90	1.83
24	0.84	-0.02	-0.22	94	2.46
25	0.88	-0.03	-0.32	98	3.01
Measured					
1	0.13	0.16	2.10	2	0.29
2	1.37	-0.02	-0.25	6	0.33
3	0.98	-0.06	-0.82	10	0.41
4	1.19	-0.05	-0.67	14	0.46
5	1.77	0.13	1.72	18	0.56
6	0.35	0.06	0.84	22	0.56
7	0.57	-0.01	-0.09	26	0.60
8	0.56	-0.01	-0.07	30	0.61
9	0.63	-0.02	-0.30	34	0.61
10	0.95	-0.06	-0.81	38	0.64
11	0.97	-0.06	-0.82	42	0.74
12	1.21	-0.05	-0.64	46	0.81
13	0.87	-0.06	-0.76	50	0.81
14	1.90	0.20	2.65	54	0.89
15	0.20	0.12	1.62	58	0.91
16	1.37	-0.02	-0.24	62	0.92
17	0.86	-0.06	-0.75	66	1.03
18	0.42	0.04	0.49	70	1.10
19	1.15	-0.05	-0.72	74	1.14
20	0.79	-0.05	-0.64	78	1.16

21	1.41	-0.01	-0.13	82	1.35
22	0.61	-0.02	-0.24	86	1.36
23	1.09	-0.06	-0.79	90	1.40
24	0.63	-0.02	-0.28	94	1.90
25	0.67	-0.03	-0.40	98	2.10

B.4 PV Residual and Probability Table – Thano Forest Range: Plot-II

Modelled					
	RESIDUAL OUTPUT			PROBABILITY OUTPUT	
Observation	PV	Res.	St. Residual	Percentile	Volume'
1	1.61	-0.11	-0.61	1.67	0.14
2	0.48	0.04	0.21	5.00	0.29
3	0.69	-0.04	-0.20	8.33	0.39
4	1.39	-0.13	-0.72	11.67	0.47
5	0.86	-0.08	-0.45	15.00	0.51
6	0.97	-0.10	-0.57	18.33	0.60
7	1.72	-0.09	-0.50	21.67	0.65
8	1.41	-0.13	-0.72	25.00	0.74
9	2.45	0.20	1.16	28.33	0.78
10	1.69	-0.09	-0.53	31.67	0.87
11	1.01	-0.11	-0.60	35.00	0.91
12	1.81	-0.07	-0.39	38.33	0.92
13	2.23	0.08	0.47	41.67	0.97
14	1.03	-0.11	-0.61	45.00	1.01
15	1.70	-0.09	-0.53	48.33	1.23
16	1.65	-0.10	-0.58	51.67	1.27
17	0.25	0.13	0.75	55.00	1.28
18	2.07	0.01	0.08	58.33	1.32
19	1.45	-0.12	-0.70	61.67	1.42
20	-0.34	0.48	2.74	65.00	1.50
21	1.13	-0.12	-0.68	68.33	1.55
22	2.24	0.09	0.50	71.67	1.59
23	2.95	0.57	3.27	75.00	1.60
24	0.41	0.06	0.36	78.33	1.63

25	1.35	-0.13	-0.73	81.67	1.74
26	1.54	-0.12	-0.66	85.00	2.08
27	0.62	-0.01	-0.07	88.33	2.31
28	0.80	-0.07	-0.37	91.67	2.33
29	0.06	0.23	1.31	95.00	2.65
30	1.09	-0.11	-0.66	98.33	3.52
Measured					
1	1.13	-0.12	-0.67	1.67	0.04
2	0.22	0.07	0.40	5.00	0.19
3	0.43	-0.02	-0.09	8.33	0.29
4	0.94	-0.12	-0.68	11.67	0.31
5	0.70	-0.09	-0.51	15.00	0.34
6	0.85	-0.11	-0.65	18.33	0.41
7	1.18	-0.11	-0.65	21.67	0.48
8	1.18	-0.11	-0.65	25.00	0.49
9	2.05	0.24	1.35	28.33	0.61
10	1.42	-0.07	-0.40	31.67	0.61
11	0.70	-0.09	-0.51	35.00	0.67
12	1.41	-0.07	-0.42	38.33	0.72
13	1.82	0.09	0.50	41.67	0.74
14	0.83	-0.11	-0.63	45.00	0.74
15	1.27	-0.10	-0.58	48.33	0.75
16	1.40	-0.08	-0.43	51.67	0.82
17	0.25	0.06	0.31	55.00	0.85
18	1.71	0.03	0.20	58.33	1.02
19	0.97	-0.12	-0.69	61.67	1.03
20	-0.53	0.57	3.20	65.00	1.07
21	0.86	-0.12	-0.65	68.33	1.07
22	1.83	0.10	0.55	71.67	1.17
23	2.39	0.52	2.95	75.00	1.32
24	0.31	0.03	0.16	78.33	1.33
25	0.77	-0.10	-0.59	81.67	1.35
26	1.15	-0.12	-0.67	85.00	1.74
27	0.52	-0.05	-0.26	88.33	1.90
28	0.54	-0.05	-0.30	91.67	1.93

29	0.00	0.19	1.06	95.00	2.29
30	0.86	-0.12	-0.65	98.33	2.91

APPENDIX C: RELATIVE ERRORS IN DBH, HEIGHT AND VOLUME IN ALL PLOTS

C.1 Relative errors in Barkot Forest Area

Relative error	Tree Name	Height	DBH	Volume
1	BKT_1	0.11	0.18	0.50
2	BKT_3	0.06	0.12	0.31
3	BKT_5	0.08	0.09	0.24
4	BKT_7	0.13	0.11	0.30
5	BKT_12	0.09	0.10	0.25
6	BKT_13	0.10	0.07	0.18
7	BKT_15	0.12	0.09	0.24
8	BKT_25	0.13	0.11	0.28
9	BKT_27	0.11	0.08	0.20
10	BKT_28	0.04	0.06	0.15
Average		0.10	0.10	0.26

C.2 Relative errors in IIRS Campus

S. No.	Tree Name	Height	DBH	Volume
1	T-1.txt	0.13	0.45	1.49
2	T-2.txt	0.14	0.10	0.26
3	T-3.txt	0.14	0.03	0.08
4	T-4.txt	0.09	0.10	0.26
5	T-5.txt	0.12	0.08	0.20
6	T-6.txt	0.18	0.08	0.22
7	T-7.txt	0.10	0.12	0.32
Average		0.13	0.14	0.40

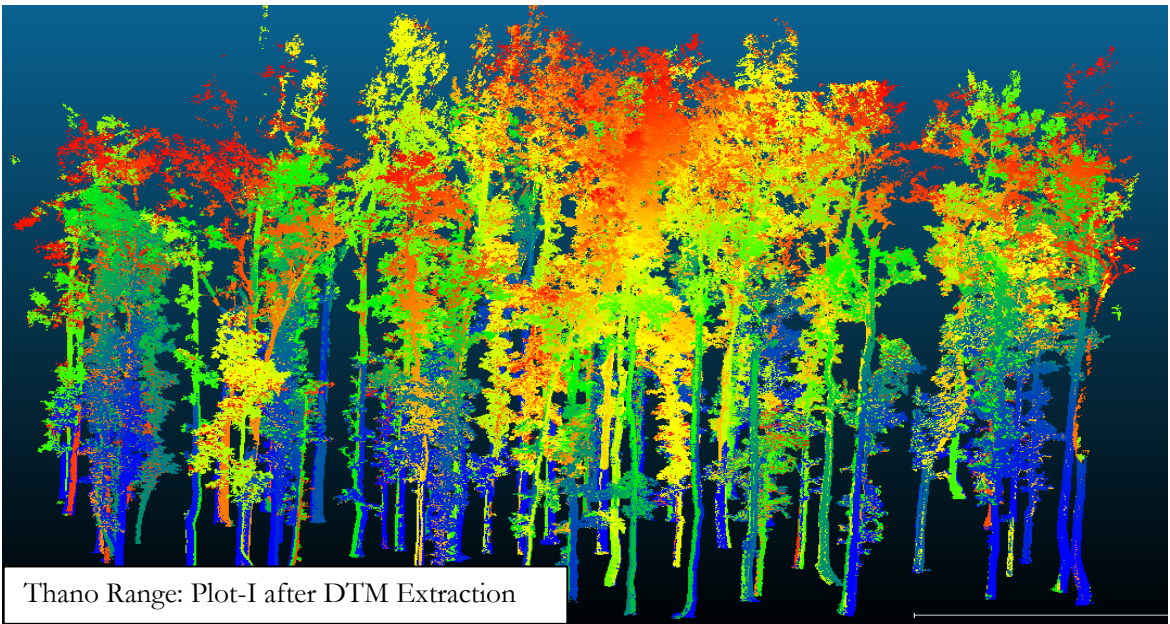
C.3 Relative errors in Thano Forest Area: Plot-I

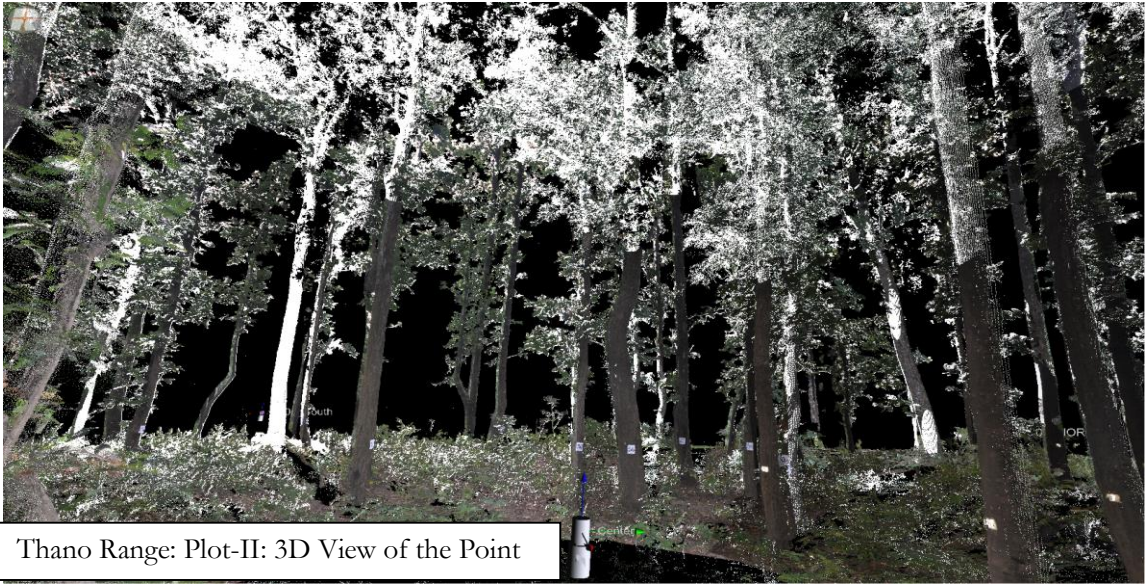
S. No.	Tree Name	Height	DBH	Volume
1	TT1_2	0.08	0.18	0.51
2	TT1_7	0.15	0.09	0.25
3	TT1_13	0.06	0.04	0.11
4	TT1_17	0.09	0.12	0.32
5	TT1_19	0.08	0.11	0.29
6	TT1_21	0.05	0.15	0.41
7	TT1_22	0.09	0.15	0.40
8	TT1_23	0.17	0.12	0.33
9	TT1_24	0.10	0.16	0.43
10	TT1_25	0.06	0.25	0.74
11	TT1_27	0.09	0.18	0.50
12	TT1_28	0.10	0.15	0.41
13	TT1_29	0.09	0.12	0.33
14	TT1_30	0.06	0.16	0.44
15	TT1_31	0.18	0.14	0.38
16	TT1_32	0.10	0.09	0.22
17	TT1_33	0.08	0.22	0.63
18	TT1_34	0.15	0.10	0.28
19	TT1_35	0.10	0.11	0.30
20	TT1_36	0.13	0.05	0.13
21	TT1_38	0.09	0.12	0.31
22	TT1_39	0.20	0.12	0.33
23	TT1_42	0.09	0.22	0.61
24	TT1_43	0.14	0.13	0.34
25	TT1_45	0.57	0.12	0.32
Average		0.12	0.14	0.37

C.4 Relative errors in Thano Forest Area: Plot-II

S. No.	Tree Name	Height	DBH	Volume
1	TT2_5	0.11	0.17	0.48
2	TT2-6	0.05	0.25	0.76
3	TT2-8	0.15	0.20	0.58
4	TT2-10	0.09	0.20	0.55
5	TT2-13	0.17	0.11	0.29
6	TT2-15	0.08	0.07	0.18
7	TT2-16	0.08	0.19	0.53
8	TT2-17	0.02	0.08	0.20
9	TT2-18	0.06	0.06	0.16
10	TT2-20	0.11	0.07	0.18
11	TT2-21	0.13	0.18	0.50
12	TT2-22	0.11	0.12	0.31
13	TT2-23	0.11	0.08	0.21
14	TT2-25	0.10	0.11	0.28
15	TT2-26	0.05	0.14	0.37
16	TT2-27	0.08	0.07	0.17
17	TT2-29	0.20	0.09	0.25
18	TT2-30	0.08	0.08	0.19
19	TT2-31	0.13	0.20	0.56
20	TT2-33	0.17	0.63	2.56
21	TT2-34	0.02	0.13	0.36
22	TT2-35	0.09	0.08	0.21
23	TT2-36	0.07	0.08	0.21
24	TT2-37	0.06	0.14	0.38
25	TT2-38	0.08	0.28	0.83
26	TT2-40	0.06	0.14	0.38
27	TT2-41	0.16	0.10	0.27
28	TT2-42	0.09	0.18	0.51
29	TT2-43	0.18	0.19	0.56
30	TT2-44	0.10	0.11	0.30
Average		0.10	0.15	0.44

APPENDIX D: 3D VIEW OF THE POINT CLOUDS





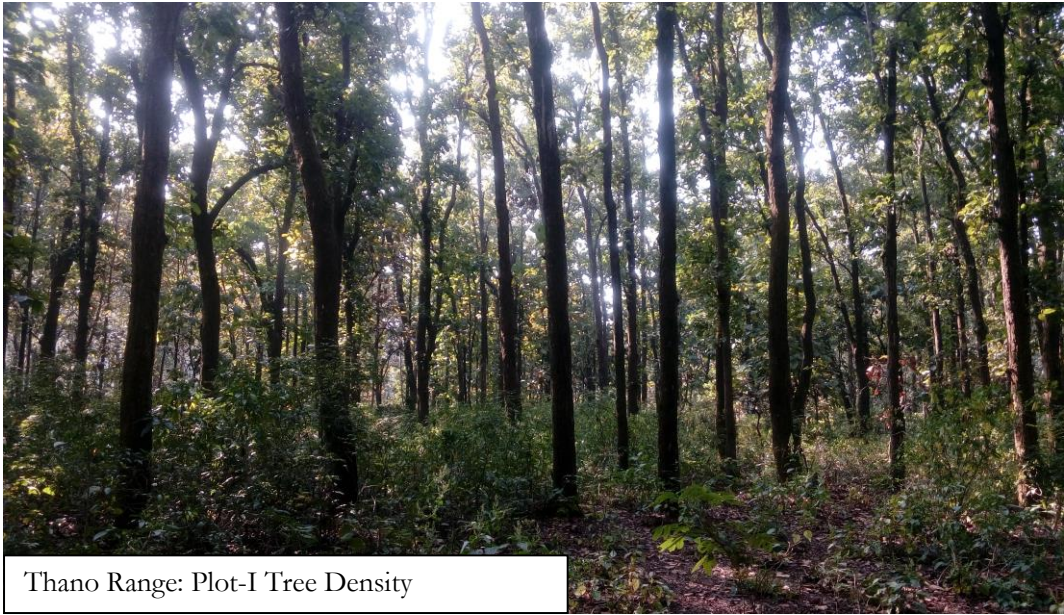
Thano Range: Plot-II: 3D View of the Point



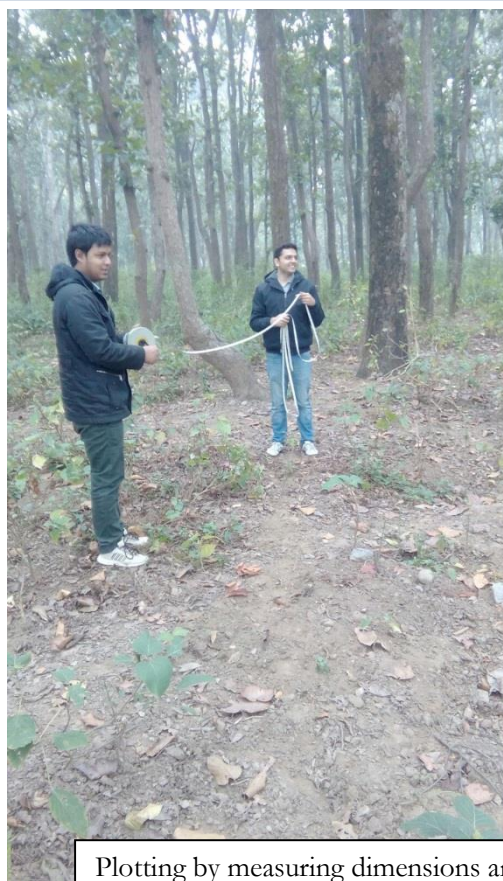
Individual Tree Extraction

APPENDIX E: FIELD VISITS – PHOTOGRAPHS





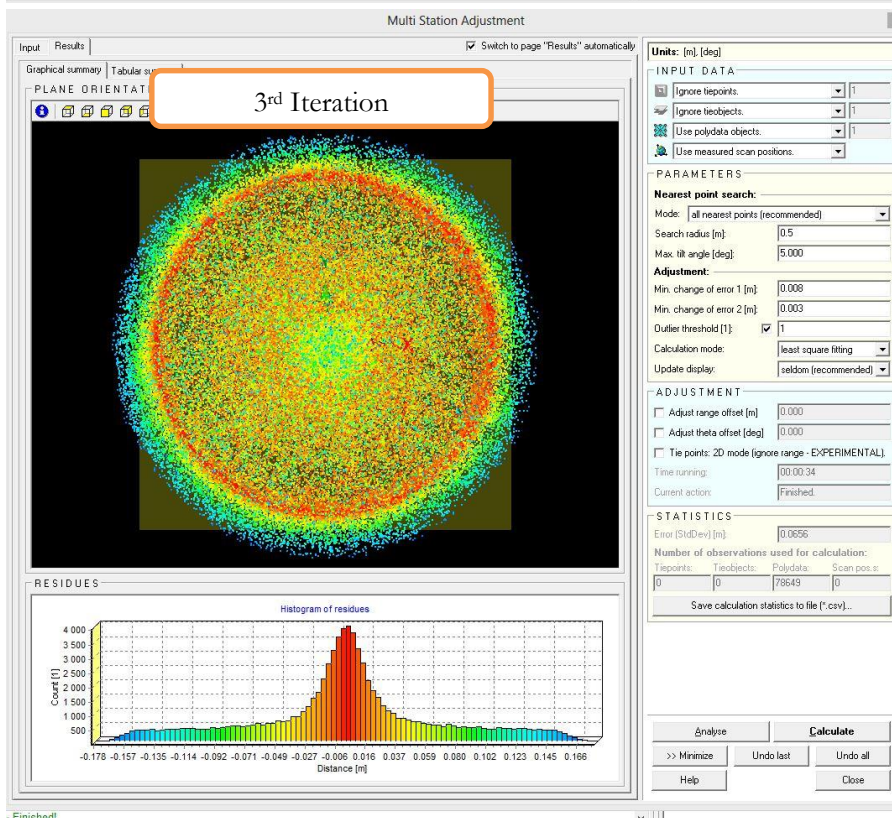
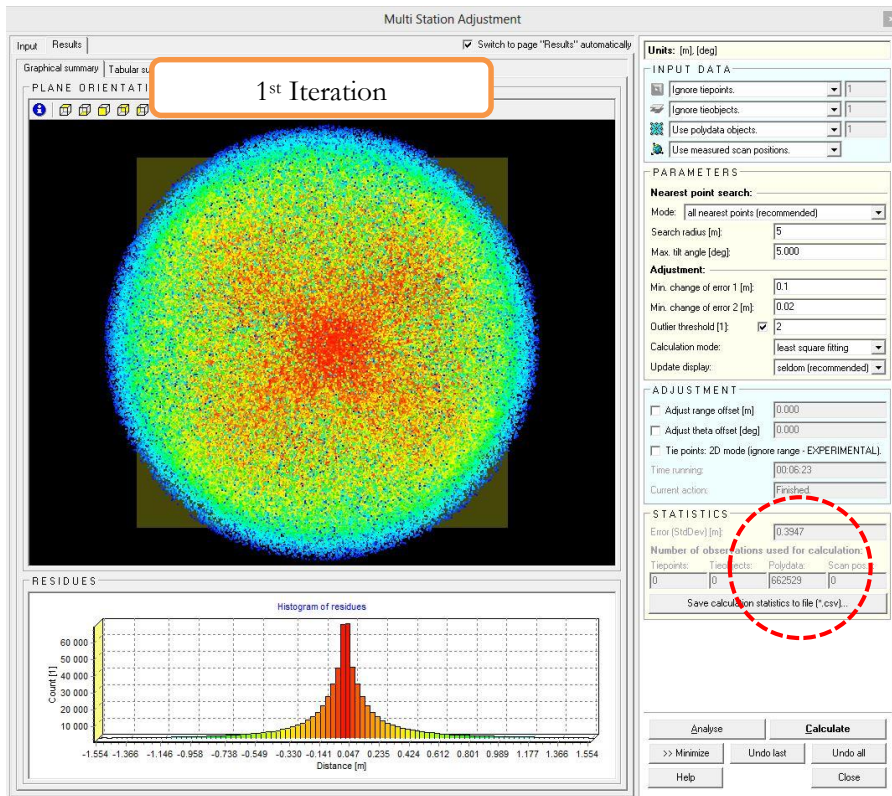
Thano Range: Plot-I Tree Density



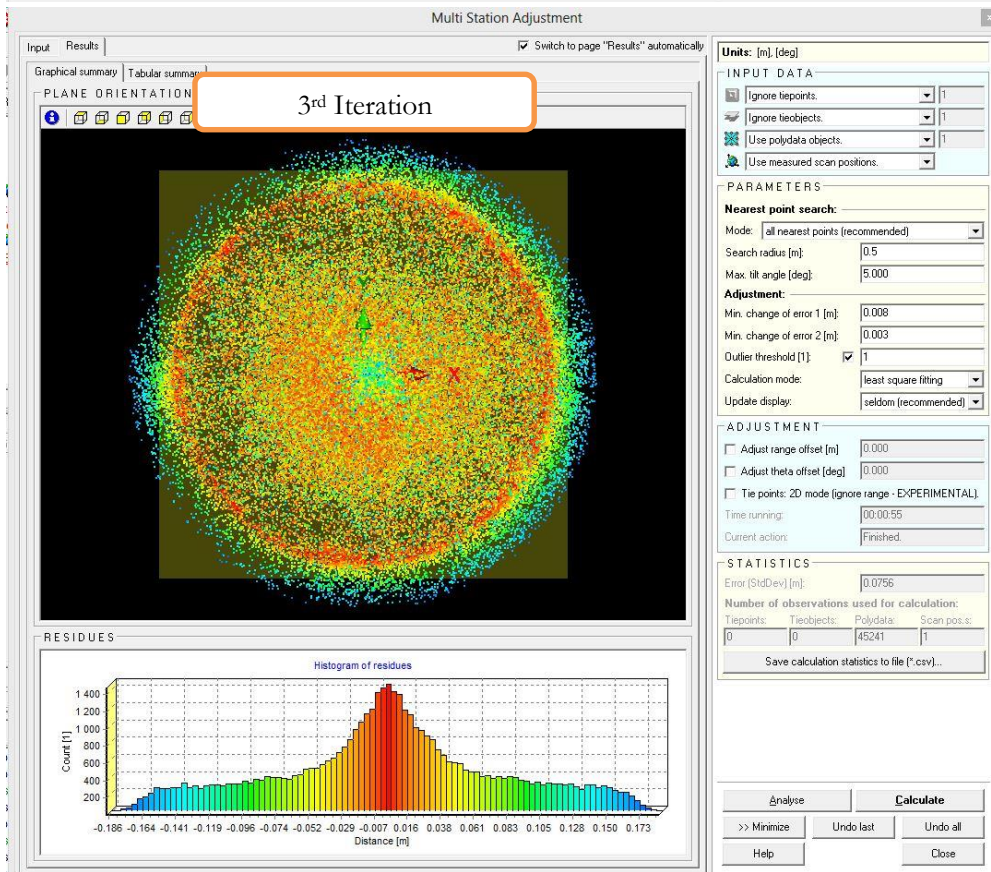
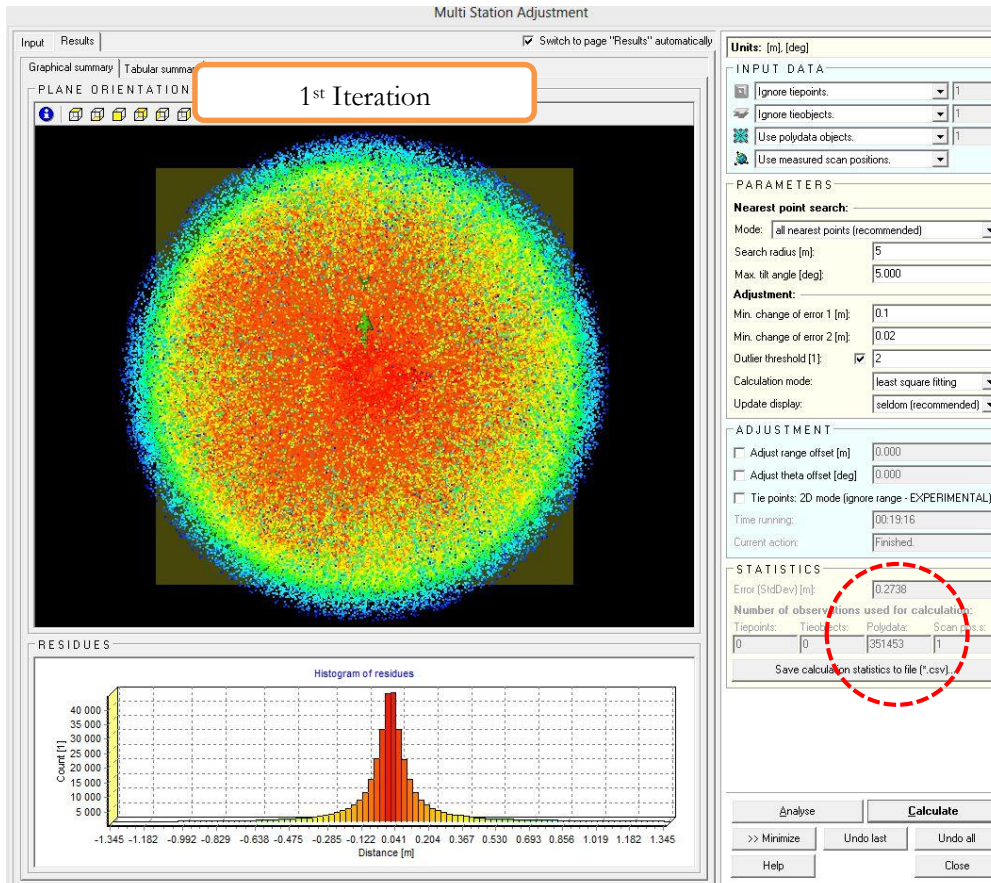
Plotting by measuring dimensions and Scanning by handling TLS Remotely

APPENDIX F: REGISTRATION QUALITY

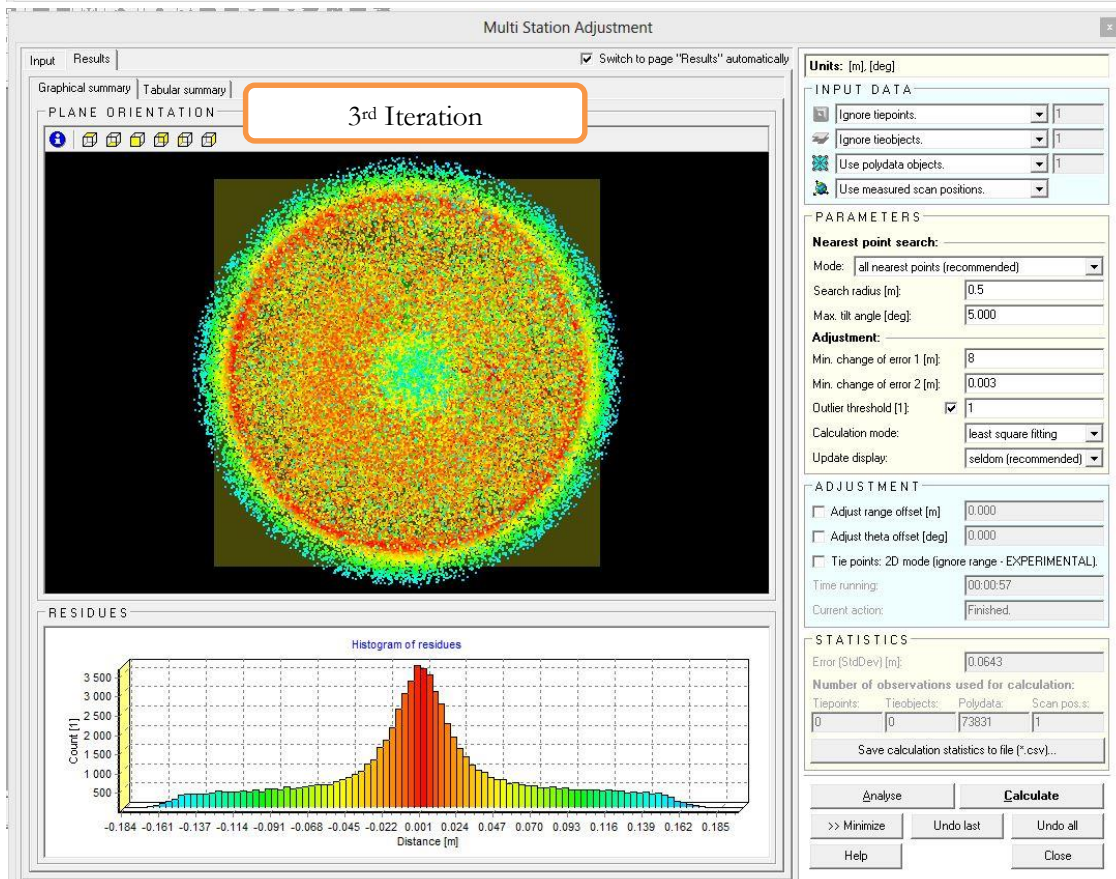
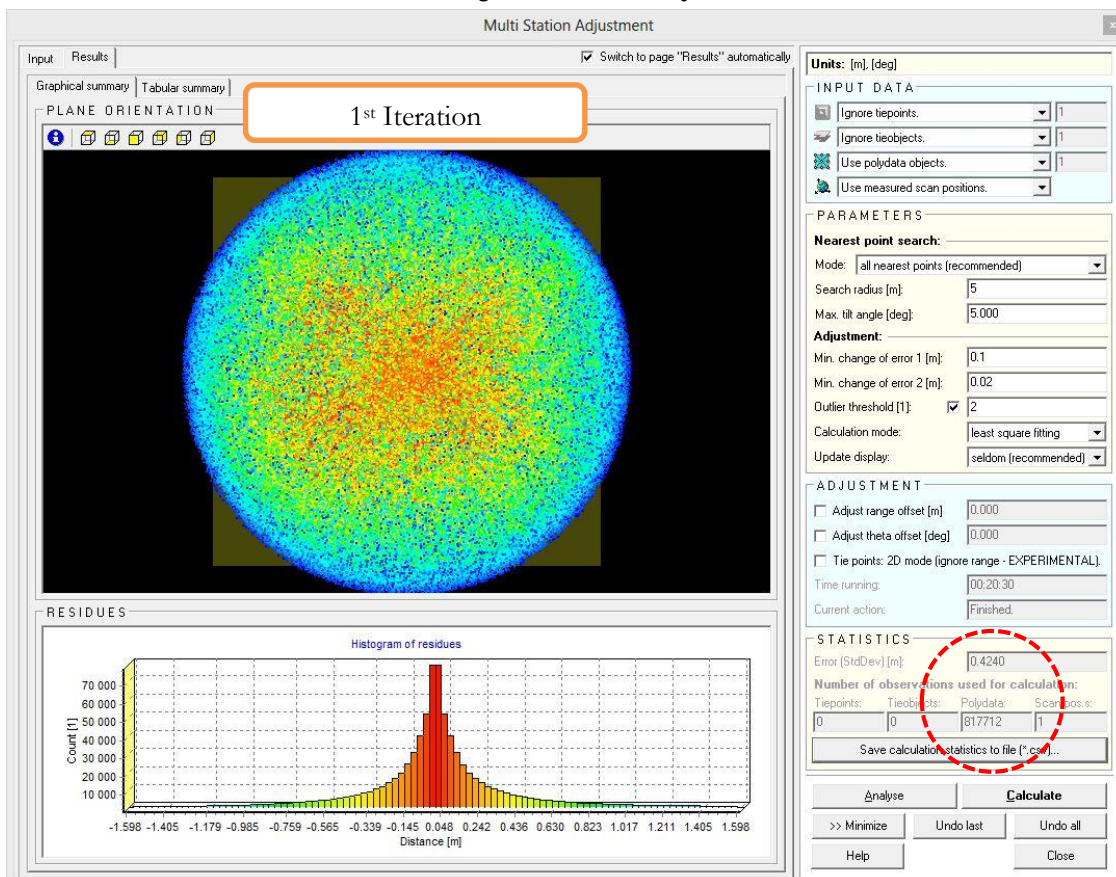
F.1 First and last iterations during Multi-Station Adjustments at Barkot Forest Area



F.2 First and last iterations during Multi-Station Adjustments at IIRS Campus



F.3 First and last iterations during Multi-Station Adjustments at Thano Forest Area: Plot-I



F.3 First and last iterations during Multi-Station Adjustments at Thano Forest Area: Plot-II

